NASA Technical Memorandum 83199
Part 1

Aircraft Noise Prediction Program Theoretical Manual

William E. Zorumski

FEBRUARY 1982

NASA

Addendum to
NASA Technical Memorandum 83199
Part 1

Aircraft Noise Prediction Program
Theoretical Manual

This addendum adds three new sections to the original document.

Please add the enclosed sections 2.4, 2.5, and 2.6 in Chapter 2 and replace the Contents page with the enclosed revised Contents page in your copy of NASA Technical Memorandum 83199, Part 1.

revised 11-93

NASA Technical Memorandum 83199
Part 1

Aircraft Noise Prediction Program Theoretical Manual

William E. Zorumski
Langley Research Center
Hampton, Virginia

National Aeronautics
and Space Administration

Scientific and Technical Information Branch

1982

1. Report No.	2. Government Accession No.	3. Recipient's Catalog No.
NASA TM-83199, Part 1		

4. Title and Subtitle	5. Report Date
AIRCRAFT NOISE PREDICTION PROGRAM THEORETICAL MANUAL	February 1982
	6. Performing Organization Code 505-32-03-01
7. Author(s) William E. Zorumski	8. Performing Organization Report No. L-14805
	10. Work Unit No.
9. Performing Organization Name and Address NASA Langley Research Center Hampton, VA 23665	11. Contract or Grant No.
	13. Type of Report and Period Covered Technical Memorandum
12. Sponsoring Agency Name and Address National Aeronautics and Space Administration Washington, DC 20546	14. Sponsoring Agency Code

15. Supplementary Notes

16. Abstract

The NASA Aircraft Noise Prediction Program (ANOPP) theoretical methods are given in this two-part manual. Part 1 deals with the prediction of data which affects noise generation and propagation. These data include the aircraft flight dynamics, the source noise parameters, and the propagation effects. Part 2 gives detailed prediction methods for specific aircraft noise sources. These sources are airframe noise, combustion noise, fan noise, single and dual stream jet noise, and turbine noise. Part 2 also gives modifications to the NASA methods which comply with the International Civil Aviation Organization (ICAO) standard method for aircraft noise prediction.

17. Key Words (Suggested by Author(s))	18. Distribution Statement
Aircraft noise Noise prediction Jet noise Turbomechanical noise	Unclassified - Unlimited Subject Category 71

19. Security Classif. (of this report)	20. Security Classif. (of this page)	21. No. of Pages	22. Price
Unclassified	Unclassified	193	A09

For sale by the National Technical Information Service, Springfield, Virginia 22161 NASA-Langley, 1982

Contents

Part 1

Part 2*

*Chapters 8 and 9 are published under separate cover.

1. INTRODUCTION

The purpose of the NASA Aircraft Noise Prediction Program (ANOPP) is to predict noise from aircraft, accounting for the effects of the aircraft characteristics, its engines, its operations, and the atmosphere. The approach to this problem has been on a fundamental basis, as depicted in figure 1. The aircraft follows an arbitrary flight path in the presence of an observer on the ground. During this operation, noise sources on the aircraft emit radiation with defined power, directional, and spectral distribution characteristics, all of which may depend on time. This source noise propagates through the atmosphere, being attenuated, to the vicinity of the observer. The observer receives the noise signal from the direct ray plus a signal from a ray reflected by the local ground surface.

A number of approaches are available for this general prediction problem. These approaches are divided in ANOPP into four categories, called functional levels, which are depicted by the schematic in figure 2. The functional levels are defined by the amount of data which is processed and by the degree of approximation in the prediction methods. Level I predicts an effective measure of noise which depends on the observer location. Level II predicts a noise level which depends on the observer and time. In Level III, frequency effects are predicted in addition to the effects of observer and time. In Levels II and III, the noise measures may be subdivided as to the noise source which generates them. Level IV predicts the same information as Level III but with more detail in the spectral data.

The present documents deal with Level III. Part 1 describes the modules which prepare the data which are required for source noise prediction and the modules which are used to process the predicted noise. Part 2 contains the source noise prediction modules. The principal modules used in Level III are depicted in the functional diagram of figure 3. Three stages of computation are shown in this diagram.

The input preparation stage has modules for preparing tables of data which are later interpolated by the prediction and output processing modules. The Atmospheric Module establishes the properties of the atmosphere: pressure, density, humidity, and related variables as a function of altitude. The Flight Dynamics Module represents a two-degree-of-freedom flight dynamic analysis wherein the power setting variable is used as a control function with a definite time dependence. A second control function, the angle of attack, is also used in this module. These control functions may be taken from standard procedure tables or may be the result of an optimization process where many flights are analyzed to find the best operational procedure for a given aircraft performance criterion. The Source Parameters Modules prepare source parameters for the noise prediction modules. These modules take the Mach number, power setting, and angle-of-attack functions of time from the Flight Dynamics Module and interpolate the engine state table to give engine state variables as a function of time. These data are then passed to the second stage of computation. Data for atmospheric absorption effects are prepared by the Atmospheric Absorption Module. This table is used in the

Propagation Module in the second stage of computation. The Geometry Module takes data on the aircraft position and orientation from the Flight Dynamics Module and evaluates the vectors from the source to each ground observer as functions of time. Each noise source will be given in a specified axis system such as engine 1 axes or aircraft wind axes so that each observer vector will be expressed in several source coordinate systems at the same time.

Noise predictions are made in several coordinate systems which are attached to the aircraft. The airframe noise predictions are made in the wind axis system by the Aircraft Noise Module. Wing noise has a dipole directivity in this system with the Z-axis being the dipole axis as shown in figure 4. Predictions are made for virtual observers at a fixed distance r and prescribed angle θ in this sytem at a sequence of times t which are widely spaced. Using the wind axis system, which has the axis of symmetry, allows for minimum use of the prediction modules since the virtual observers are located by only the single coordinate θ. After making the predictions for wing noise for a few virtual observers and times in the wind axis system, the Propagation Module interpolates these data, using the rapidly varying true observer vectors given by the Geometry Module, to give free-field unattenuated predictions at actual observer positions. The Propagation Module then adds air absorption and ground effects by interpolating a previously prepared table from the Atmospheric Absorption Module to give actual noise at the observers due to the wing noise component from the Aircraft Noise Module. Other noise source components in the Airframe Noise Module may be added to the wing noise at the source if they are conveniently expressed in the wind axis system. Otherwise, the looping process depicted in figure 3 is used to propagate the noise to the observer before summation takes place.

The engine axis systems depicted in figure 3 contain noise source components, such as jet and fan noise, with a common axis of symmetry, the engine axis. Noise sources are conveniently summed at virtual observer locations in these systems before they are processed through the Propagation Module and taken to actual observers. Figure 5 illustrates this process. Within the engine axis system, modules for fan, combustor, turbine, and jet noise are called to make predictions at virtual observer positions. Each component noise prediction is expressed at the same set of virtual observer positions so that direct summation of the noise may be made before propagation to the observers. This summation saves excessive use of the computational procedures in the Propagation Module.

Output processing, the third stage of prediction process, involves operations on predicted noise at the observer. These predictions are functions of frequency, time, source coordinate system, and observer. The output processing modules reduce these data by taking summations and integrals over these four variables. The Noise Levels Module removes the frequency dependence by converting spectra into weighted noise levels such as A-level and D-level to further reduce the amount of data. Perceived Noise Level, a nonlinear measure of noise, is also computed by this module. Time integrals are made in the Effective Noise Module to evaluate variables such as Effective Perceived Noise.

An ANOPP Level III noise prediction module is characterized by the prediction of 1/3-octave-band noise. The band centers are based on

observer frequencies and are independent of time. All other inputs to the prediction modules are time dependent. The vectors from the source to the observer are naturally dependent on time and observer so that the output from a source module is a function of frequency, time, and observer, in that order.

The prediction of 1/3-octave-band noise is a serious limitation which should not be passed over quickly. Some of the most important noise sources are actually tones, for example, from the fan rotor of a bypass-type engine. In the prediction modules, these tones are assigned to a 1/3-octave band and subsequently treated as broadband noise. This will cause errors in the prediction of atmospheric attenuation, ground effects, and even noise levels. Nevertheless, the added complexity of carrying a separate procedure for tones suggests that this is not an appropriate task for ANOPP Level III and this type of analysis has been relegated to the Level IV manual.

Input and output of the functional modules may be a combination of dimensional and dimensionless variables. Two systems of dimensions are used, the preferred SI system and alternate U.S. Customary system. One principal distinction must be made about the use of the U.S. Customary system. The unit of pound-mass is not permitted and must be replaced by the less popular unit of slugs. The reason for this is that $F = ma$ only if the mass is expressed in slugs. Variables involving heat energy are used within the program. These variables, such as c_p, the specific heat at constant pressure, are always expressed in mechanical units rather than calories or BTU. This facilitates the dimensional balancing of equations and the formation of dimensionless groups.

Within each module the essential computations are made by using dimensionless groups. This approach eliminates extraneous variables, accounts for scaling, permits the use of an empirical data base, and facilitates the use of different systems of units. When the dependent data have been generated in dimensionless form, they may be converted to dimensional variables for output if this is desired. In many cases, it is not desirable to convert to dimensional units since this would increase the amount of computation and data. For example, dimensional engine data are often tabulated as a function of altitude, velocity, and engine speed (or some power setting variable), whereas it is only necessary to tabulate dimensionless data as a function of Mach number and power setting. The use of dimensionless groups thus reduces the three-dimensional arrays to two-dimensional arrays, a great savings in computation and storage of data.

The sections of this manual are organized along the lines of the diagram in figure 3. In each section, a module is described by briefly stating its purpose and function, its input and output data, and the method or computation process. References are given to the appropriate technical literature from which the methods are developed. The module description, like the module, is written as an independent section so that some duplication naturally results. On the other hand, since modules must interface, it is necessary to refer from one module to another in the output sections. All variables which are not naturally dimensionless will have dimensions shown with SI units first followed by U.S. Customary units in parentheses. Variables which have been converted to dimensionless

groups through division by a reference variable are given with their conventional dimensional description followed by re and the group for the reference variable. As an example, the dimensionless group (T/T_a) would be described as

T^* absolute temperature, re T_a

and, in the symbols list, T_a would be found with a description

T_a absolute ambient temperature, K (^oR).

Symbol lists are provided with each section to aid in clarifying all nomenclature.

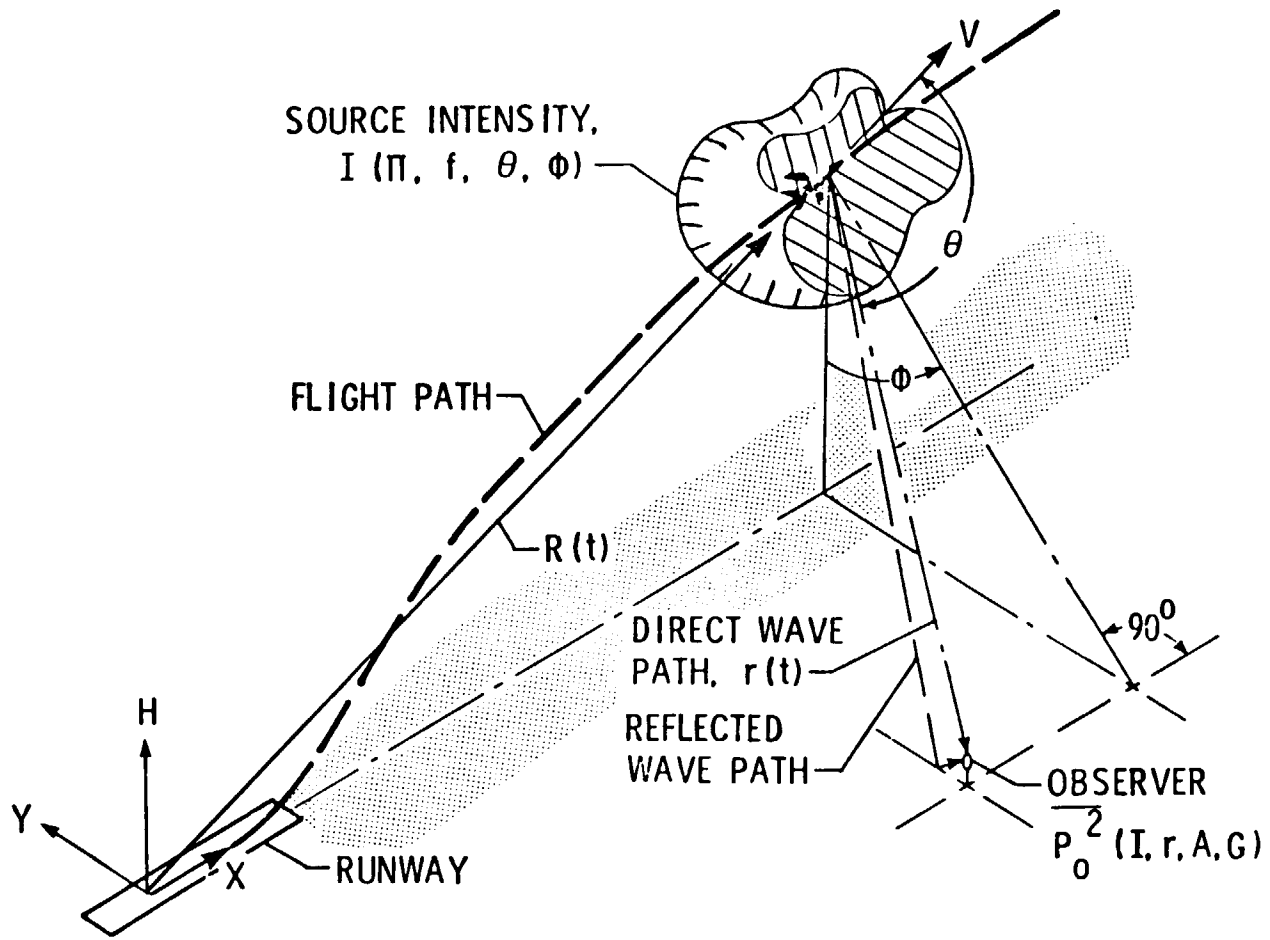

Figure 1.- Overall prediction methodology.

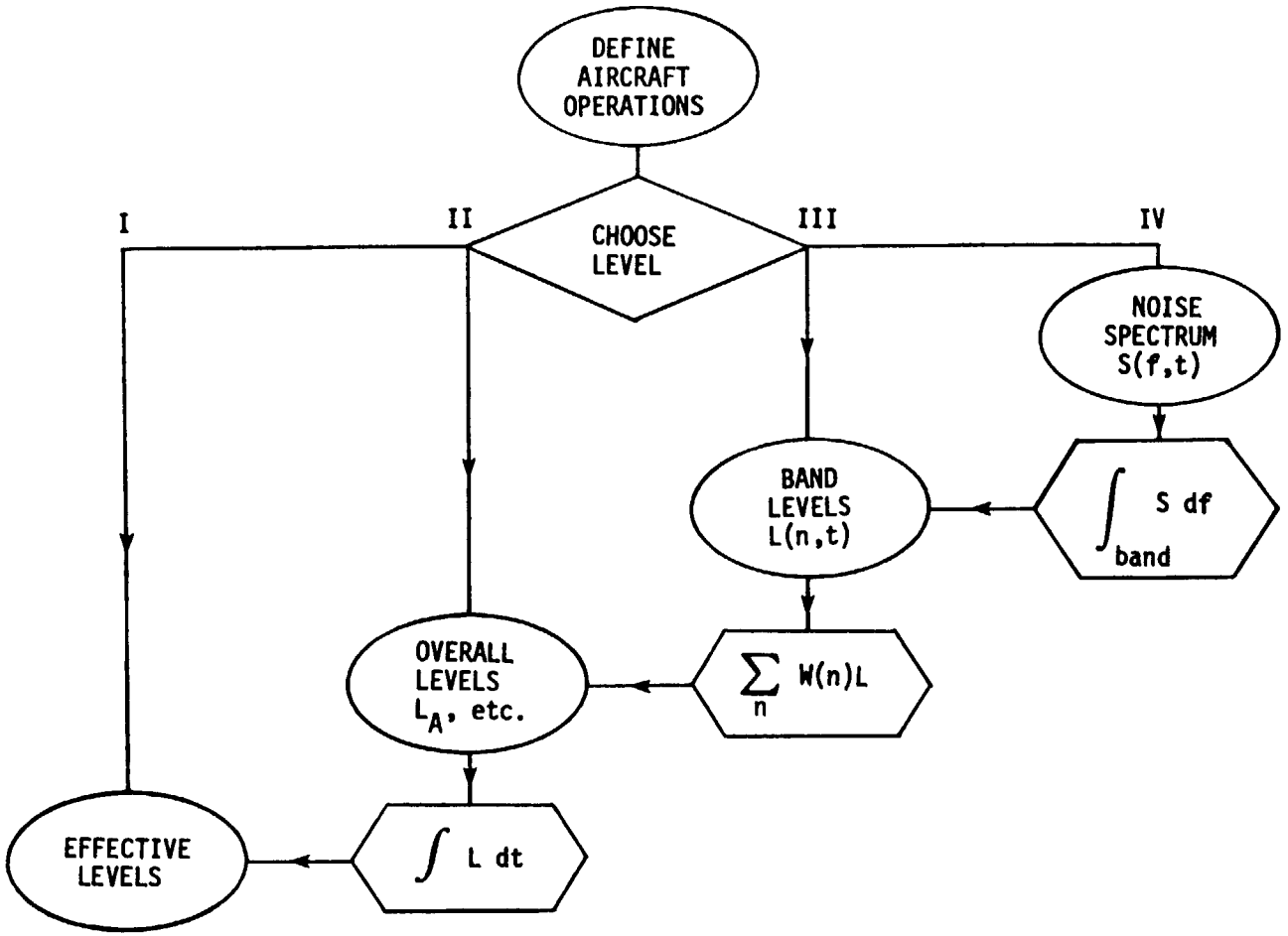

Figure 2.- ANOPP functional level computation flow diagram.

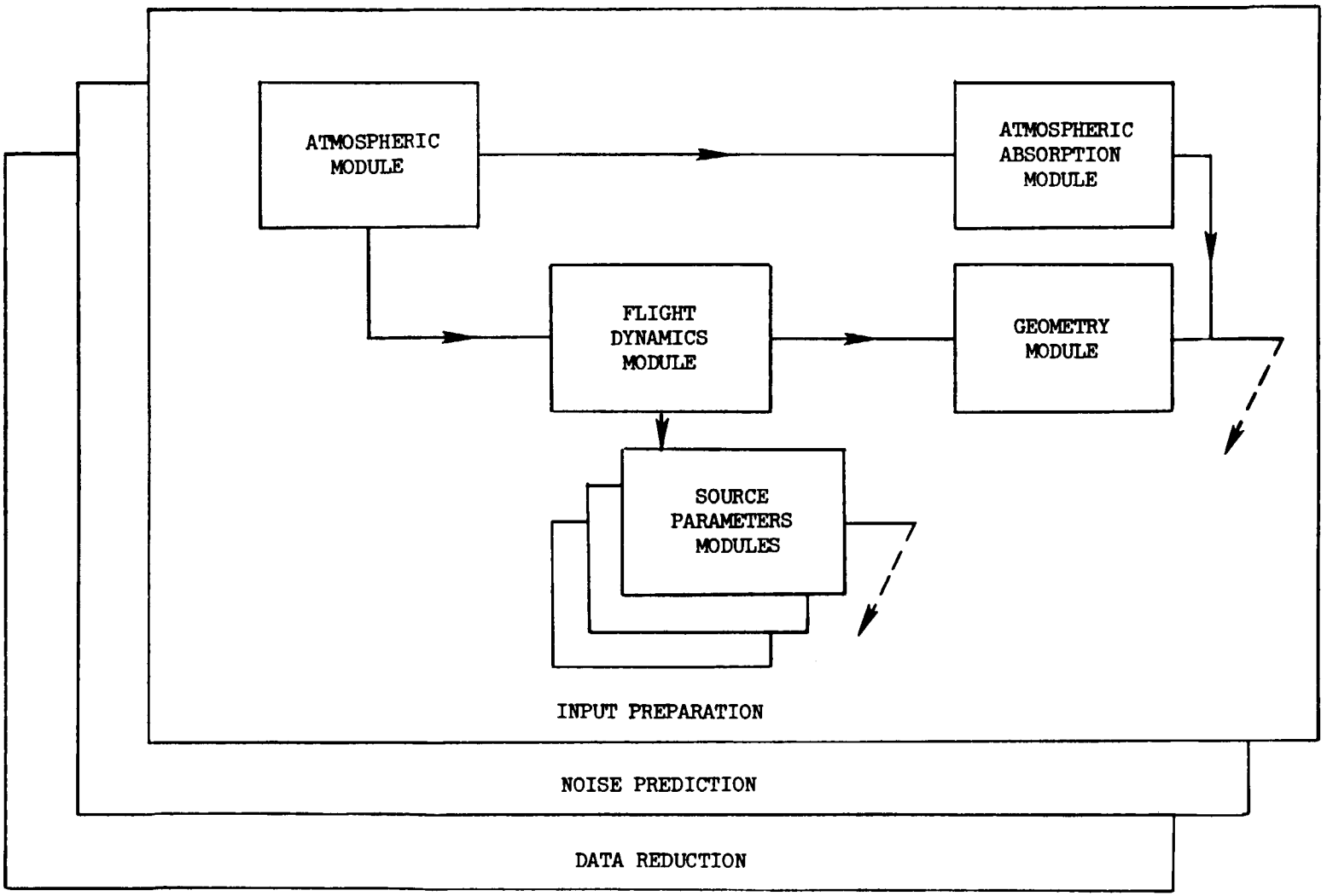

Figure 3.- ANOPP Level III functional diagram.

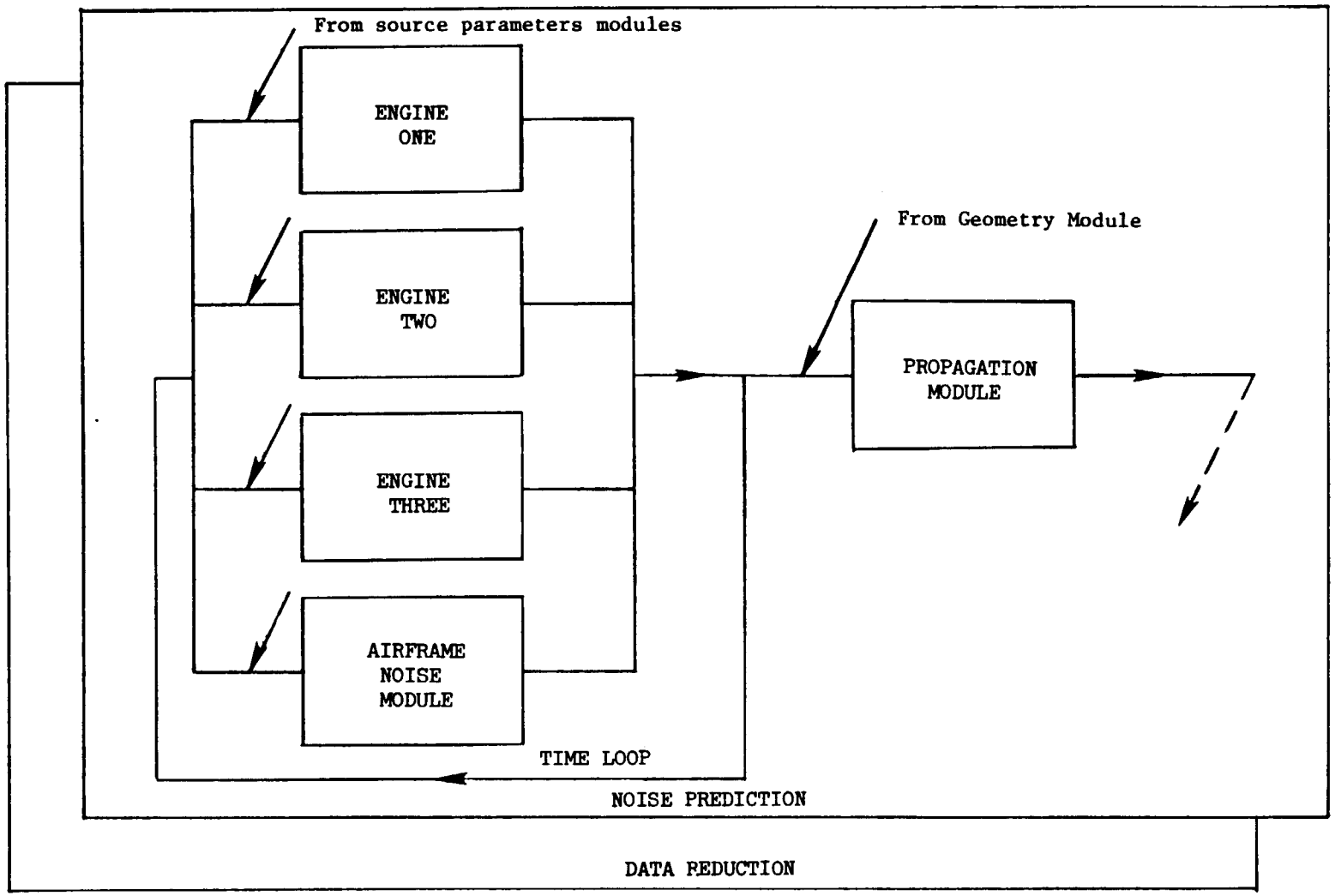

Figure 3.- Continued.

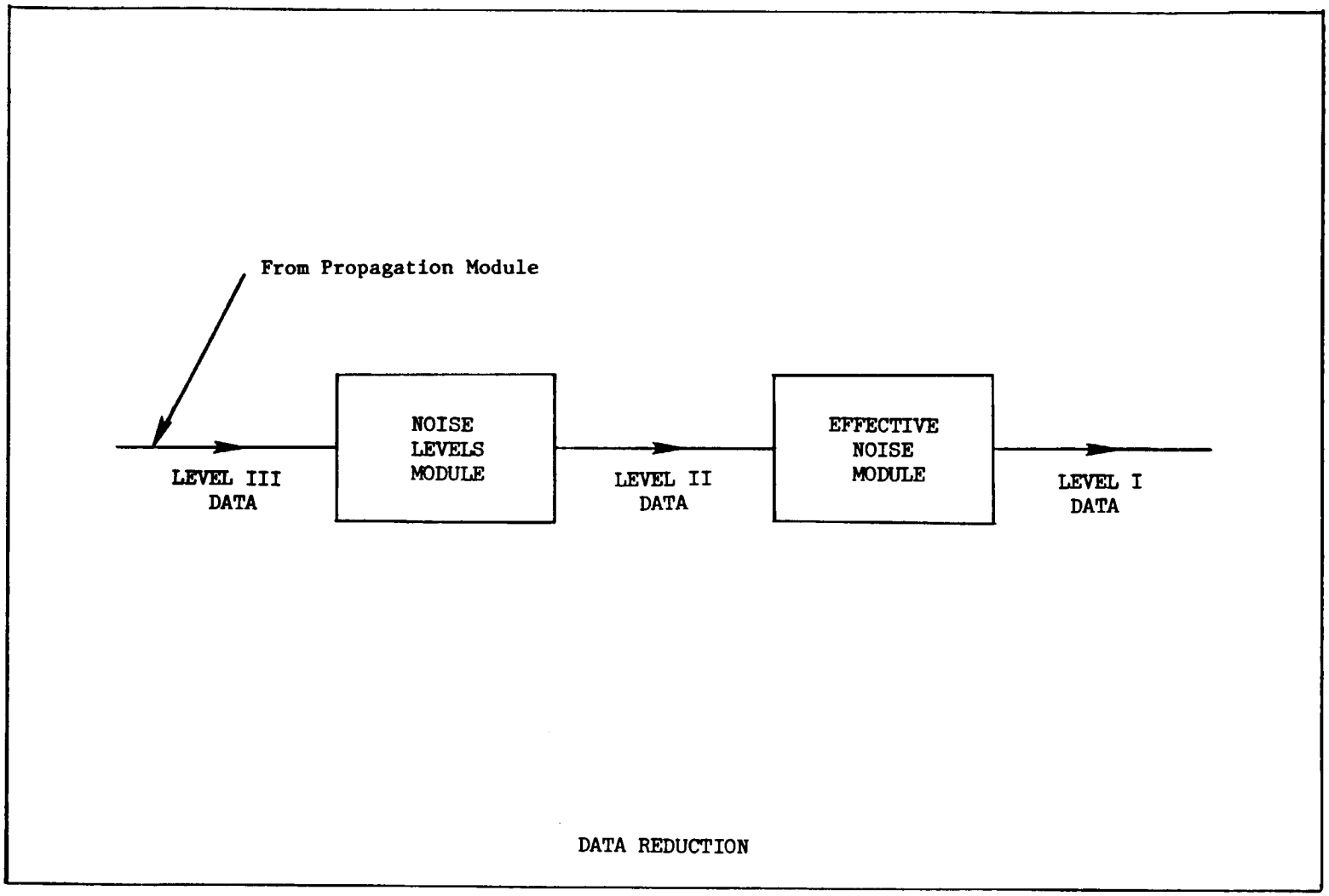

Figure 3.- Concluded.

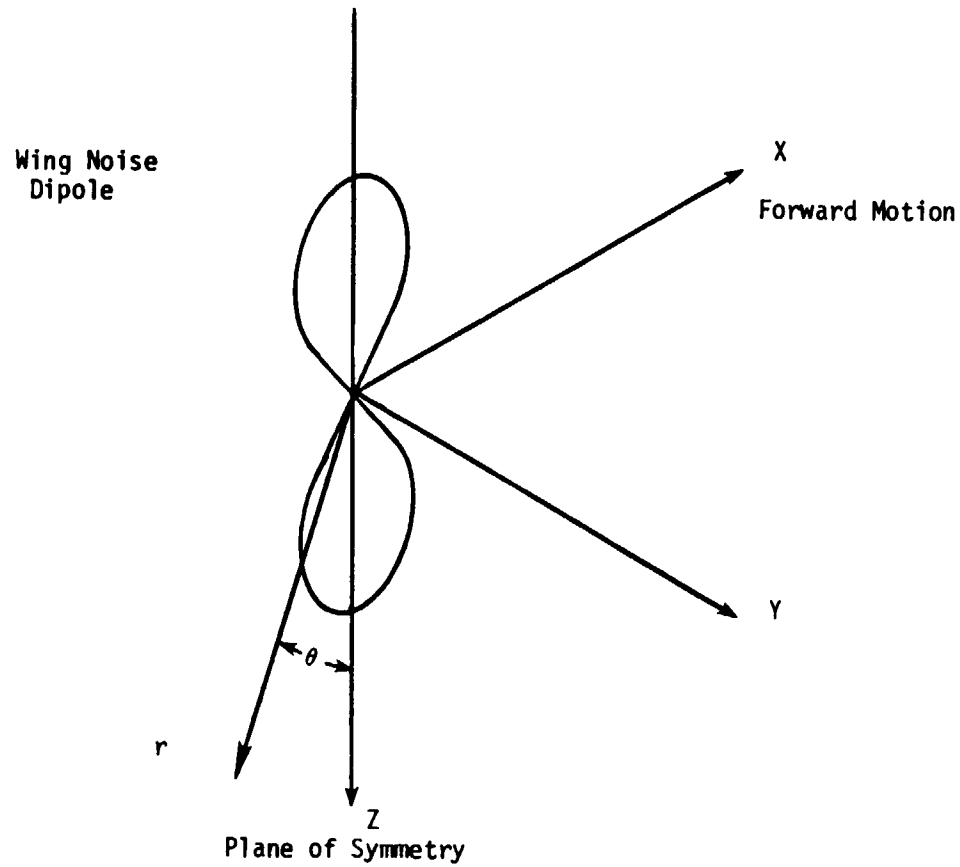

Figure 4.- Wing noise in the wind axis system.

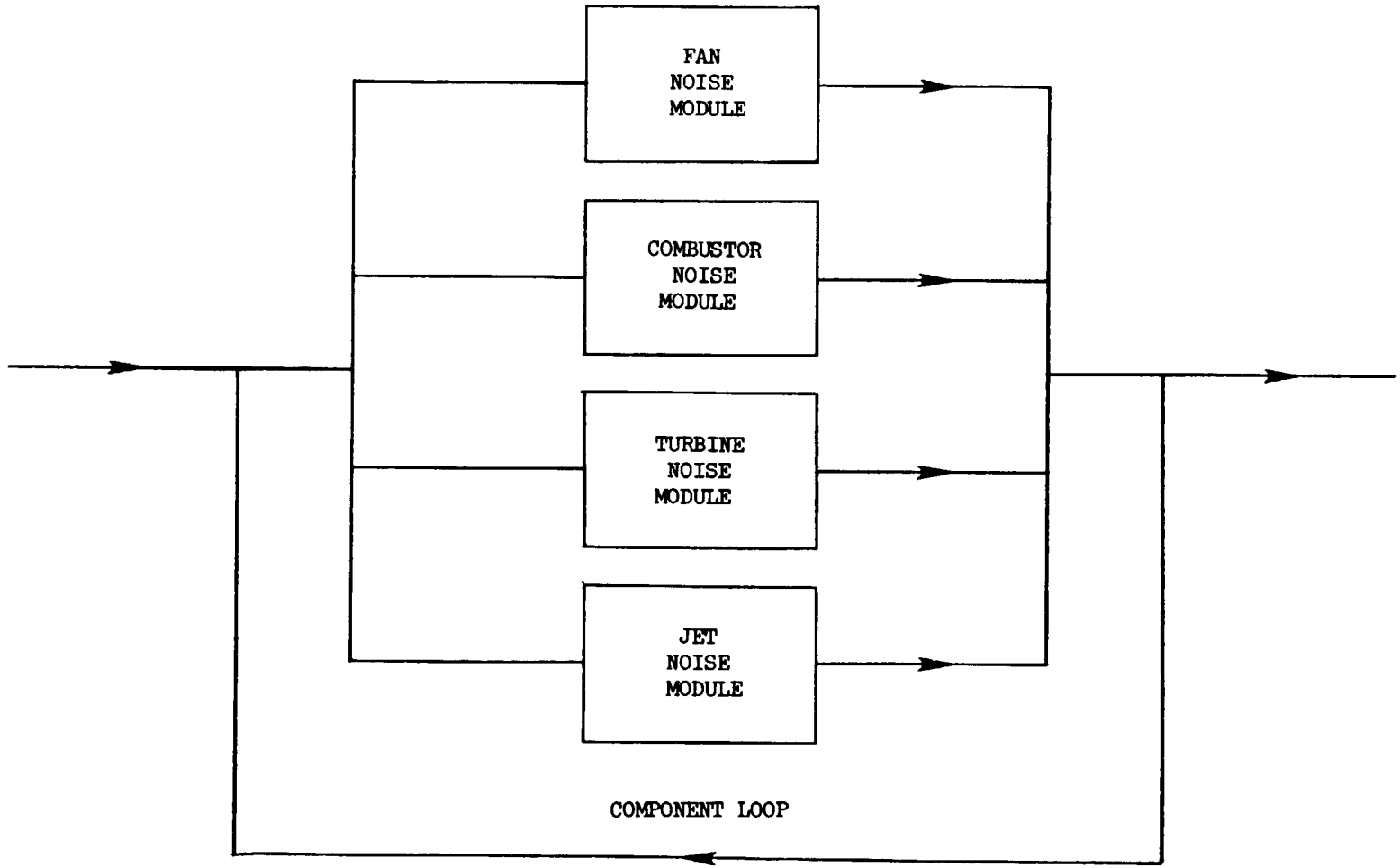

Figure 5.- Engine component noise prediction for a given engine axis.

2. AIRCRAFT FLIGHT DYNAMICS

2.1 ATMOSPHERIC MODULE

INTRODUCTION

Selection of an atmospheric model is the first step in predicting aircraft noise. Atmospheric properties affect the performance of the aircraft, the noise generated by the aircraft and its engines, and the propagation of this noise through the atmosphere. Since noise is most significant during terminal operations (take-off and landing), this model is only representative of the atmosphere below 10 km.

Four approximations are used in this model. The first approximation is that acceleration due to gravity is constant and is assigned the sea level value. This assumption is usually made in the analysis of aircraft performance. The second approximation is to neglect the effect of water vapor on the pressure, density, and viscosity of air. Consequently, the molecular weight of air is taken as the standard sea level value (scale: $C^{12} = 12.0000$). The third approximation is that geopotential altitude is equal to geometric altitude. For each of these assumptions the maximum relative error is of the order 10^{-3} at 10 km. The fourth approximation is that atmospheric properties are functions of altitude only. All equations and constants used in this model are taken from references 1 and 2.

The primary purpose of the Atmospheric Module is to generate dimensionless arrays of ambient atmospheric parameters at equal increments of altitude. Dimensionless parameters are used to provide simplified forms for the equations and to facilitate working in different systems of units.

SYMBOLS

c	speed of sound, m/s (ft/s)
g	acceleration due to gravity, m/s^2 (ft/s^2)
H	altitude (geometric assumed equal to geopotential), m (ft)
ΔH	output altitude increment, m (ft)
h	absolute humidity, percent mole fraction (ratio of number of H_2O molecules to total number of molecules in mixture, 1.178 percent at 70 percent relative humidity and standard pressure and temperature)
k	coefficient of thermal conductivity, W/m-K (BTU/ft-s-^oR)
M	molecular weight of air
n	number of output values
p	atmospheric pressure, Pa (lb/ft^2)

$\bar{R}$ universal gas constant, kg-m^2/K-s^2 (slug-$ft^2/{}^oR$-s^2)

rh relative humidity, percent

S Sutherland's constant, 110.4 K (198.72^oR)

T temperature, K (^oR)

y $= Mg_r(H - H_1)/\bar{R}T_r$

γ ratio of specific heats

μ coefficient of viscosity, kg/m-s (lb/ft-s)

ρ density, kg/m^3 (slugs/ft^3)

Subscripts:

i input array values

j output array values

r standard sea level value

1 ground level value

Superscripts:

* dimensionless value

- average

INPUT

Input for constructing the atmospheric model consists of ΔH, the desired output altitude increment; H_1 and p_1, the ground level altitude and pressure; and a table of temperatures and humidities as functions of altitude. Input of one atmospheric set at ground level consisting of altitude, temperature, and relative humidity results in a constant atmospheric model. Input of more than one set results in a hydrostatic atmospheric model generated according to the preset altitude increment ΔH. The input altitudes do not have to be supplied at equal increments; however, the ground level altitude must be supplied. Output altitudes are generated at equal increments. Table I gives the recommended ranges and the default values for the input parameters.

Input Constants

H_1 ground level altitude, m (ft)

ΔH output altitude increment, m (ft)

p_1 pressure at ground level, Pa (lb/ft^2)

Atmosphere Input Table

H	altitude, m (ft)
T(H)	temperature, K (^{o}R)
rh(H)	relative humidity, percent

OUTPUT

The output is a table of dimensionless pressures, densities, temperatures, humidities, sound speeds, average sound speeds, coefficients of viscosity and thermal conductivity, and characteristic acoustic impedances as a function of altitude.

Atmospheric Properties Table

y	altitude, $Mg_r(H - H_1)/\bar{R}T_r$
$p^*(y)$	pressure, re p_r
$\rho^*(y)$	density, re ρ_r
$T^*(y)$	temperature, re T_r
h(y)	humidity, percent mole fraction
$c^*(y)$	sound speed, re c_r
$\bar{c}^*(y)$	average sound speed, re c_r
$\mu^*(y)$	coefficient of viscosity, re μ_r
$k^*(y)$	coefficient of thermal conductivity, re k_r
$\rho^* c^*(y)$	characteristic acoustic impedance, re $\rho_r c_r$

METHOD

The generation of an atmospheric model requires that numerical values be established for certain primary constants relevant to the Earth's atmosphere. These primary constants are given in table II. All computations within the atmospheric model module are based on dimensionless equations formed with these primary constants. The basic equations used in the computational sequence are:

Perfect gas law:

$$p = \rho\bar{R}T/M \tag{1a}$$

which in dimensionless form becomes

$$p^* = \rho^* T^* \tag{1b}$$

Equation for speed of sound:

$$c^2 = \gamma \bar{R} T / M \tag{2a}$$

which in dimensionless form becomes

$$(c^*)^2 = T^* \tag{2b}$$

Hydrostatic equation:

$$dp/p = -Mg_r \, dH/\bar{R}T \tag{3a}$$

which in dimensionless form becomes

$$dp^*/p^* = -dy/T^* \tag{3b}$$

where

$$y = Mg_r (H - H_1) \Big/ \bar{R} T_r \tag{4}$$

Figure 1 is a graphic representation of the atmospheric coordinates.

Using the atmospheric variables supplied as input, along with the basic equations, the atmospheric model is computed as follows. An altitude vector y_j is defined for incremental altitude changes ΔH by

$$\Delta y = Mg_r \, \Delta H \Big/ \bar{R} T_r \tag{5}$$

with

$$y_j = (j - 1) \, \Delta y \qquad (j = 1, 2, \ldots, n) \tag{6}$$

where n is the number of output altitudes.

The dimensionless temperature is computed by

$$T_i^* = T(H_i)/T_r \tag{7}$$

Output values for temperature T_j^* are then found by linear interpolation with respect to y.

Dimensionless pressures are computed by integrating equation (3b). If temperature is assumed to vary linearly between y_j and y_{j+1}, the integration may be carried out exactly to yield the recurrence formula:

$$p_j^* = p_{j-1}^* \left(T_j^* / T_{j-1}^* \right)^{-\Delta y / \left(T_j^* - T_{j-1}^* \right)} \qquad \left(T_j^* \neq T_{j-1}^*; \; j = 2, 3, \ldots, n \right) \tag{8a}$$

or

$$p_j^* = p_{j-1}^* e^{-\Delta y / T_j^*} \qquad \left(T_j^* = T_{j-1}^*; \; j = 2, 3, \ldots, n \right) \tag{8b}$$

where

$$p_1^* = p_1 / p_r \tag{8c}$$

Once the dimensionless temperature and pressure vectors are prepared, the other required dimensionless atmospheric vectors are computed as follows:

Density:

$$\rho_j^* = p_j^* / T_j^* \tag{9}$$

Sound speed:

$$c_j^* = \left(T_j^* \right)^{1/2} \tag{10}$$

Coefficient of viscosity:

$$\mu_j^* = \frac{1.38313 \left(T_j^* \right)^{3/2}}{T_j^* + 0.38313} \tag{11}$$

Coefficient of thermal conductivity:

$$k_j^* = \frac{1.77385 \left(T_j^* \right)^{3/2}}{T_j^* + 0.8516 \times 10^{-0.0416 / T_j^*}} \tag{12}$$

Characteristic impedance:

$$\rho^* c_j^* = p_j^* / \left(T_j^* \right)^{1/2} \tag{13}$$

The constant 0.38313 is the ratio of S/T_r, where S is Sutherland's constant.

Average sound speed is defined by

$$\bar{c}(y) = \frac{y}{\int_0^y \left[c(y)\right]^{-1} dy} \tag{14}$$

where the denominator of equation (14) is the time for vertical transmission. If temperature is again assumed to vary linearly between y_j and y_{j+1}, the denominator of equation (14) can be integrated exactly to yield the following recurrence formula:

$$I_j = I_{j-1} + \frac{2(\Delta y)}{\left(T_j^*\right)^{1/2} + \left(T_{j-1}^*\right)^{1/2}} \tag{15a}$$

where

$$\int_0^{y_j} \left[\left(T_j^*\right)\right]^{-1/2} dy = I_j \tag{15b}$$

with the following condition:

$$y_1 = 0 \qquad I_1 = 0 \tag{15c}$$

Equation (14) is then computed in dimensionless form for altitude y_j by

$$\bar{c}^*(y_j) = y_j/I_j \tag{16}$$

The input humidity is expressed as relative humidity in percent. For computational purposes, it is more convenient to express humidity in absolute terms as the mole ratio (in percent) of H_2O molecules relative to the total number of molecules in a mixture. The absolute humidity is defined in terms of temperature, pressure, and relative humidity by

$$h_j = \left(rh_j/p_j^*\right)10^{8.4256-\left(10.1995/T_j^*\right)-4.922 \log T_j^*} \tag{17}$$

where rh_j is computed by linearly interpolating with respect to y.

Once the atmospheric values are computed in dimensionless form, dimensional values for printed output are computed using the following equations:

$$H_j = (RT_r/Mg_r)y_j + H_1 \tag{18}$$

$$p_j = p_r p_j^* \tag{19}$$

$$T_j = T_r T_j^* \tag{20}$$

$$\rho_j = \rho_r \rho_j^* \tag{21}$$

$$c_j = c_r c_j^* \tag{22}$$

$$\bar{c}_j = c_r \bar{c}_j^* \tag{23}$$

$$\mu_j = \mu_r \mu_j^* \tag{24}$$

$$k_j = k_r k_j^* \tag{25}$$

$$\rho c_j = \rho_r^* c_r \rho c_j^* \tag{26}$$

REFERENCES

1. U.S. Standard Atmosphere, 1976. NOAA, NASA, and U.S. Air Force, Oct. 1976.

2. Sutherland, Louis C.: Review of Experimental Data in Support of a Proposed New Method for Computing Atmospheric Absorption Losses. DOT-TST-75-87, U.S. Dep. Transp., May 1975.

TABLE I.- RANGE AND DEFAULT VALUES OF INPUT PARAMETERS

Input parameter	Minimum	Default	Maximum
ΔH, m	1	100	100
p_1, N/m^2 . . .	90 000	101 325	110 000
H, H_1, m	-300	0	10 000
T, K	200	288.15	300
rh, %	0	70	100

TABLE II.- STORED PRIMARY CONSTANTS

Constant	SI Units	U.S. Customary Units
g_r	9.806 65 m/s^2	32.1741 ft/s^2
M	28.9644	28.9644
$\bar{R}$	8314.32 $m^2/K\text{-}s^2$	49 718.96 $ft^2/{}^oR\text{-}s^2$
γ	1.40	1.40
p_r	$1.013\ 25 \times 10^5$ Pa	2116.22 lb/ft^2
ρ_r	1.225 kg/m^3	0.002 377 $slug/ft^3$
T_r	288.15 K	518.67 ^oR
c_r	340.294 m/s	1116.45 ft/s
μ_r	1.7894×10^{-5} kg/m-s	3.737×10^{-7} slug/ft-s
k_r	6.0530×10^{-6} W/m-K	4.0674×10^{-6} BTU/ft-s-^oR
$\bar{R}T_r/Mg_r$	$8.434\ 515\ 6 \times 10^3$ m	$2.767\ 210\ 65 \times 10^4$ ft

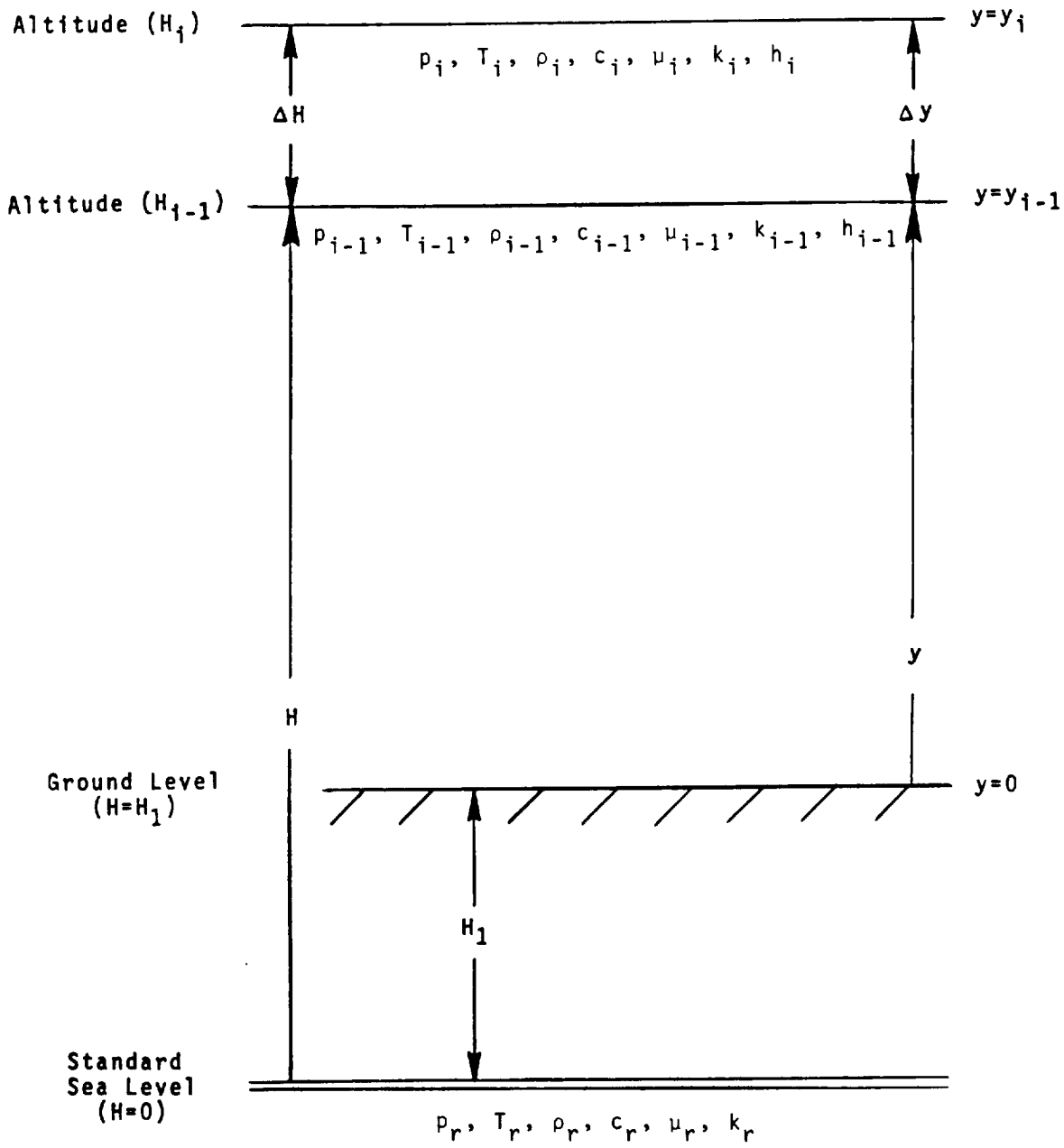

Figure 1.- Dimensional and dimensionless altitudes for the atmospheric model.

2.2 GEOMETRY MODULE

INTRODUCTION

The calculation of aircraft noise requires a complete spatial and temporal definition of the noise propagation paths. The geometric relationship between the noise source components and the observers must be defined for the duration of the aircraft flight. The aircraft position is given, either from input or from the Flight Dynamics Module (FLI), in an Earth-fixed coordinate system as a function of time. The aircraft orientation is also given with respect to the Earth-fixed coordinate system in terms of Euler angles. These coordinate system conventions are described in detail in reference 1 and in other standard texts on aerodynamics of the airplane. Although the Flight Dynamics Module uses two-degree-of-freedom equations, the Geometry Module will be valid for six degrees of freedom so that ANOPP may be extended to the more general case of three-dimensional flight paths by input of a three-dimensional path or by addition of a more general flight module.

Observer positions are given as input to the program in an Earth-fixed coordinate system. The task of the Geometry Module is to find the vectors from the noise source on the aircraft to the observers and to express these vectors in terms of a coordinate system at the aircraft. These vectors are functions of time because the noise source moves with the aircraft.

It is not desirable to make noise predictions for each observer at all times during the flight. An observer close to the point of brake release will have large values of noise at different times than the observer several miles down the flight track. Noise at an observer which is more than 20 dB below the maximum value is of little interest in most cases. Consequently, a significant savings in computation results when the times for which the noise is certain to be negligible are eliminated in advance.

The noise emitted from an aircraft takes a finite time to reach the observer. Since noise predictions are desired at evenly spaced values of the reception time, the reception times are treated as an independent variable and a set of flight emission times are determined. The aircraft position and orientation are then found at these emission times for each observer. Intermediate reception time points are selected at sufficiently small increments to ensure that the changes in noise characteristics between successive time points are not large.

This module produces a table of the emission time, distance, polar directivity angle, azimuthal directivity angle, and elevation angle to each observer as a function of reception time and source coordinate system. This table is used by the Propagation Module (PRO) for the computation of propagation effects.

SYMBOLS

A_w	reference area of aircraft, m^2 (ft^2)
c	speed of sound, m/s (ft/s)
ΔdB	limiting noise level, down from peak level
g_r	standard acceleration due to gravity, m/s^2 (ft/s^2)
h	observer height, m (ft)
$\vec{i},\vec{j},\vec{k}$	base vectors
k	constant
M	molecular weight of air
m_o	initial mass of aircraft
(n_1,n_2,n_3)	direction cosines
o	observer index
R	universal gas constant, $m^2/K\text{-}s^2$ ($ft^2/^oR\text{-}s^2$)
r	distance, m (ft)
s	source coordinate system name
T	transformation matrix
T_r	standard sea level temperature, K (^oR)
t	time, s
Δt	reception time increment, s
(x,y,z)	position coordinates, m (ft)
y	altitude, re RT_r/Mg_r
γ	elevation angle, deg
θ	polar directivity angle, deg
$\Delta\theta$	polar directivity angle limit, deg
ρ	density, kg/m^3 ($slugs/ft^3$)
ϕ	azimuthal directivity angle, deg
Ψ,Θ,Φ	Euler angles, deg

Subscripts:

a	aircraft or Earth-fixed flight axes
i	time index
m	local minimum
min	global minimum
o	observer or Earth-fixed observer axes
r	standard sea level
s	source coordinate system
w	wind axis

Superscripts:

*	dimensionless value
-	average

INPUT

Input to the Geometry Module consists of the aircraft body axis position and orientation vector. It is understood that these data are given with respect to the Earth-fixed flight axis system of figure 1. The orientation vector is taken to be the set of three Euler angles described in reference 1. The average speed of sound as a function of altitude is obtained from the atmospheric properties table. There may be several noise source axis systems located within the aircraft body system. The orientation of these systems are given as input with respect to the body axis system. All source coordinate systems are assumed to have the same origin. Observer positions are given in the Earth-fixed observer system shown in figure 1. Table I gives the recommended ranges and the default values for the input parameters.

Input Constants

A_w	reference area of aircraft, m^2 (ft^2)
ΔdB	limiting noise level, down from peak level
k	constant
m_o	reference mass of aircraft, kg (slugs)
t_1	initial time, s
t_n	final time, s

Δt reception time increment, s

$\Delta\theta$ maximum polar directivity angle limit, deg

Flight Dynamics Table

t flight time, s

$\begin{bmatrix} x_a(t) \\ y_a(t) \\ z_a(t) \end{bmatrix}$ aircraft body coordinates, m (ft)

$\begin{bmatrix} \Psi_a(t) \\ \Theta_a(t) \\ \Phi_a(t) \end{bmatrix}$ aircraft body Euler angles, deg

$\begin{bmatrix} \Psi_w(t) \\ \Theta_w(t) \\ \Phi_w(t) \end{bmatrix}$ aircraft wind axis Euler angles, deg

Observer Table

o observer index

$\begin{bmatrix} x_o(o) \\ y_o(o) \\ z_o(o) \end{bmatrix}$ observer coordinates, m (ft)

Source Coordinate System Table

s source system name

$\begin{bmatrix} \Psi_s(s) \\ \Theta_s(s) \\ \Phi_s(s) \end{bmatrix}$ source Euler angles, relative to body axis, deg

Atmospheric Properties Table

y	altitude, re RT_r/Mg_r
$\bar{c}^*(y)$	average speed of sound, re c_r

OUTPUT

Output from the Geometry Module is the vectors from the source to the observer. These are expressed as spherical components in the source coordinate system. In addition, the elevation angle from the observer to the source is provided for use in the Propagation Module.

Geometry Table

t_o	reception time, s
o	observer index
s	source coordinate system name
$t_e(t_o,o,s)$	emission time, s
$r(t_o,o,s)$	distance, m (ft)
$\theta(t_o,o,s)$	polar directivity angle, deg
$\phi(t_o,o,s)$	azimuthal directivity angle, deg
$\gamma(t_o,o,s)$	elevation angle, deg

METHOD

Each observer has an associated time segment during which the emitted noise dominates over other times during the flight. This time segment (or segments) is to be estimated based on relative distance to the observer. This estimation can be done by scanning the vector from the source for each observer as a function of time, recording its minimum magnitude, and then eliminating those times for which the magnitude is greater than a fixed constant, say 10, times the minimum value. This operation will define a limited time slice for each observer and further computation of noise for that observer may be made within that time slice only.

Elimination of Excess Data

First, the flight times from the flight dynamics table are examined and all times less than the initial time t_1 and greater than the final time t_n are discarded. In addition, if the points are closer together than the characteristic flight time increment Δt_f given as

$$\Delta t_f = \frac{km_o}{\rho_r c_r A_w} \tag{1}$$

the extra points are discarded. The constant k in equation (1) is a user parameter.

Supplementing Sparse Data

Input to the Geometry Module may consist of data at widely spaced time points. If the time points are spaced at time intervals greater than the input interval limit Δt, the aircraft body coordinates, body Euler angles, and wind axis Euler angles are interpolated with a cubic spline to produce intermediate values spaced at intervals less than Δt.

Location of Minimum Distance

The computations now proceed separately for each observer, and the process continues until all observers have been completed. The observer coordinates are transformed into the Earth-fixed flight coordinate system by the axis reflection transformation:

$$\begin{bmatrix} x_o \\ y_o \\ z_o \end{bmatrix} = \begin{bmatrix} 1 & 0 & 0 \\ 0 & -1 & 0 \\ 0 & 0 & -1 \end{bmatrix} \begin{bmatrix} x_o \\ y_o \\ h \end{bmatrix} \tag{2}$$

The position of the observer relative to the aircraft is then

$$\begin{bmatrix} x_{oa}(t) \\ y_{oa}(t) \\ z_{oa}(t) \end{bmatrix} = \begin{bmatrix} x_o \\ y_o \\ z_o \end{bmatrix} - \begin{bmatrix} x_a(t) \\ y_a(t) \\ z_a(t) \end{bmatrix} \tag{3}$$

Let the flight times be designated by an index i which ranges from 1 to I and let the observer vector $\vec{r}(t_i) = \vec{r}_i$ be

$$\vec{r}_i = \vec{i}x_{oa}(t_i) + \vec{j}y_{oa}(t_i) + \vec{k}z_{oa}(t_i) \qquad (i = 1, 2, \ldots, I) \tag{4}$$

In addition define a discrete path vector by

$$\vec{s}_i = \vec{r}_i - \vec{r}_{i+1} \qquad (i = 1, 2, \ldots, I-1) \tag{5}$$

These vectors, shown in figure 2, are used to find a minimum distance to the observer and the time at which the minimum occurs.

To find the minimum distance, the first segment is checked to see if the projection of $\vec{r}_i$ on $\vec{s}_i$, that is, point P in figure 2(b), lies within the length of $\vec{s}_i$. This is expressed by

$$0 \leq \vec{n}_{r,i} \cdot \vec{n}_{s,i} \leq 1 \tag{6}$$

where $\vec{n}_r$ and $\vec{n}_s$ are unit vectors in the direction of $\vec{r}$ and $\vec{s}$. If this condition is not satisfied, then there is no minimum distance within the segment. The equality is included in order that the case of a minimum at the end point will be acceptable. For each segment which passes the test of equation (6), a local minimum and time is computed by

$$\vec{r}_{m,i} = \vec{n}_{s,i} \times \left(\vec{r}_i \times \vec{n}_{s,i}\right) \tag{7}$$

$$t_{m,i} = t_i + \left(\vec{n}_{r,i} \cdot \vec{n}_{s,i}\right)\left(t_{i+1} - t_i\right) \tag{8}$$

For each local minimum, a time point $t_{m,i}$ is added to the aircraft position, aircraft orientation, and observer vector data by linear interpolation on time.

Finally, the set of values $r_{m,i}$ is examined to select the global minimum. Then the global minimum distance $r_{min}(o)$ and time $t_{min}(o)$ are recorded for the observer. In the event that there is no local minimum, then there can be no global minimum so that the program issues a warning message.

Determination of Time Segments

The maximum distance of interest is given by

$$r_{max} = 10^{\Delta dB/20} r_{min} \tag{9}$$

on the basis that spherical spreading alone will give a relative noise reduction of ΔdB in comparison to the noise at the closest point of approach. It is desired to find those points r_i which satisfy the condition

$$r_{min} \leq r_i \leq r_{max} \tag{10}$$

and their associated times. This condition is depicted in figure 3. The process is one of examining the magnitudes r_i to find the starting time

$$r_i \geq r(t_s) = r_{max} > r_{i+1} \tag{10a}$$

and the ending time

$$r_j < r(t_f) = r_{max} \leq r_{j+1} \tag{10b}$$

as depicted in figure 4. Note that the set of values $\vec{r}_i$ must include the minimum distance vector and at least two other vectors, as depicted in figure 5, in order for both equation (10a) and (10b) to have possible solutions.

In order to find the starting and finishing times, each segment is examined in turn to find if it contains a limiting point ℓ. As shown in figure 6, the equation for the end point can be written as

$$\left| a_i \vec{s}_i - \vec{r}_i \right| = r_{max} \tag{11}$$

where

$$a_i = \frac{t_\ell - t_i}{t_{i+1} - t_i} \qquad (i = 1, 2, \ldots, I-1) \tag{12}$$

and t_ℓ may be either a start or an end time. Equation (11) gives

$$a_i = \frac{\left(\vec{s}_i \vec{r}_i\right) \pm \sqrt{\left(\vec{s}_i \vec{r}_i\right)^2 - s_i^2\left(r_i^2 - r_{max}^2\right)}}{s_i^2} \tag{13}$$

For the first segment, the condition is added that $a_1 < 1$. This means, as depicted in figure 6(a), that the circle with radius r_{max} intersects the vector $\vec{s}_1$ or its extension behind time t_1. If $a < 0$, then the starting time is before t_1 as shown by equation (12). For all intermediate segments, it is required that

$$0 \leq a_i \leq 1 \qquad (i = 2, 3, \ldots, I-2) \tag{14}$$

as shown in figure 6(b). It is possible that both roots will occur and define a complete time segment as shown in figure 6(a); however, it will generally turn out that only one root of equation (13) satisfies the limits in equation (14). For the final time, the condition $0 < \vec{a}$ allows the final time to lie on the extension of the last path vector $\vec{s}_{I-1}$.

Limit on Directivity Variation

The directivity angle between the path vector $\vec{s}$ and the observer vector $\vec{r}$ must be limited to a change $\Delta\theta$ within each time step.

The directivity angle is

$$\theta_i = \text{Arcsin} \left| \vec{n}_{r,i} \times \vec{n}_{s,i} \right| \tag{15}$$

and

$$\Delta\theta_i = \theta_{i+1} - \theta_i \tag{16}$$

If $\Delta\theta_i > \Delta\theta$, then intermediate time points must be added.

Output Computation

The direction cosines from the source to the observer in the Earth-fixed flight coordinate system are now computed. The position of the observer $\vec{r}$ was computed by equation (3). Then the direction cosines are given by

$$\begin{bmatrix} n_{r,1} \\ n_{r,2} \\ n_{r,3} \end{bmatrix} = \vec{r}/r \tag{17}$$

The average speed of sound is known as a function of altitude y from the Atmospheric Properties Table. This variable is converted to be a function of the flight time by setting

$$y(t) = \frac{Mg_r \left[r\ n_{r,3}(t) \right]}{RT_r} \tag{18}$$

and

$$\bar{c}(t) = c_r c(y)^* \tag{19}$$

where $n_{r,3}$ is the direction cosine computed by equation (17). The value of reception time t_o that corresponds to each value of t_f can now be computed by

$$t_o = t_f + r/\bar{c}(t) \tag{20}$$

and a table of t_f as a function of t_o is created. The reception times are naturally grouped into segments by the time segments previously defined. The reception times found by this process will naturally occur at uneven intervals.

The elevation angle γ from the observer to the source can now be computed as

$$\gamma = \text{Arcsin } n_{r,3} \tag{21}$$

where $n_{r,3}$ is the direction cosine.

For computation of the directivity angles, the direction cosines of equation (17) must be rotated to the source coordinate system. This transformation is accomplished with the use of Euler angles for each coordinate system as defined in figure 7.

$$\begin{bmatrix} n_{r,1} \\ n_{r,2} \\ n_{r,3} \end{bmatrix}_s = \left[T(\Phi_s)\right]\left[T(\Theta_s)\right]\left[T(\Psi_s)\right]\begin{bmatrix} n_{r,1} \\ n_{r,2} \\ n_{r,3} \end{bmatrix}_a \tag{22}$$

where

$$T(\Psi) = \begin{bmatrix} \cos\Psi & \sin\Psi & 0 \\ -\sin\Psi & \cos\Psi & 0 \\ 0 & 0 & 1 \end{bmatrix} \tag{23}$$

$$T(\Theta) = \begin{bmatrix} \cos\Theta & 0 & -\sin\Theta \\ 0 & 1 & 0 \\ \sin\Theta & 0 & \cos\Theta \end{bmatrix} \tag{24}$$

$$T(\Phi) = \begin{bmatrix} 1 & 0 & 0 \\ 0 & \cos\Phi & \sin\Phi \\ 0 & -\sin\Phi & \cos\Phi \end{bmatrix} \tag{25}$$

Then, the polar directivity angle θ is given by

$$\theta(t_o,o,s) = \text{Arccos}\left(n_{r,1}\right)_s \tag{26}$$

and the azimuthal directivity angle ϕ is given by

$$\phi(t_o,o,s) = \text{Arctan}\left(n_{r,2}/n_{r,3}\right)_s \tag{27}$$

The preceding procedure is repeated until the outputs for all reception times, time segments, observers, and sources have been computed and the geometry table is complete. The aircraft body axes and wind axes are always used for source coordinate systems. Additional source coordinate systems may be provided by the user.

REFERENCE

1. Etkin, Bernard: Dynamics of Atmospheric Flight. John Wiley & Sons, Inc., c.1972.

TABLE I.- RANGE AND DEFAULT VALUES OF INPUT PARAMETERS

Input parameter	Minimum	Default	Maximum
A_w, m^2	1	1	1×10^4
ΔdB	10	20	30
k	0.1	1	10
m_o, kg	1	416.8	1×10^6
t_l, s	0	0	
t_n, s		1×10^5	1×10^5
Δt, s	0.1	0.5	2.0
$\Delta\theta$, deg	5	10	20

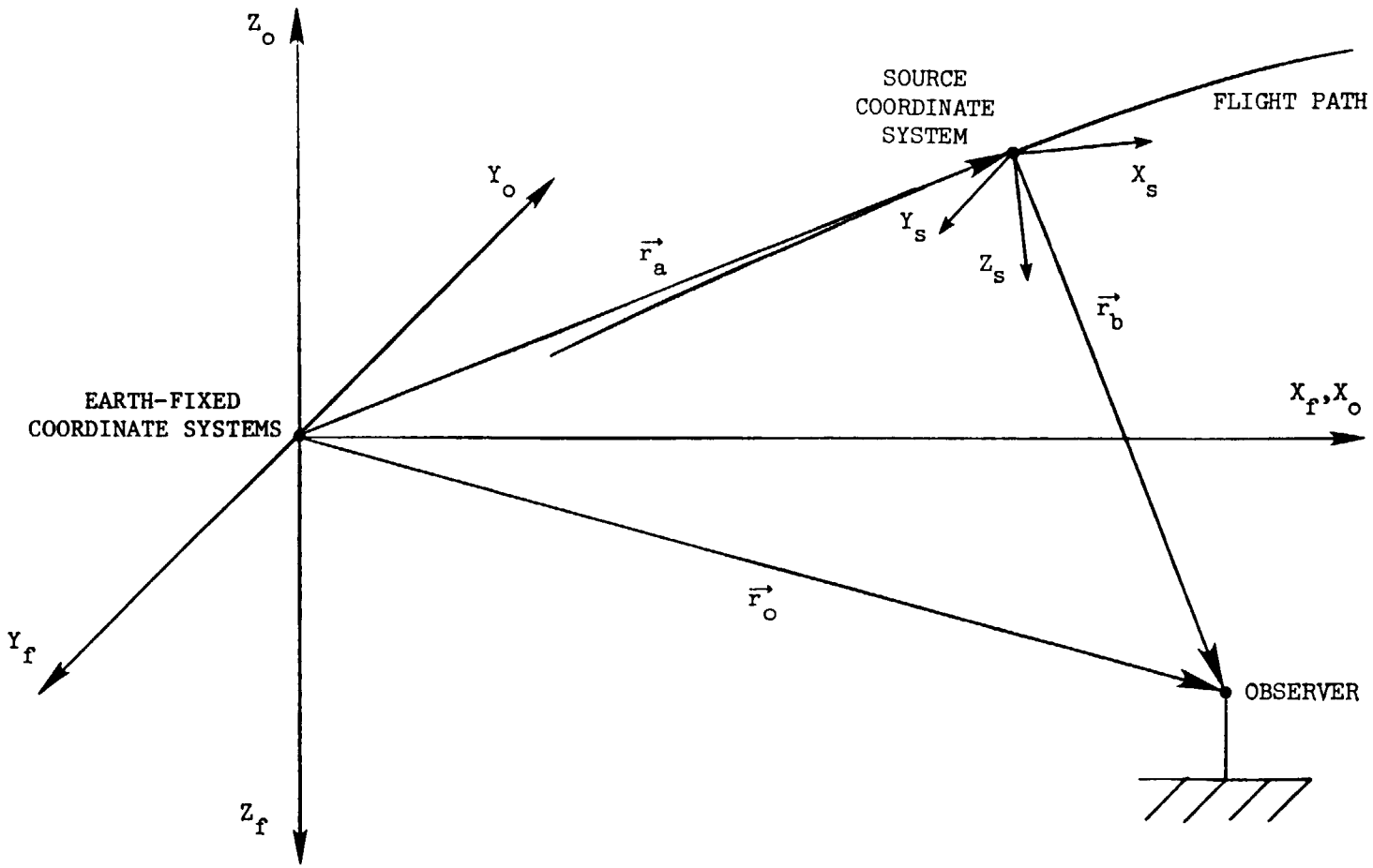

Figure 1.- Coordinate system definitions for description of source to observer geometry.

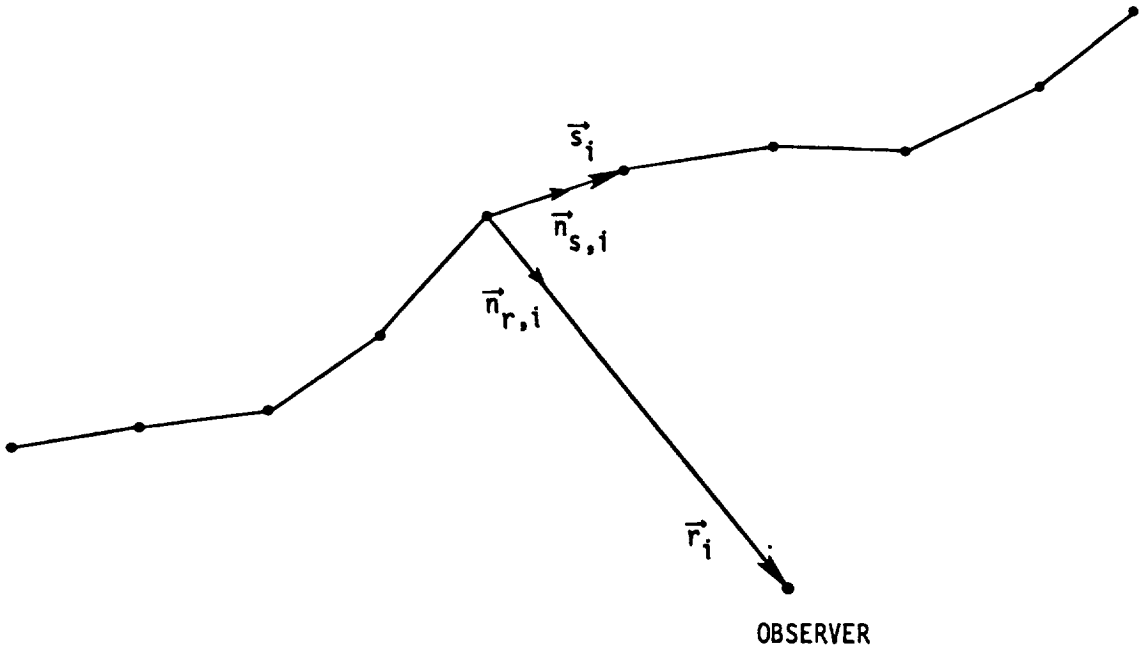

(a) Discrete representation of flight path.

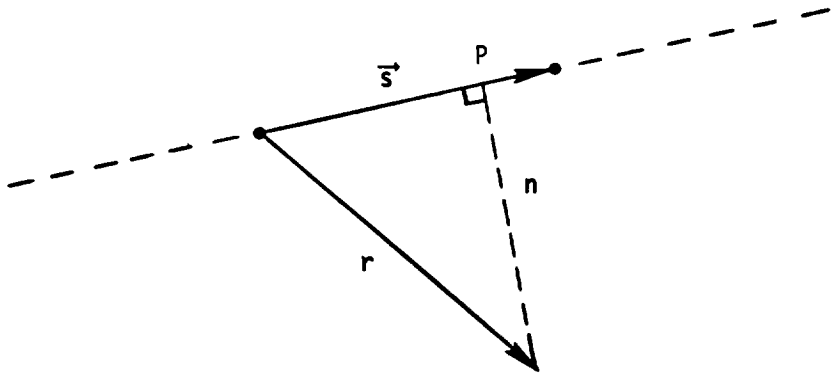

(b) Conditions for minimum distance in path segment.

Figure 2.- Location of minimum distance.

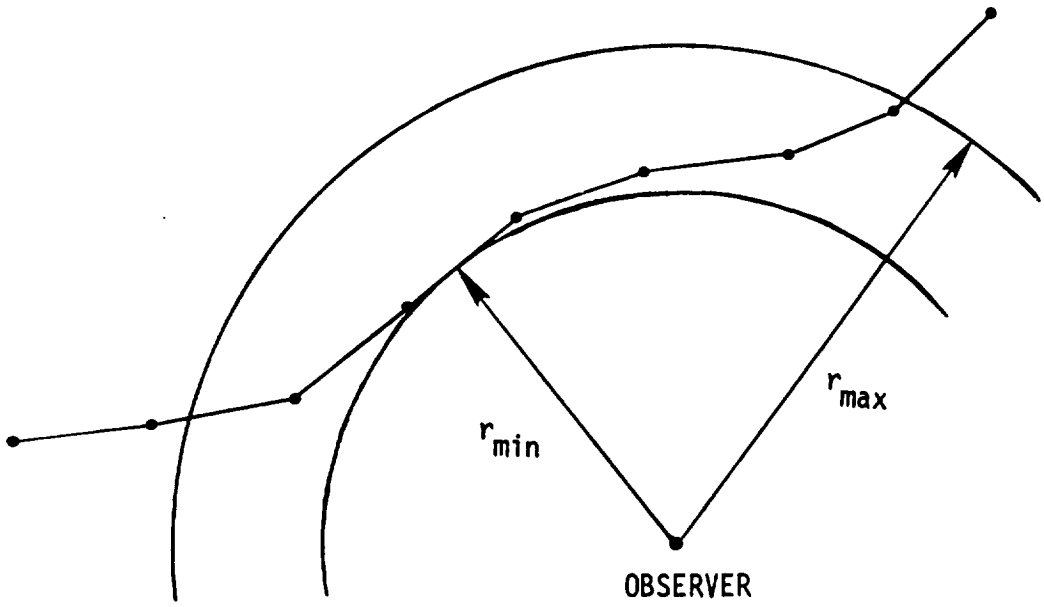

Figure 3.- Determination of time segments for observer.

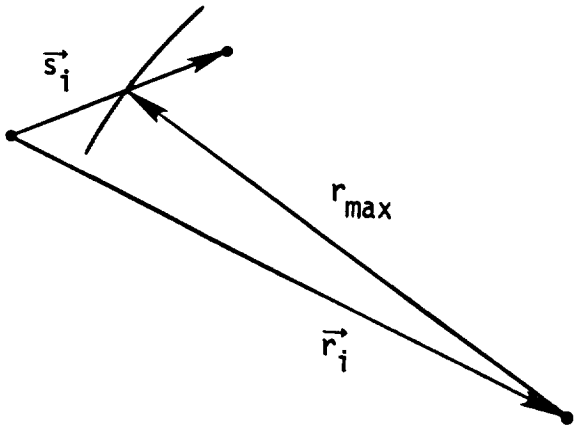

(a) Starting time.

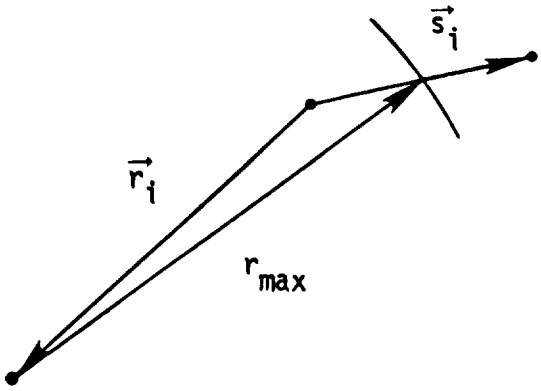

(b) Ending time.

Figure 4.- Limit points on time segments.

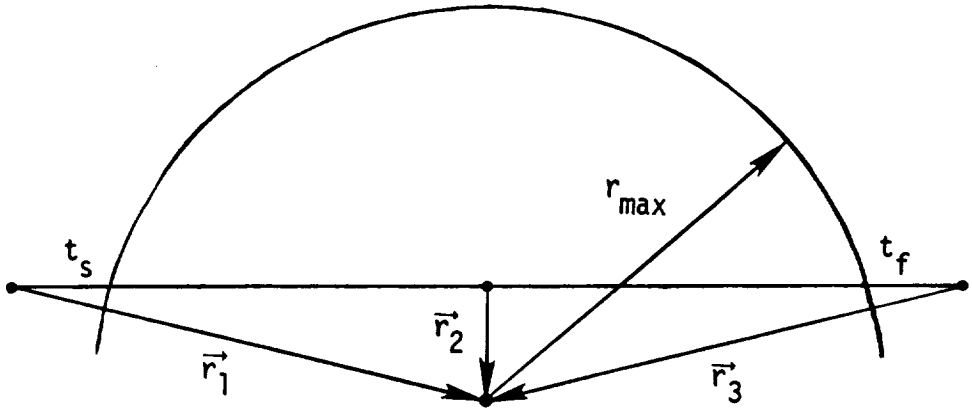

Figure 5.- Minimum set of three vectors for determination of single time segment.

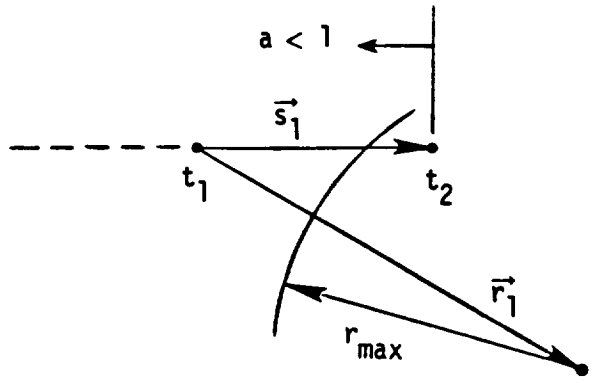

(a) First segment.

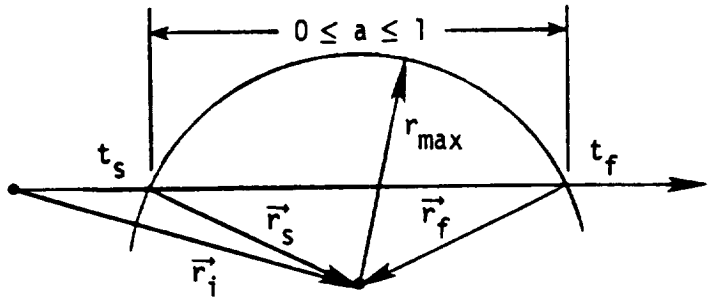

(b) Intermediate segment.

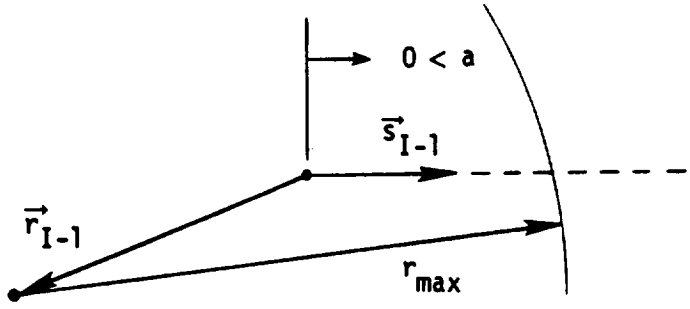

(c) Final segment.

Figure 6.- Solution for starting and finishing times for time segments.

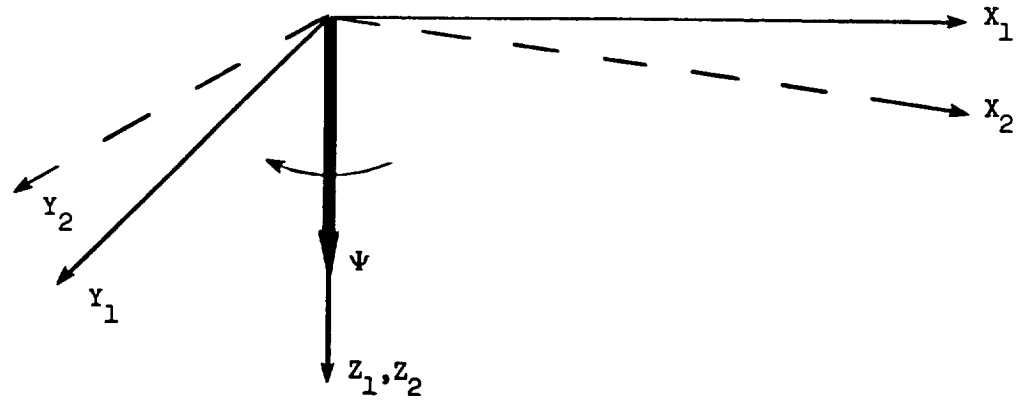

(a) Azimuth.

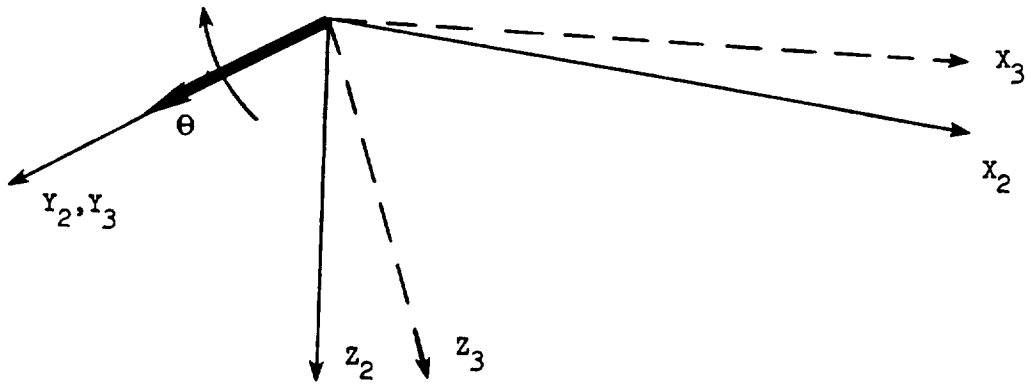

(b) Elevation.

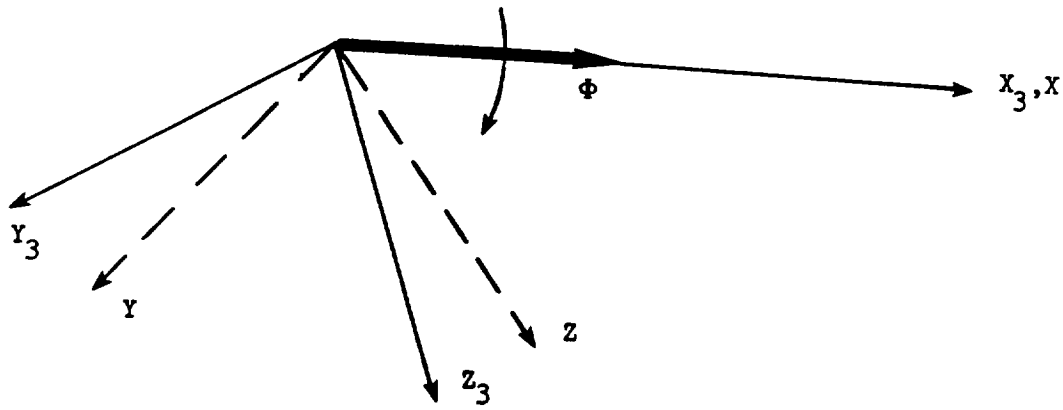

(c) Bank.

Figure 7.- Definition of Euler angles.

2.3 FLIGHT DYNAMICS MODULE

INTRODUCTION

Accurate prediction of the noise produced by an aircraft in flight requires a detailed knowledge of the aircraft position as a function of time. The dynamic behavior of any aircraft is a complex problem. A complete description of the problem requires the solution of six ordinary differential equations for the three force components and the three moment components in three-dimensional space. The six unknowns for this problem are the three position coordinates and the three attitude coordinates (Euler angles) of the aircraft. This theory can be found in typical textbooks such as references 1 and 2.

Several approximations can be made to simplify this problem; however, each simplification reduces the generality of the description of the flight. The first simplification is to restrict the flight trajectory to two dimensions. This reduces the problem to three ordinary differential equations, two force equations and one moment equation, eliminating any consideration of yaw and roll effects. A second simplification is made by assuming that all forces act through the center of mass of the aircraft so that all moments about the lateral axis of the aircraft are zero. This assumption is valid if the aircraft is constantly maintained in a trimmed condition. The problem is now reduced to simultaneously solving two ordinary differential equations for the unknown longitudinal and vertical position of the aircraft as a function of time. These approximations are used within ANOPP for computation of the aircraft trajectory. If a different flight trajectory is required, the data can be inserted directly as a function of time.

The Flight Dynamics Module computes the two-dimensional trajectory of an aircraft as a function of time. From the module inputs of control settings, aerodynamic coefficients, engine performance, atmospheric properties, and initial/final conditions, the two force balance equations are solved for the aircraft position, attitude, and Mach number as a function of time.

SYMBOLS

A_e reference area of aircraft-engine inlet-face cross section, m^2 (ft^2)

A_w aircraft wing reference area, m^2 (ft^2)

b wing span, m (ft)

C_D aerodynamic drag coefficient, $\dfrac{D}{\frac{1}{2}\rho_a V^2 A_w}$

$C_{D,\ell g}$	landing-gear drag coefficient
C_L	aerodynamic lift coefficient, $\frac{L}{\frac{1}{2}\rho_a V^2 A_w}$
c	speed of sound, m/s (ft/s)
D	aerodynamic drag, N (lb)
F_g	ground force, N (lb)
g_r	acceleration of gravity, m/s^2 (ft/s^2)
H	Heaviside step function
h	local altitude, m (ft)
h_a	absolute humidity, percent mole fraction
$I_{\ell g}$	landing-gear position
L	aerodynamic lift, N (lb)
M	aircraft Mach number, V/c
m	aircraft mass, kg (slugs)
$\dot{m}_a$	engine air flow rate, kg/s (slugs/s)
$\dot{m}_e$	engine mass flow rate, kg/s (slugs/s)
$\dot{m}_f$	engine fuel flow rate, kg/s (slugs/s)
N	number of engines
T	thrust, N (lb)
T_r	standard sea level temperature, K ($^{\circ}R$)
t	time, s
t_e	engine specific thrust, m/s (ft/s)
V	aircraft velocity, m/s (ft/s)
W	aircraft weight, N (lb)
(x,y,z)	aircraft position in Earth-fixed coordinates, m (ft)
α	angle of attack, deg

δ_f flap control variable, deg

ε engine inclination angle, deg

Θ aircraft Euler angle, deg

θ inclination of flight path with respect to horizontal, deg

μ dynamic viscosity, kg/m-s (slugs/ft-s)

π power setting

ρ air density, kg/m^3 ($slugs/m^3$)

τ coefficient of rolling friction

Subscripts:

a ambient

b body axis

e engine

n final limit

o break release

r standard sea level

1 initial value

Superscript:

* dimensionless value

INPUT

The amount of information required to define a flight trajectory is extensive because of the complex nature of the problem. Description of the aircraft geometry must be provided. Initial and final conditions are necessary to solve the differential equations and to terminate the solution in a finite time. A control variable table defines the aircraft attitude and engine setting. An aerodynamic coefficient table and an engine performance table describe the characteristics of the airframe and engine. Finally, the atmosphere is described by an atmospheric properties table. Default values for the input parameters are given in table I.

Input Constant

ΔV maximum velocity increment for engine variable table, m/s (ft/s)

Aircraft Configuration Table

A_w	aircraft wing reference area, m^2 (ft^2)
A_e	engine inlet reference area, m^2 (ft^2)
b	wing span, m (ft)
m_o	fully loaded reference mass, kg (slugs)
N	number of engines
h_o	altitude at break release, m (ft)
τ	coefficient of rolling friction
ε_e	engine inclination angle for each engine, deg

Initial/Final Conditions Table

m_1	initial mass, kg (slugs)
t_1	initial time, s
V_1	initial velocity, m/s (ft/s)
x_1	initial distance from origin, m (ft)
y_1	lateral position, m (ft)
h_1	initial altitude, m (ft)
θ_1	initial flight-path angle, deg
t_n	final time, s
V_n	final velocity, m/s (ft/s)
x_n	final distance from origin, m (ft)
h_n	final altitude, m (ft)

Control Variable Table

t	time, s
$\alpha(t)$	angle of attack, deg
$\delta_f(t)$	flap setting, deg

$\pi_e(t)$ power setting for each engine

$t_{\ell g}$ landing-gear retraction time, s

Aerodynamic Coefficient Table

α angle of attack, deg

δ_f flap angle, deg

h/b wing height to span ratio

$C_D(\alpha,\delta_f,h/b)$ drag coefficient

$C_L(\alpha,\delta_f,h/b)$ lift coefficient

$C_{D,\ell g}(C_L)$ landing-gear drag coefficient

Engine Performance Table

π power setting

M aircraft Mach number

$\dot{m}_a^*(M,\pi)$ air flow rate, re $\rho_a c_a A_e$

$\dot{m}_f^*(M,\pi)$ fuel flow rate, re $\rho_a c_a A_e$

$t_e^*(M,\pi)$ specific thrust, re c_a

Atmospheric Properties Table

h^* altitude, $M_a g_r h/\bar{R}T_r$

$c^*(h^*)$ speed of sound, re c_r

$\rho^*(h^*)$ density, re ρ_r

$\mu^*(h^*)$ dynamic viscosity, re μ_r

$h_a(h^*)$ absolute humidity, percent mole fraction

OUTPUT

The Flight Dynamics Module produces two tables that are used within ANOPP. The first is the flight trajectory as a function of time. The output times for this table are the ones used in integrating the differential equations. This table is expressed as a full six-degree-of-freedom array, even though the two-degree-of-freedom assumption is made, to be compatible with the Geometry Module. The second is the engine variable

table as a function of source time for use in the source parameters modules. The output times for this table are the control variable input times augmented, if necessary, to adequately define the data.

Flight Trajectory Table

t_f	flight time, s
$(x(t),y_1,z(t))$	aircraft coordinates, m (ft)
$(0,\Theta_b(t),0)$	aircraft body axis Euler angles, deg
$(0,\Theta(t),0)$	aircraft wind axis Euler angles relative to body axes, deg

Engine Variable Table

t_s	source time, s
$M(t_s)$	Mach number
$\pi_e(t_s)$	engine power settings
$\delta_f(t_s)$	flap setting, deg
$I_{\ell G}(t_s)$	landing-gear position
$\rho_a(t_s)$	ambient density, kg/m^3 (slugs/ft^3)
$c_a(t_s)$	ambient speed of sound, m/s (ft/s)
$\mu_a(t_s)$	ambient dynamic viscosity, kg/m-s (slugs/ft-s)
$h_a(t_s)$	absolute humidity, percent mole fraction

METHOD

The two-degree-of-freedom flight trajectory used by this module is governed by two ordinary differential equations. The sum of the forces along the flight path must be zero and the sum of the forces normal to the flight path must be zero. These equations are expressed as

$$F_g + L - mg_r \cos\theta + \sum_{e=1}^{N} T_e \sin(\alpha + \varepsilon_e) = mV \frac{d\theta}{dt} \tag{1}$$

and

$$-\tau F_g + \sum_{e=1}^{N} T_e \cos(\alpha + \varepsilon_e) - mg_r \sin\theta - D = m \frac{dV}{dt} \tag{2}$$

The definition of the force terms in equations (1) and (2) are shown in figure 1 for the aircraft during the ground roll and in figure 2 for the aircraft in flight. The term $V\,d\theta/dt$ in equation (1) is the centrifugal acceleration normal to the flight path and the term dV/dt is the acceleration along the flight path.

The ground force term F_g is nonzero only during the ground roll. In addition, the centrifugal acceleration and the flight-path angle θ are zero during the ground roll. Therefore, applying equation (1) during the ground roll yields

$$F_g = \begin{cases} mg_r - L - \sum_{e=1}^{N} T_e \sin(\alpha + \varepsilon_e) & (h = h_o) \\ 0 & (h > h_o) \end{cases} \tag{3}$$

where h is the local altitude. The coefficient of friction τ is a function of the landing-gear and surface characteristics. The surface is assumed to be uniform throughout the ground roll. It is further assumed that the friction force results solely from the main landing gear so that it remains constant during aircraft rotation. Since most of the aircraft weight is supported by the main gear, the error introduced is small.

The total thrust T_e for each engine is related to the specific thrust and the mass flow rates by

$$T_e = \dot{m}_e c_a t_e^*(M,\pi) \tag{4}$$

where

$$\dot{m}_e = \dot{m}_a + \dot{m}_f \tag{5}$$

The aircraft lift L and drag D is computed from the lift and drag coefficients as

$$L = \frac{1}{2}\rho_a V^2 A_w \left[C_L(\alpha,\delta_f,h/b)\right] \tag{6}$$

and

$$D = \frac{1}{2}\rho_a V^2 A_w \left[C_D(\alpha,\delta_f,h/b) + C_{D,\ell g}(C_L)\right] \tag{7}$$

In general, the lift coefficient C_L and the drag coefficient C_D are a function of angle of attack α, flap setting δ_f, and altitude h/b. Figures 3 and 4 are examples of the effect of flap setting on C_L and C_D and figures 5 and 6 are examples of the ground effect on C_L and C_D.

There is an additional source of drag $C_{D,\ell g}$ which is present when the landing gear is extended. Figure 7 demonstrates the relationship between the landing-gear drag coefficient and the lift coefficient.

The mass of the aircraft changes as a function of time due to the consumption of fuel by the engines. The rate of change of the aircraft mass as a function of time is given by

$$\frac{dm}{dt} = - \sum_{e=1}^{N} \dot{m}_f(M,\pi_e) \tag{8}$$

Finally, the position of the aircraft as a function of time in Cartesian coordinates is determined from

$$\frac{dx}{dt} = V \cos \theta \tag{9}$$

and

$$\frac{dz}{dt} = -V \cos \theta \tag{10}$$

The numerical solution of differential equations is made easier if the differential equations are expressed in dimensionless form. This scales the independent and dependent variables and prevents insignificant error terms from dominating the solution. Rewriting equations (1), (2), (3), (8), (9), and (10) in dimensionless form yields

$$Mm^* \frac{d\theta}{dt^*} = \sum_{e=1}^{N} \dot{m}_e^* \left(\frac{A_e}{A_w}\right) t_e^* \sin(\alpha + \varepsilon_e) - m^* W_o^* \cos \theta + \frac{1}{2} M^2 C_L \tag{11}$$

$$m^* \frac{dM}{dt} = \sum_{e=1}^{N} \dot{m}_e^* \left(\frac{A_e}{A_w}\right) t_e^* \cos(\alpha + \varepsilon_e) - \frac{1}{2} M^2 C_D$$

$$- m^* W_o^* \sin \theta - \tau F_g^* H(-z^*) \tag{12}$$

$$F_g^* = m^* W_o^* - \frac{1}{2} M^2 C_L - \sum_{e=1}^{N} \dot{m}_e^* \left(\frac{A_e}{A_w}\right) t_e^* \sin(\alpha + \varepsilon_e) \tag{13}$$

$$\frac{dm^*}{dt^*} = - \sum_{e=1}^{N} \left(\frac{A_e}{A_w}\right) \dot{m}_f^* \tag{14}$$

$$\dot{m}_e^* = \dot{m}_a^* + \dot{m}_f^* \tag{15}$$

$$\frac{dx^*}{dt^*} = M \cos \theta \tag{16}$$

$$\frac{dz^*}{dt^*} = -M \sin \theta \tag{17}$$

where

$$W_o^* = \frac{m_o g_r}{\rho_a c_a^2 A_w} \tag{18}$$

$$t^* = \frac{\rho_a c_a A_w}{m_o} t \tag{19}$$

$$x^* = \frac{\rho_a A_w}{m_o} x \tag{20}$$

$$z^* = \frac{\rho_a A_w}{m_o}(h_o - h) \tag{21}$$

$$m^* = m/m_o \tag{22}$$

and H is the Heaviside function

$$H(s) = \begin{cases} 1 & (s \geq 0) \\ 0 & (s < 0) \end{cases} \tag{23}$$

Other symbols in equations (11) through (17) have been previously defined. Now, all required outputs for the flight module can be computed. The aircraft body axis Euler angle Θ_b is related to the angle of attack and flight-path incidence angle by

$$\Theta_b = \alpha + \theta \tag{24}$$

and the wind axis Euler angle relative to the body axis is

$$\Theta = -\alpha \tag{25}$$

The Mach number, power setting, flap setting, and landing-gear position must be expressed in terms of the source time set, which is the input control time set augmented with each time when the velocity changes by ΔV. The quantity ΔV is a user-supplied parameter. In addition, the atmospheric properties are expressed as a function of the source time set.

REFERENCES

1. Etkin, Bernard: Dynamics of Atmospheric Flight. John Wiley & Sons, Inc., c.1972.

2. Dommasch, Daniel O.; Sherby, Sydney S.; and Connolly, Thomas F.: Airplane Aerodynamics, Fourth ed. Pitman Pub. Corp., 1967.

TABLE I.- DEFAULT VALUES OF INPUT PARAMETERS

Input parameter	Default
ΔV, m/s	30
A_w, m^2	100
A_e, m^2	$\pi/4$
b, m	20
m_o, kg	10 000
N	1
h_o, m	0.0
τ	0.01
ε_e, deg	0.0
m_l, kg	10 000
t_l, s	0.0
V_l, m/s	0.0
x_l, m	0.0
y_l, m	0.0
h_l, m	0.0
θ_l, deg	0.0
t_n, s	100
V_n, m/s	125
x_n, m	10 000
h_n, m	10 000

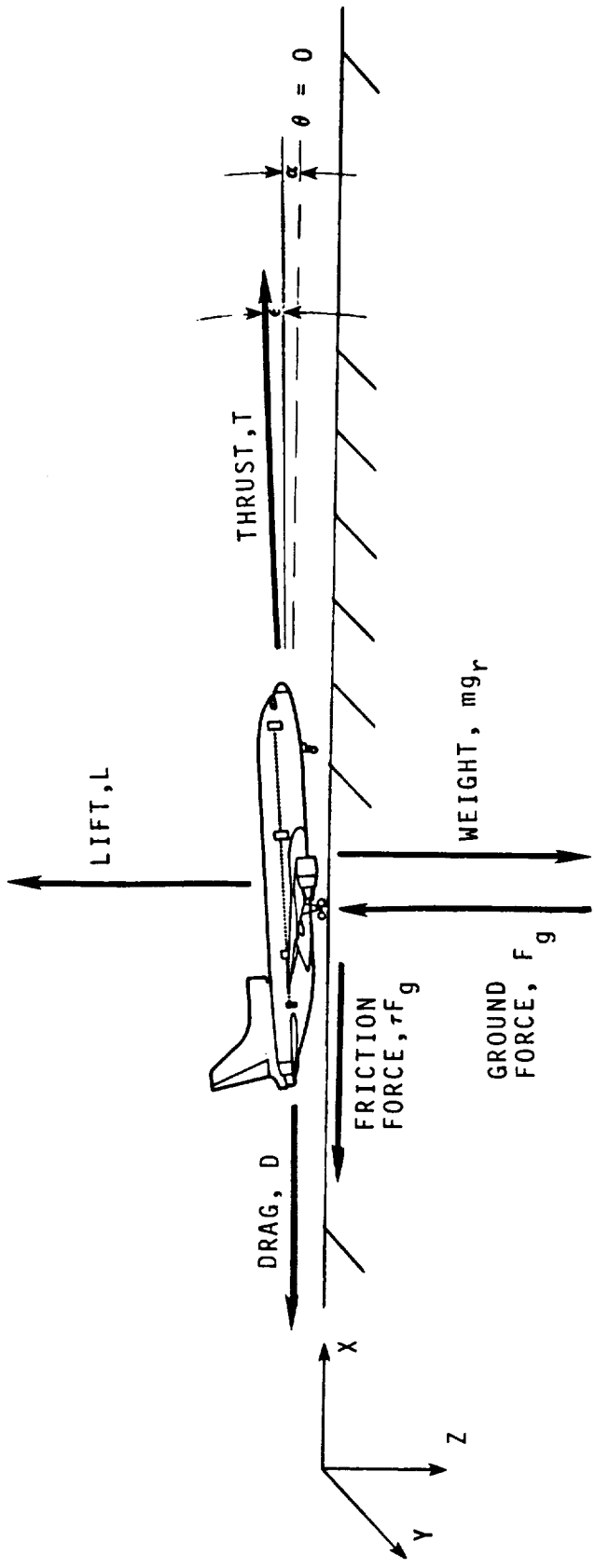

Figure 1.- Forces acting on aircraft during ground roll.

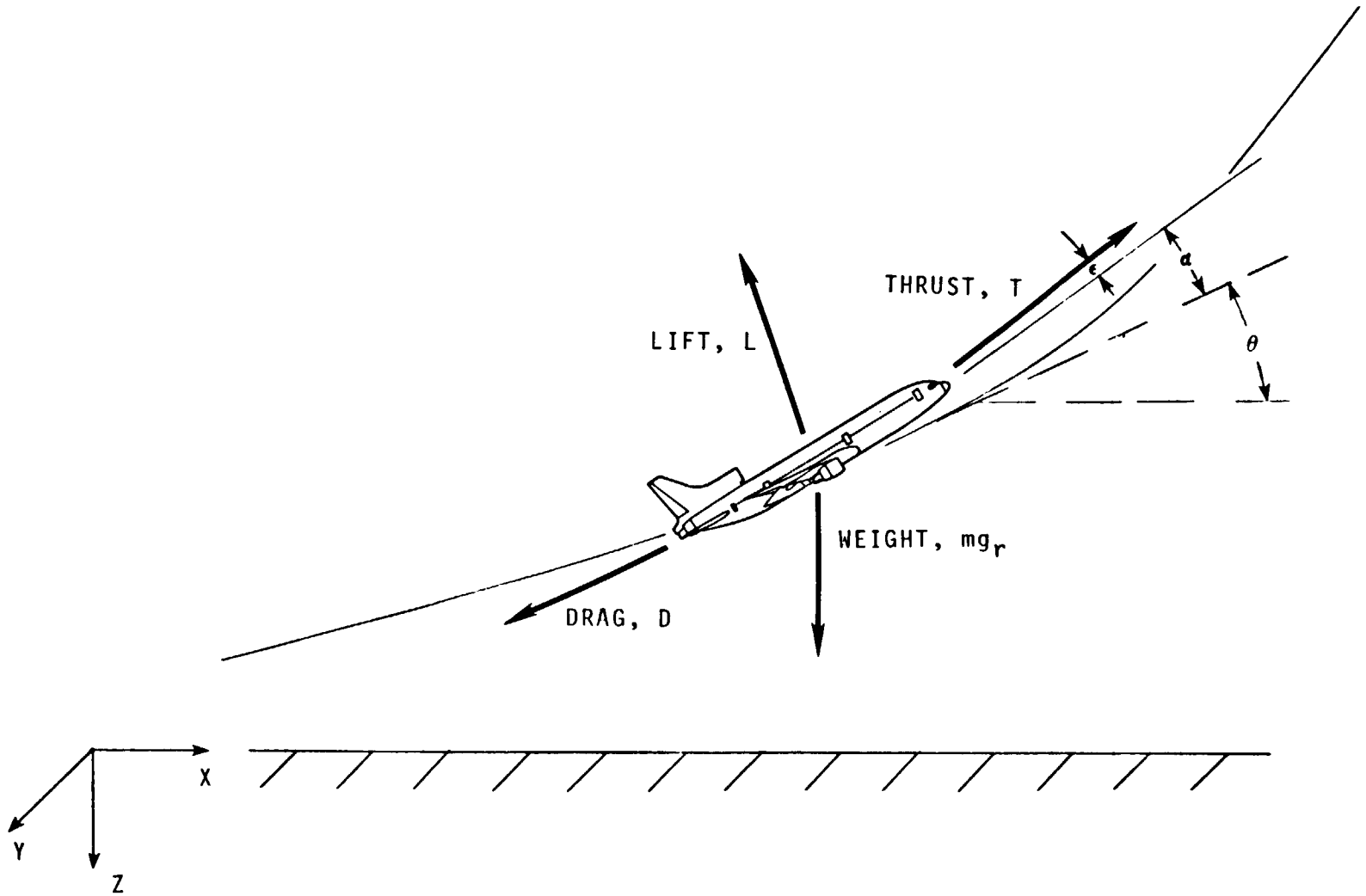

Figure 2.- Forces acting on aircraft during flight.

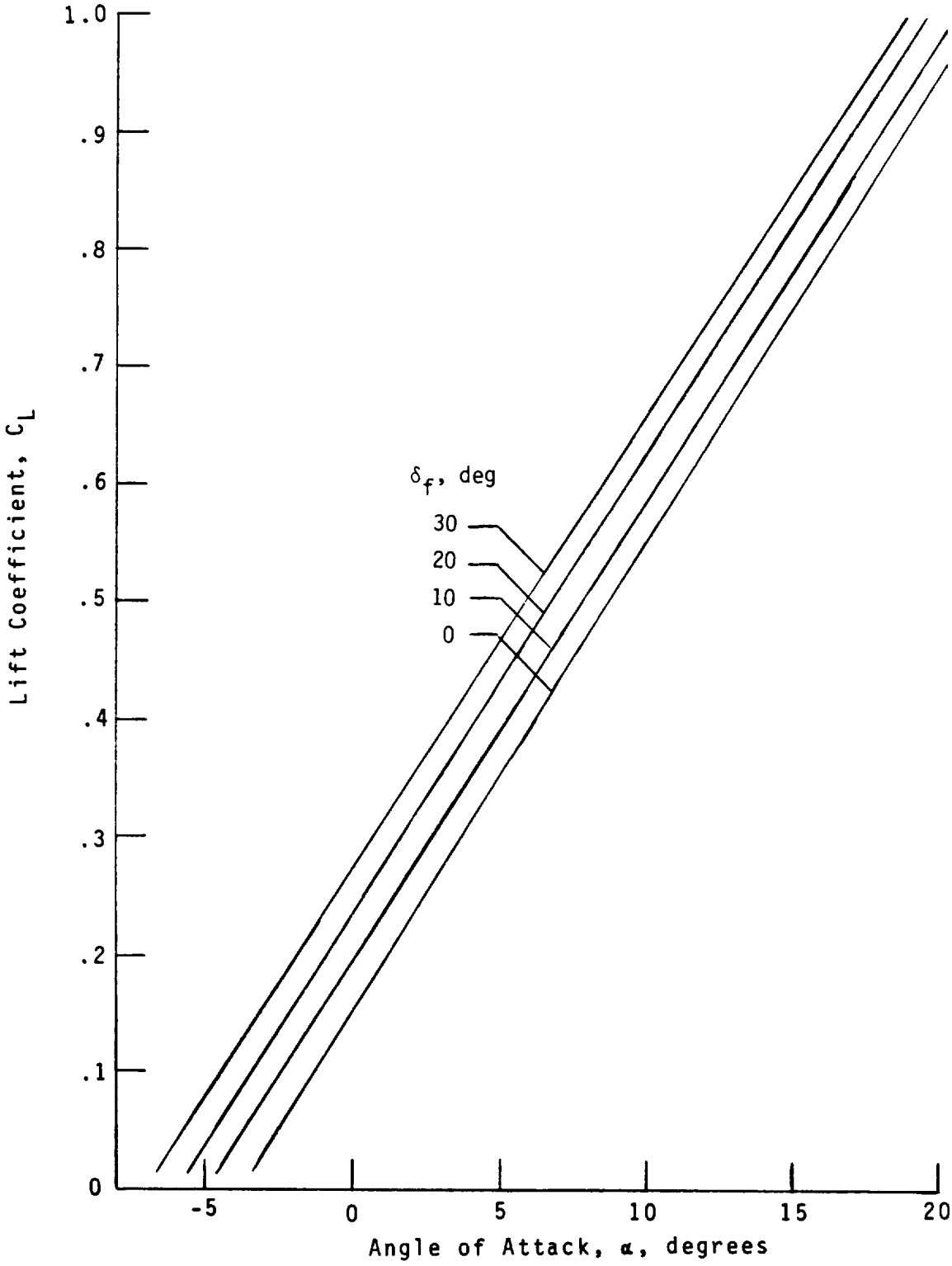

Figure 3.- Typical lift coefficient for low-speed operation with no ground effect.

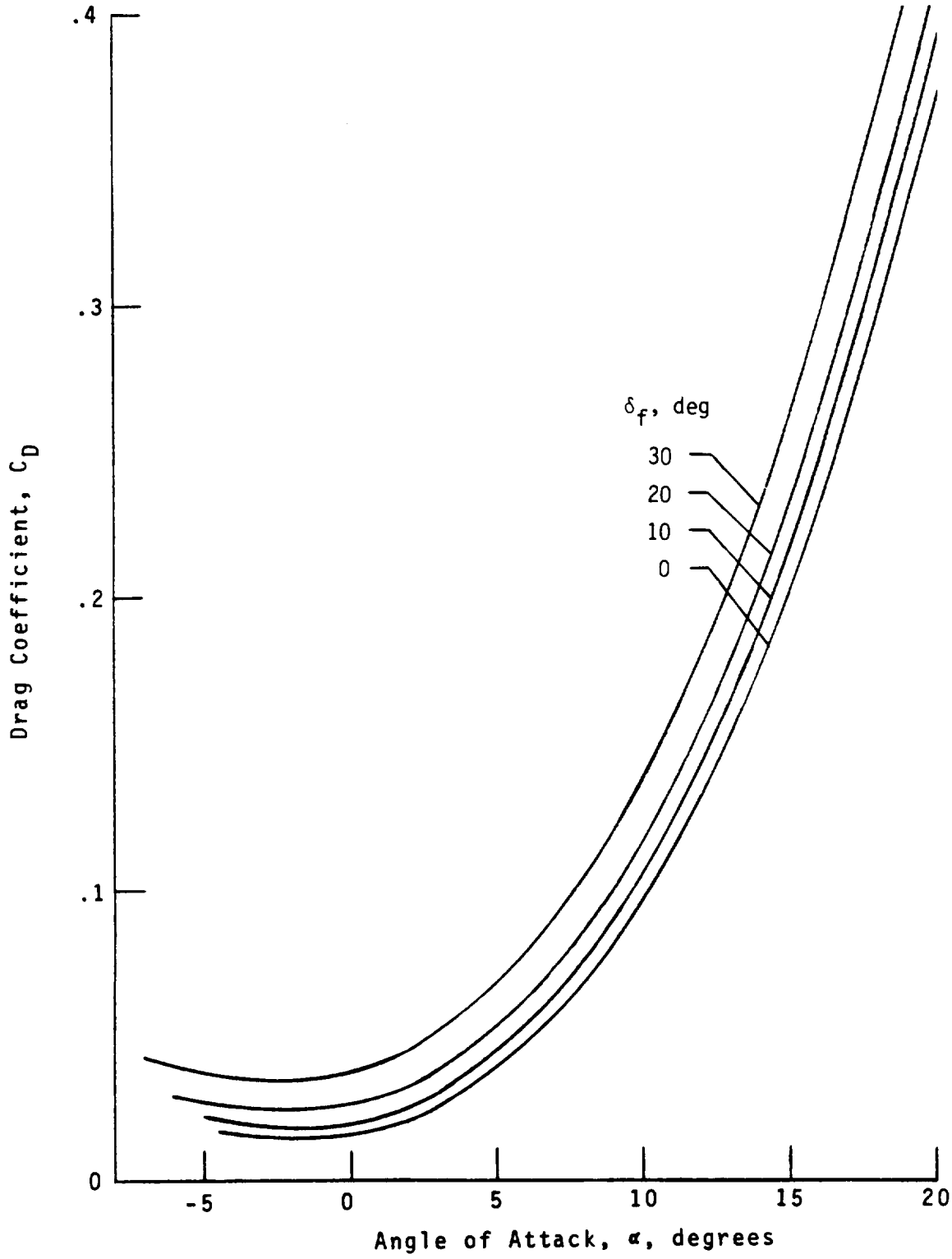

Figure 4.- Typical drag coefficient for low-speed operation with no ground effect.

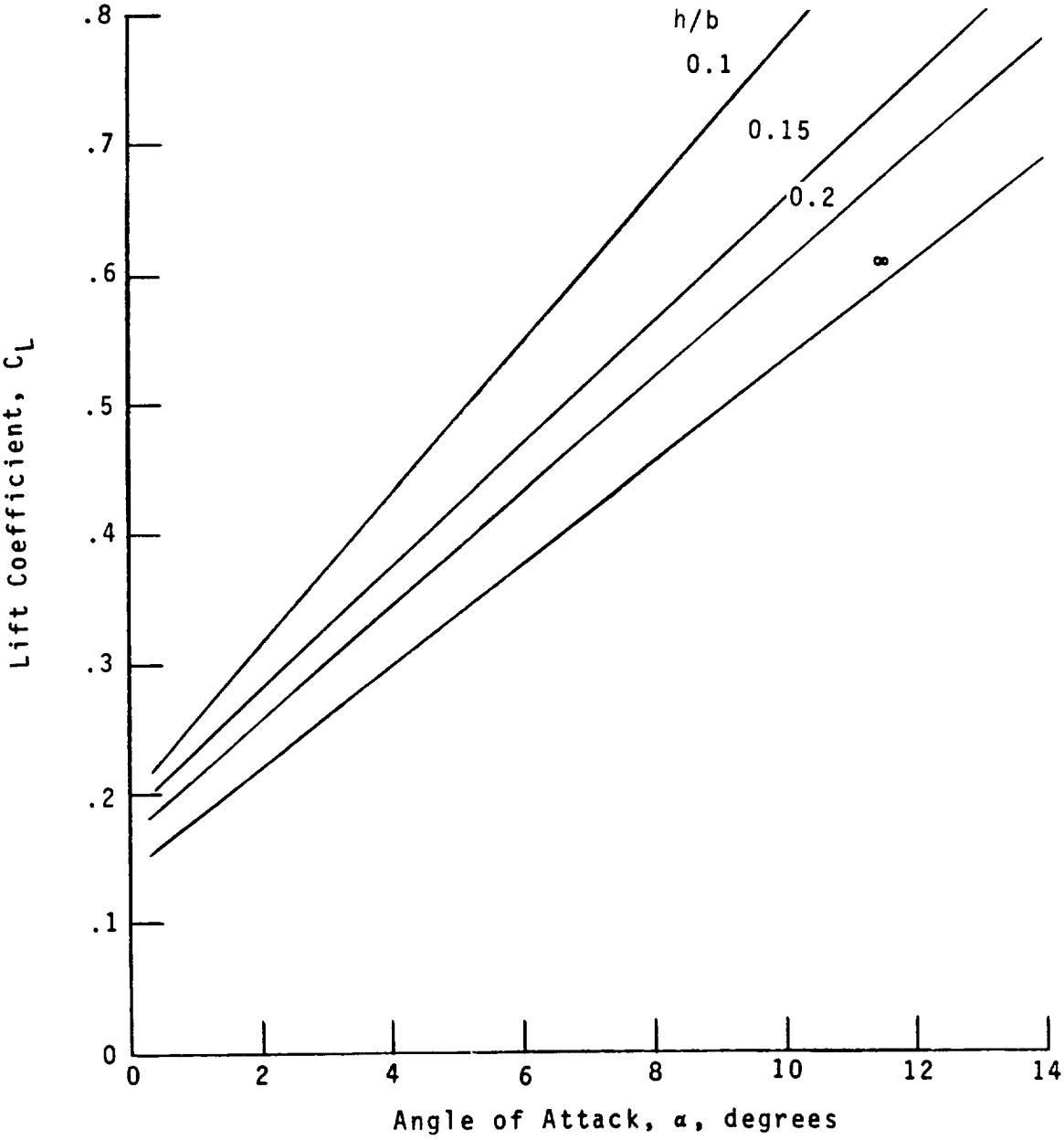

Figure 5.- Typical lift coefficient for ground effect.

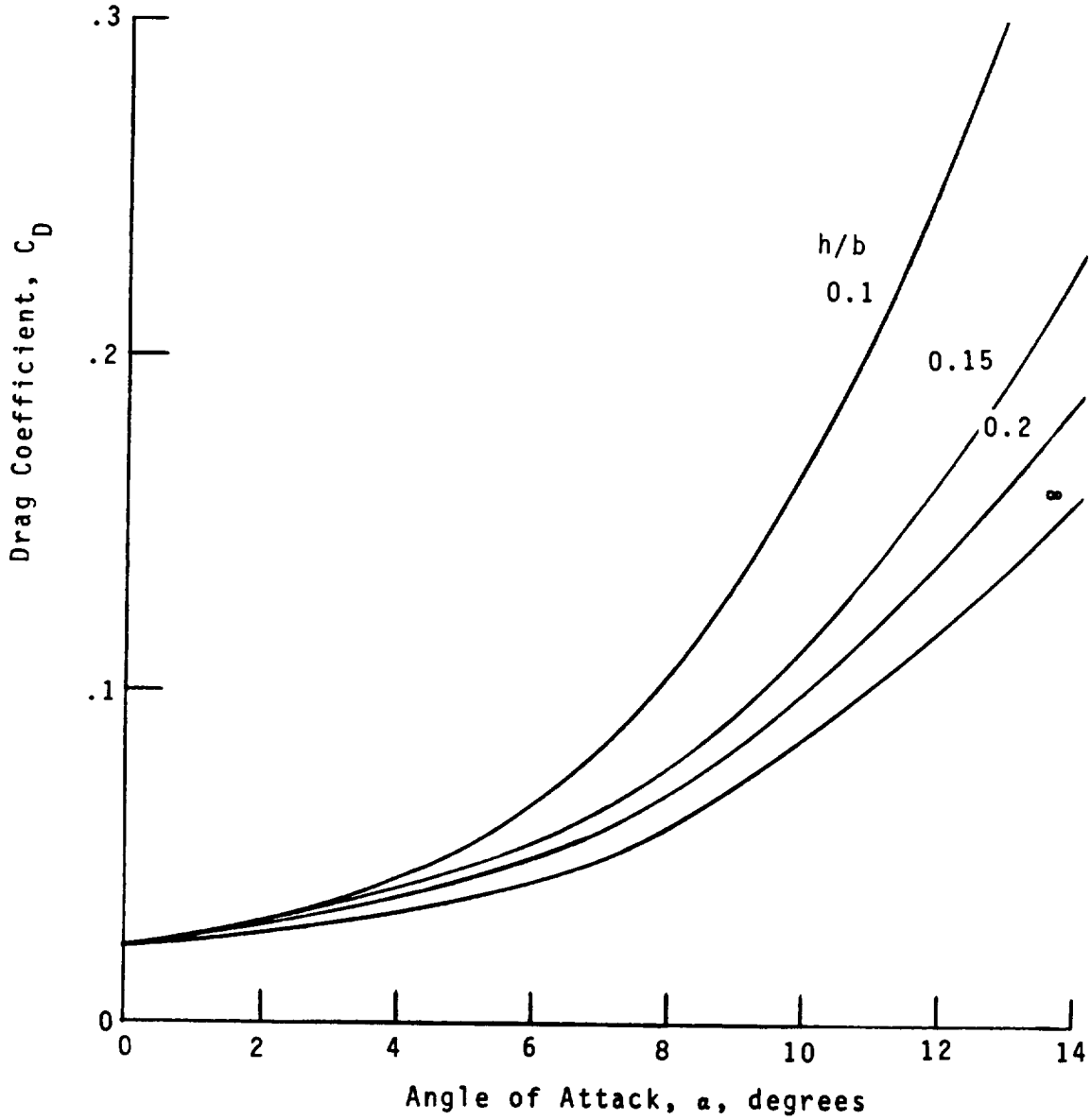

Figure 6.- Typical drag coefficient for ground effect.

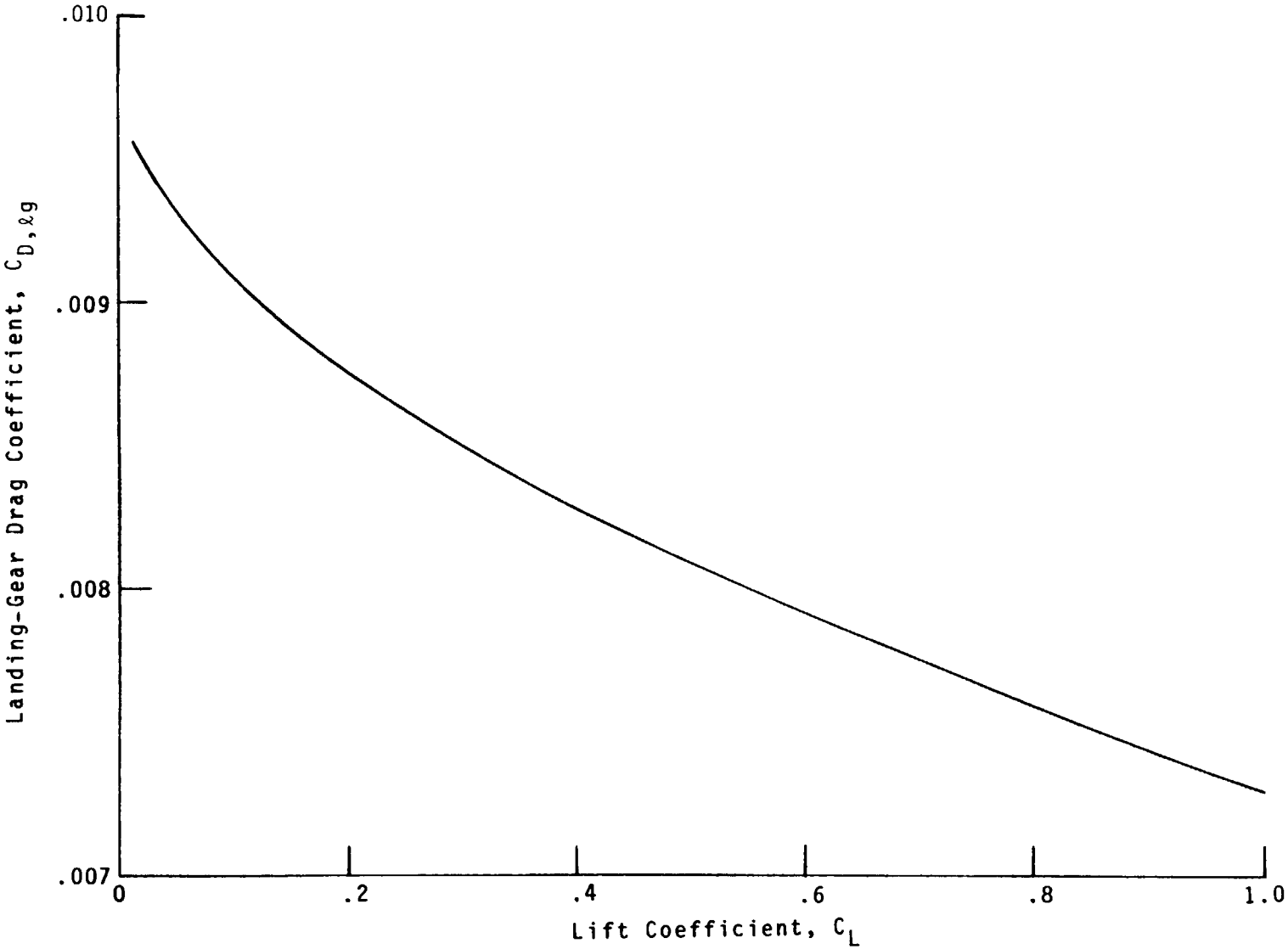

Figure 7.- Typical landing-gear drag coefficient.

2.4 Jet Takeoff (JTO) Module

John Rawls, Jr.

Lockheed Engineering & Sciences Company

Introduction

The purpose of the Jet Takeoff (JTO) Module is to calculate the position of an aircraft during takeoff. The basic takeoff profile consists of ground roll and climb as shown in figure 1. Two optional maneuvers may be appended to the basic takeoff profile. One is cutback (in engine power) which is a procedure used to reduce noise levels on the ground. The other is a steady turn which may be initiated after a steady-state solution to the equations of motion has been obtained.

An arbitrary fight profile requires a solution to nine differential equations: three force equations, three moment equations, and three equations to determine the position of the aircraft relative to an Earth-fixed coordinate system. During takeoff, these equations conveniently reduce to four first-order nonlinear differential equations which are solved numerically with a fourth-order Runge-Kutta technique. Several assumptions are made in this module to simplify the analysis. These assumptions include zero wind, a level runway, zero aerodynamic ground effects, and zero weight reduction from the burning of fuel.

Symbols

A_w	aircraft wing reference area, m^2 (ft^2)
C_D	aerodynamic drag coefficient, $\frac{D}{\frac{1}{2}\rho_a V^2 A_w}$
$C_{D.\mathrm{Lg}}$	aerodynamic drag coefficient due to landing gear
C_L	aerodynamic lift coefficient, $\frac{L}{\frac{1}{2}\rho_a V^2 A_w}$
c	speed of sound, m/s (ft/s)
D	aerodynamic drag, N (lb)
F_g	ground force, N (lb)
G	steady-state climb function
g_r	gravitational constant, 9.8066 m/s^2 (32.1741 ft/s^2)
H	altitude, m (ft)
h_a	absolute humidity, percent mole fraction
L	aerodynamic lift, N (lb)
L_{Lg}	landing gear position, Up or Down
M	molecular weight of dry air, 28.9644
M_∞	aircraft Mach number, V/c
m	aircraft mass, W/g_r, kg (slugs)
N_{eng}	number of engines
p_w	roll rate, deg/s

q_w	pitch rate, deg/s
$\overline{R}$	universal gas constant, 8314.32 $m^2/K\text{-}s^2$ (49 718.96 $ft^2/°R\text{-}s^2$)
r_w	yaw rate, deg/s
T_e	thrust, N (lb)
T_r	standard sea level temperature, 288.15 K (518.67°R)
t	time, s
t_s	source time, s
Δt	incremental time step, s
V	aircraft velocity, m/s (ft/s)
W	aircraft weight, N (lb)
x	aircraft longitudinal distance from origin, m (ft)
y	aircraft lateral distance from origin, m (ft)
z	aircraft altitude above runway, m (ft)
α	aircraft angle of attack, deg
β	sideslip angle, deg
δ_f	flap control variable, deg
ϵ	engine inclination angle, deg
ϵ_{tol}	error tolerance
μ	dynamic viscosity, kg/m-s (slugs/ft-s)
ξ	integration step size, s
Π	engine power setting, percent maximum thrust
ρ	air density, kg/m^3 ($slugs/ft^3$)
τ	coefficient of rolling friction
$(\psi_b, \theta_b, \phi_b)$	body axis Euler angles, deg
$(\psi_w, \theta_w, \phi_w)$	wind axis Euler angles, deg
$(\psi_{wb}, \theta_{wb}, \phi_{wb})$	Euler angles relative to body axis, deg
Ω	turn rate, deg/s
Subscripts:	
a	ambient
b	body axis
bank	steady turn
climb	climb segment of takeoff
cutback	cutback segment of takeoff
i	initial
max	maximum

min	minimum
rot	rotation
w	wind axis

Superscripts:

*	nondimensional
·	derivative with respect to time

Input

The JTO Module requires an extensive set of parameters and tables to define the performance characteristics of the aircraft and the engines, the aircraft geometry, and the takeoff procedure. The Aircraft Configuration Parameters describe the geometric properties of the aircraft. Note in this set of parameters that the weight of the aircraft is the maximum takeoff weight since weight reduction due to the burning of fuel is neglected. Aircraft and engine performance characteristics are input through the Aerodynamic Lift and Drag Coefficient Table, the Landing Gear Drag Coefficient Table, and the Engine Performance Table.

The takeoff procedure begins at brake release and ends when the aircraft reaches a designated altitude, a designated distance from brake release, or a designated elapsed flight time. The basic takeoff procedure is defined by setting the rotation speed, the desired climb speed, and the desired climb angle. In order for the aircraft to become airborne, the speed at rotation must be greater than the stall speed and the climb velocity should be at least 20 percent greater than the stall speed. Note that the climb speed and the climb angle are labeled "desired." If one or both of these parameters is chosen too large, there will be insufficient thrust to obtain the anticipated flight profile. Should this occur, reduce θ_w to the minimum acceptable climb angle or set θ_w to the default value of 2.3°. This establishes an initial climb angle θ_w which allows the aircraft to attain the climb velocity as soon after liftoff as possible. Once the climb speed is attained, the JTO Module automatically computes a new climb angle which achieves the maximum rate of climb for a steady-state solution. The maximum angle of attack during rotation ensures that the tail of the aircraft does not scrape the runway.

The takeoff procedure may include two optional maneuvers: cutback and steady turn. The cutback procedure is implemented by setting the CUTBACK flag to TRUE, designating the altitude at which cutback is to occur, indicating the cutback climb angle, and indicating the time required for the cutback procedure to be completed. To include a turn in the takeoff procedure, set the BANK parameter to TRUE, indicate the altitude at which the turn is to begin, indicate the turn rate, and specify the new flight-path heading. Note that a steady turn will not be executed unless a steady-state condition has been achieved.

The final steps are to establish the origin of the Earth-fixed coordinate system, position the aircraft on the runway, and define the initial conditions. Usually, the origin of the Earth-fixed coordinate system coincides with the location of the aircraft at brake release; therefore, x_i is zero. The initial altitude z_i indicates the height of the aircraft above the runway and should be greater than zero. Setting z_i to zero may cause an error in later noise calculations if the location of the aircraft and an observer coincide. (This results is a singularity in the noise calculation.) The user must also configure the aircraft for takeoff by defining an initial angle of attack and an initial flap setting.

The last input data are the Differential Equation Parameters and the Atmospheric Properties Table. Under most circumstances, the default values for the Differential

Equation Parameters are adequate. Atmospheric parameters required for the calculation of lift, drag, and sound speed are described by the Atmospheric Properties Table.

Aircraft Configuration Parameters

A_w	aircraft wing reference area, m^2 (ft^2)
N_{eng}	number of engines
W	aircraft weight, N (lb)
ε	engine inclination angle, deg

Initial Condition Parameters

t_i	initial time, s
x_i	initial longitudinal distance from origin of Earth-fixed coordinate system, m (ft)
z_i	initial altitude above runway, m (ft)
α_i	initial angle of attack, deg
δ_i	initial flap setting, deg

Final Condition Parameters

t_{max}	maximum time, s
x_{max}	maximum distance from origin, m (ft)
z_{max}	maximum altitude, m (ft)

Aircraft Performance Parameters

V_{climb}	desired climb velocity, m/s (ft/s)
V_{rot}	rotation velocity, m/s (ft/s)
θ_{climb}	desired flight-path angle during climb, deg
Π	engine power setting, percent maximum net thrust
$\dot{\alpha}$	rotation rate, deg/s
α_{max}	maximum angle of attack during rotation, deg
τ	coefficient of rolling friction

Steady Turn Parameters

BANK	turn flag
z_{bank}	turn altitude, m (ft)
Ω	turn rate, deg/s
ψ_{bank}	desired flight-path heading after completion of turn, ψ_{bank} positive initiates right turn and ψ_{bank} negative initiates left turn, deg

Cutback Parameters

CUTBACK	cutback flag
z_{cutback}	cutback altitude, m (ft)
θ_{cutback}	cutback climb angle, deg
$\Delta t_{\text{cutback}}$	time required to complete cutback, s

Differential Equation Parameters

Δt	flight time increment, s
ϵ_{tol}	error tolerance
ξ	integration step size, s
ξ_{max}	maximum integration step size, s
ξ_{min}	minimum integration step size, s

Aerodynamic Lift and Drag Coefficient Table

α	aircraft angle of attack, deg
δ_f	flap control variable, deg
$C_L(\alpha, \delta_f)$	aerodynamic lift coefficient, $\frac{L}{\frac{1}{2}\rho_a V^2 A_w}$
$C_D(\alpha, \delta_f)$	aerodynamic drag coefficient, $\frac{D}{\frac{1}{2}\rho_a V^2 A_w}$

Landing Gear Drag Coefficient Table

C_L	aerodynamic lift coefficient, $\frac{L}{\frac{1}{2}\rho_a V^2 A_w}$
$C_{D,\text{Lg}}(C_L)$	aerodynamic drag coefficient due to landing gear extension

Atmospheric Properties Table (ATM)

H^*	altitude, re $\frac{\bar{R}T_r}{Mg_r}$
$c^*(H^*)$	speed of sound, re c_a
$\rho^*(H^*)$	air density, re ρ_a
$\mu^*(H^*)$	dynamic viscosity, re μ_a
$h_a(H^*)$	absolute humidity, percent mole fraction

Engine Performance Table

Π	engine power setting, percent maximum net thrust
M_∞	aircraft Mach number
$T_e(\Pi, M_\infty)$	net thrust per engine, N (lb)

Output

Two output tables are created by the JTO module. The Flight-Path Table gives the aircraft ground coordinates and Euler angles in both the body axis and the wind axis coordinates systems. The Source Variables Table is a function of source time with eight dependent variables including Mach number, engine power setting, flap setting, landing gear position, and ambient atmospheric conditions. A new source time is added to the Source Variables Table whenever one of the eight dependent quantities changes value.

Flight-Path Table

t	flight time, s
$(x(t), y(t), z(t))$	aircraft ground coordinates, m (ft)
$(\psi_b(t), \theta_b(t), \phi_b(t))$	aircraft body axis Euler angles, deg
$(0, \theta_{wb}(t), 0)$	aircraft wind axis Euler angles relative to the body axis, deg

Source Variables Table

t_s	source time, s
$M_\infty(t_s)$	Mach number
$\Pi(t_s)$	engine power setting, percent maximum thrust
$\delta_f(t_s)$	flap setting, deg
$L_{\mathrm{Lg}}(t_s)$	landing gear position, Up or Down
$\rho_a(t_s)$	ambient air density, kg/m^3 (slugs/ft^3)
$c_a(t_s)$	ambient speed of sound, m/s (ft/s)
$\mu_a(t_s)$	ambient dynamic viscosity, kg/m-s (slugs/ft-s)
$h_a(t_s)$	absolute humidity, percent mole fraction

Method

The JTO Module defines the takeoff profile of an aircraft relative to a fixed position on Earth. Three frames of reference are used to describe the motion of the aircraft. One is fixed to the Earth with the origin placed at brake release, as shown in figure 1. The x axis is parallel to the runway with positive x in the direction of takeoff. The y and z axes form a right-handed coordinate system with the z axis pointing positive "downward." The other two reference frames are fixed to the aircraft with the origin located at the center of mass.

The two aircraft reference frames used in this module are shown in figure 2. One reference frame is the body axis coordinate system denoted by (x_b, y_b, z_b). The positive x_b axis extends forward from the center of the aircraft. The y_b and z_b axes form a right-handed coordinate system with the z_b axis pointing positive downward. The other reference frame is the wind axis coordinate system denoted by (x_w, y_w, z_w). In the wind axis coordinate system, the x_w axis is aligned with the aircraft velocity vector. The wind axis coordinate system is used to solve the equations of motion.

The orientation of the Earth-fixed axes and the aircraft body axes are defined by the Euler angles denoted by $(\psi_b, \theta_b, \phi_b)$ as shown in figure 3. In the wind axis coordinate system,

the Euler angles are denoted by $(\psi_w, \theta_w, \phi_w)$. The body and wind axis Euler angles are related by the angle of attack α and the sideslip angle β as follows:

$$\psi_b = \psi_w + \beta \tag{1}$$

$$\theta_b = \theta_w + \alpha \tag{2}$$

$$\phi_b = \phi_w \tag{3}$$

In this analysis, the sideslip angle β is always zero.

The JTO Module computes the Earth-fixed coordinates (x, y, z), the body axis Euler angles $(\psi_b, \theta_b, \phi_b)$ and the wind axis Euler angles relative to the body axes $(\psi_{wb}, \theta_{wb}, \phi_{wb})$. The wind axis Euler angles relative to the body axes are given by

$$\theta_{wb} = \theta_w - \theta_b = -\alpha \tag{4}$$

$$\psi_{wb} = \psi_w - \psi_b = 0 \tag{5}$$

$$\phi_{wb} = \phi_w - \phi_b = 0 \tag{6}$$

The equations governing the position and velocity of the aircraft in the wind axis coordinate system in a still atmosphere (refs. 1 and 2) are

$$m\frac{dV}{dt} = \sum_{e=1}^{N_{\text{eng}}} T_e \cos(\alpha + \varepsilon) - \tau F_g - D - W \sin\theta_w \tag{7}$$

$$mVr_w = W \cos\theta_w \sin\phi_w \tag{8}$$

$$mVq_w = \sum_{e=1}^{N_{\text{eng}}} T_e \sin(\alpha + \varepsilon) + F_g + L - W \cos\theta_w \cos\phi_w \tag{9}$$

$$p_w = \frac{d\phi_w}{dt} - \psi_w \sin\theta_w \tag{10}$$

$$q_w = \frac{d\theta_w}{dt}\cos\phi_w + \psi_w \sin\theta_w \tag{11}$$

$$r_w = \frac{d\psi_w}{dt}\cos\theta_w \cos\phi_w - \frac{d\theta_w}{dt}\sin\phi_w \tag{12}$$

$$\frac{dx}{dt} = V \cos\theta_w \cos\psi_w \tag{13}$$

$$\frac{dy}{dt} = V \cos\theta_w \sin\psi_w \tag{14}$$

$$\frac{dz}{dt} = -V \sin\theta_w \tag{15}$$

Equations (7), (8), and (9) represent the equations of motion of the aircraft in the x_w, y_w, and z_w directions. Equations (10), (11), and (12) are expressions for the roll, pitch, and yaw rates, respectively. Equations (13), (14), and (15) give the change in the ground coordinates as a function of time. These equations are simplified during takeoff since the bank and flight-path heading angles are zero (i.e., $\phi_w = 0$ and $\psi_w = 0$). With this simplification, the roll and yaw rates are also zero (i.e., $p_w = 0$ and $r_w = 0$) and the pitch rate reduces to

$$q_w = \frac{d\theta_w}{dt} \tag{16}$$

The system of equations now reduces to the following first-order nonlinear differential equations

$$\frac{dV}{dt} = \left[\sum_{e=1}^{N_{\text{eng}}} T_e \cos(\alpha + \varepsilon) - \tau F_g - D - W \sin\theta_w\right]\frac{1}{m} \tag{17}$$

$$\frac{d\theta_w}{dt} = \left[\sum_{e=1}^{N_{\text{eng}}} T_e \sin(\alpha + \varepsilon) + F_g + L - W \cos\theta_w\right]\frac{1}{mV} \tag{18}$$

$$\frac{dx}{dt} = V\cos\theta_w \tag{19}$$

$$\frac{dz}{dt} = -V\sin\theta_w \tag{20}$$

Equations (17) through (20) are solved numerically with a fourth-order Runge-Kutta technique. A solution is obtained at each flight time specified by

$$t_{\text{new}} = t_{\text{old}} + \Delta t \tag{21}$$

An integration step size ξ is chosen such that

$$\xi \leq \Delta t \tag{22}$$

and

$$\xi_{\min} \leq \xi \leq \xi_{\max} \tag{23}$$

The integration scheme adjusts the step size to meet the desired error tolerance. Figures 4 and 5 show the forces acting on the aircraft during the ground roll and climb. The ground force term F_g in equations (17) and (18) represents the resistance due to friction resulting from contact between the aircraft wheels and the runway. This force is positive as long as the wheels remain in contact with the runway and becomes zero at the point of liftoff. An expression for the ground force is obtained by noting that the flight-path angle θ_w and pitch rate $\dot{\theta}_w$ in equation (18) are zero during ground roll. Consequently,

$$F_g = \begin{cases} W\cos\theta_w - L - \sum_{e=1}^{N_{\text{eng}}} T_e \sin(\alpha + \varepsilon) & (z = 0) \\ 0 & (z < 0) \end{cases} \tag{24}$$

The rolling friction coefficient τ in equation (17) is a function of the landing gear and the surface characteristics of the runway. Two assumptions are made to simplify this parameter. The surface is assumed to be uniform during the ground roll and the ground force F_g is assumed to result solely from the main landing gear. This assumption allows the friction coefficient to remain constant until liftoff. The aircraft lift and drag are computed by

$$L = \frac{1}{2}\rho_a V^2 A_w \left[C_L(\alpha, \delta_f)\right] \tag{25}$$

and

$$D = \begin{cases} \frac{1}{2}\rho_a V^2 A_w \left[C_D(\alpha, \delta_f) + C_{D,\text{Lg}}(C_L)\right] & (\Delta t_{\text{climb}} < 3) \\ \frac{1}{2}\rho_a V^2 A_w \left[C_D(\alpha, \delta_f) + \cos\left[\frac{(\Delta t_{\text{climb}} - 3)\pi}{6}\right] C_{D,\text{Lg}}(C_L)\right] & (3 \leq \Delta t_{\text{climb}} \leq 6) \\ \frac{1}{2}\rho_a V^2 A_w C_D(\alpha, \delta_f) & (\Delta t_{\text{climb}} > 6) \end{cases} \tag{26}$$

In equation (26), Δt_{climb} is

$$\Delta t_{\text{climb}} = t - t_{\text{climb}} \tag{27}$$

and t_{climb} is the time at the start of the climb stage. The lift coefficient C_L and the drag coefficient C_D are functions of the aircraft angle of attack and flap settings. An additional source of drag $C_{D,\text{Lg}}$, which is a function of the lift coefficient, is due to the extension of the landing gear. Landing gear drag is present during the ground roll stage and the first 3 seconds after liftoff. The landing gear drag coefficient is multiplied by a cosine term to ensure a smooth transition in the drag force. These coefficients are obtained from the Aerodynamic Lift and Drag Coefficient Table and the Landing Gear Drag Coefficient Table.

The net thrust T_e is a function of the engine power setting and the flight Mach number. Values for the net thrust are obtained from the Engine Performance Table.

Takeoff Procedure

The takeoff procedure is divided into four stages: ground roll, climb, cutback, and steady turn. Ground roll and climb are the basis for all takeoff profiles. Cutback and steady turn are optional stages.

Ground roll. Ground roll begins with the aircraft at rest. During the ground roll stage, the climb angle θ_w and the pitch rate $\dot{\theta}_w$ are zero. With these restrictions, the problem is one-dimensional and requires solutions to equations (17) and (19). The initial conditions for the ground roll stage are

$$V(t_i) = 0 \tag{28}$$

$$x(t_i) = x_i \tag{29}$$

The angle of attack α, climb angle θ_w, and coordinates y and z remain constant during ground roll; that is, $\alpha = \alpha_i$, $\theta_w = 0$, $y = 0$, and $z = z_i$. Equations (17) and (19) are solved iteratively until the rotation velocity is achieved. After reaching the rotation velocity, the angle of attack is increased by

$$\alpha_{\text{new}} = \alpha_{\text{old}} + \dot{\alpha}\,\Delta t \tag{30}$$

until the maximum angle of attack has been achieved. As the nose of the aircraft rotates "upward," the velocity and the angle of attack continue to increase. The velocity vector however remains parallel to the runway. The ground roll stage terminates when the ground force term F_g becomes zero.

Climb. Climb begins at the point of liftoff when the aircraft main landing gear leaves the ground, and 3 seconds into the climb stage, the landing gear is automatically retracted. During the climb stage, the aircraft accelerates to the desired climb velocity, and simultaneously, the climb angle increases from zero until the desired climb angle is obtained. The aircraft coordinates are obtained by solving equations (17) through (20). During the solution of these equations, one of the following conditions will arise:

Condition 1 ($V < V_{\text{climb}}$ and $\theta_w < \theta_{\text{climb}}$): Every climb stage begins with the aircraft velocity and climb angle less than the desired values. The angle of attack is evaluated at the beginning of the climb stage to determine if rotation has been completed. If rotation has not been completed, the angle of attack continues to increase until the maximum angle of attack is achieved or until the aircraft acceleration rate becomes negative. If the acceleration rate becomes negative, the aircraft has "overrotated"; in which case, the angle of attack is reduced by 1 deg/s until the acceleration rate becomes positive. Equations (17) through (20) are solved numerically until one of the conditions described subsequently occurs or until a steady-state solution is obtained.

Condition 2 ($V = V_{\text{climb}}$ and $\theta_w < \theta_{\text{climb}}$): When the aircraft attains the climb velocity before attaining the desired climb angle, the angle of attack is adjusted so that the aircraft no longer accelerates. The appropriate angle of attack is computed by setting equation (17) to zero

$$\left[\sum_{e=1}^{N_{\text{eng}}} T_e \cos(\alpha + \varepsilon) - D - W \sin\theta_w\right] = 0 \tag{31}$$

and solving for α numerically. The remaining energy in the system is used to gain altitude. If additional energy is available after the climb angle is attained, a second climb segment is automatically initiated as described by condition 4.

Condition 3 ($V < V_{\text{climb}}$ and $\theta_w = \theta_{\text{climb}}$): The alternative to condition 2 is when the aircraft attains the climb angle before attaining the desired climb velocity. For most takeoff procedures, setting a climb angle less than the maximum climb angle attainable by the aircraft is desirable. This establishes θ_{climb} as an initial climb angle which is held constant to allow the climb velocity to be achieved as quickly as possible. To ensure that the initial climb angle is maintained, equation (18) is set to zero and solved numerically for α:

$$\left[\sum_{e=1}^{N_{\text{eng}}} T_e \sin(\alpha + \varepsilon) + L - W \cos\theta_w\right] = 0 \tag{32}$$

The angle of attack now controls the climb angle, and the remaining energy in the system is used to accelerate the aircraft. If additional energy is available after the climb velocity is attained, a second climb segment is automatically initiated as described by condition 4.

Condition 4 ($V = V_{\text{climb}}$ and $\theta_w = \theta_{\text{climb}}$): Condition 4 arises when the aircraft is capable of a greater climb speed or climb angle than is specified by the input parameters. When this condition occurs, V_{climb} is held constant and the excess energy is used to increase the rate of climb. A new climb angle is computed by setting the right side of equations (17) and (18) to zero and simultaneously solving for θ_w. The new climb angle can be written in terms of the lift-drag ratio and the thrust-weight ratio as

$$\theta_w = \sin^{-1}\left\{\frac{(L/D)G}{1+(L/D)^2} - \sqrt{\left[\frac{(L/D)G}{1+(L/D)^2}\right]^2 + \left[\frac{1-G^2}{1+(L/D)^2}\right]}\right\} \tag{33}$$

where the steady-state climb function G is defined as

$$G = \frac{\sum_{e=1}^{N_{\text{eng}}} T_e}{W}\left[\frac{L}{D}\cos(\alpha + \varepsilon) + \sin(\alpha + \varepsilon)\right] \tag{34}$$

Steady-state solution: A steady-state solution is defined when both the acceleration rate and the pitch rate satisfy the following criteria:

$$m\left|\frac{dV}{dt}\right| \leq \varepsilon_{\text{tol}} \tag{35}$$

and

$$mV\left|\frac{d\theta_w}{dt}\right| \leq \varepsilon_{\text{tol}} \tag{36}$$

The Earth-fixed coordinates can now be computed by

$$x_{\text{new}} = x_{\text{old}} + V\Delta t\cos\theta_w \tag{37}$$

and

$$z_{\text{new}} = z_{\text{old}} - V\Delta t\sin\theta_w \tag{38}$$

The climb stage ends when one of the following conditions are met:

$$x \geq x_{\max} \tag{39}$$

$$z \geq z_{\max} \tag{40}$$

or

$$t \geq t_{\max} \tag{41}$$

The climb stage may also end when the cutback altitude is obtained or when a steady-state solution is obtained and a steady turn maneuver is to be performed.

Cutback. Cutback is initiated when the aircraft reaches the user-specified cutback altitude. With the aircraft angle of attack and the climb velocity remaining constant throughout the maneuver, the thrust required to obtain the cutback climb angle is computed by

$$T_{\text{cutback}} = \frac{W\left[\cos\theta_{\text{cutback}} + (L/D)\sin\theta_{\text{cutback}}\right]}{(L/D)\cos(\alpha+\varepsilon) + \sin(\alpha+\varepsilon)} \tag{42}$$

Thrust is reduced linearly such that

$$\sum_{e=1}^{N_{\text{eng}}} T_{e,\text{new}} = \sum_{e=1}^{N_{\text{eng}}} T_{e,\text{old}} - \sum_{e=1}^{N_{\text{eng}}} \Delta T_e \tag{43}$$

where the thrust increment $\sum_{e=1}^{N_{\text{eng}}} \Delta T_e$ is given by

$$\sum_{e=1}^{N_{\text{eng}}} \Delta T_e = \frac{\left(\sum_{e=1}^{N_{\text{eng}}} T_e(\Pi) - T_{\text{cutback}}\right)\Delta t}{\Delta t_{\text{cutback}}} \tag{44}$$

and $T_e(\Pi)$ is a function of the power setting at the beginning of the cutback maneuver. The climb angle corresponding to each new thrust setting is computed by equation (33) with $T_e = T_{e,\text{new}}$ in equation (34). At the end of $\Delta t_{\text{cutback}}$, in seconds, cutback is completed and a steady-state solution to equations (17) and (18) is obtained with the new climb angle equal to the cutback climb angle.

Steady turn. When an aircraft executes a steady turn, the aircraft velocity, climb angle, and roll angle are required to be constant. Consequently, a steady-state solution to equations (17) and (18) is required before a turn can be initiated. Once this condition is met, a steady turn is initiated as soon as the user-specified turn altitude is achieved.

The flight-path heading during the turn varies as

$$\psi_{w,\text{new}} = \psi_{w,\text{old}} + \Omega\,\Delta t \tag{45}$$

where the turn rate Ω is constant. A positive value for Ω produces a right turn, from the pilot's perspective. Under these conditions, the yaw rate is

$$r_w = \Omega \cos\theta_w \cos\phi_w \tag{46}$$

and the balance of forces in the y_w direction is

$$mV\Omega \cos\theta_w \cos\phi_w = W \cos\theta_w \sin\phi_w \tag{47}$$

when solving equation (47) for ϕ_w, an angle

$$\phi_w = \tan^{-1}\frac{V\Omega}{g_r} \tag{48}$$

was found to be required to execute the turn. The Earth-fixed coordinates are obtained from the following equations:

$$x_{\text{new}} = x_{\text{old}} + \frac{V_{\text{climb}}}{\Omega}\cos\theta_w\,[\sin\psi_w - \sin(\psi_w - \Omega\,\Delta t)] \tag{49}$$

$$y_{\text{new}} = y_{\text{old}} + \frac{V_{\text{climb}}}{\Omega}\cos\theta_w\,[\cos(\psi_w - \Omega\,\Delta T) - \cos\psi_w] \tag{50}$$

$$z_{\text{new}} = z_{\text{old}} - V_{\text{climb}}\,\Delta t\,\sin\theta_w \tag{51}$$

The steady turn procedure is terminated when

$$\psi_w = \psi_{\text{bank}} \tag{52}$$

or when x, z, or t exceed the maximum values given by equations (39), (40), and (41).

References

1. Etkin, Bernard: *Dynamics of Atmospheric Flight*. John Wiley & Sons, Inc., c.1972.
2. Dommasch, Daniel O.; Sherby, Sydney S.; and Connolly, Thomas F.: *Airplane Aerodynamics*. Fourth ed. Pitman Publ. Corp., c.1967.

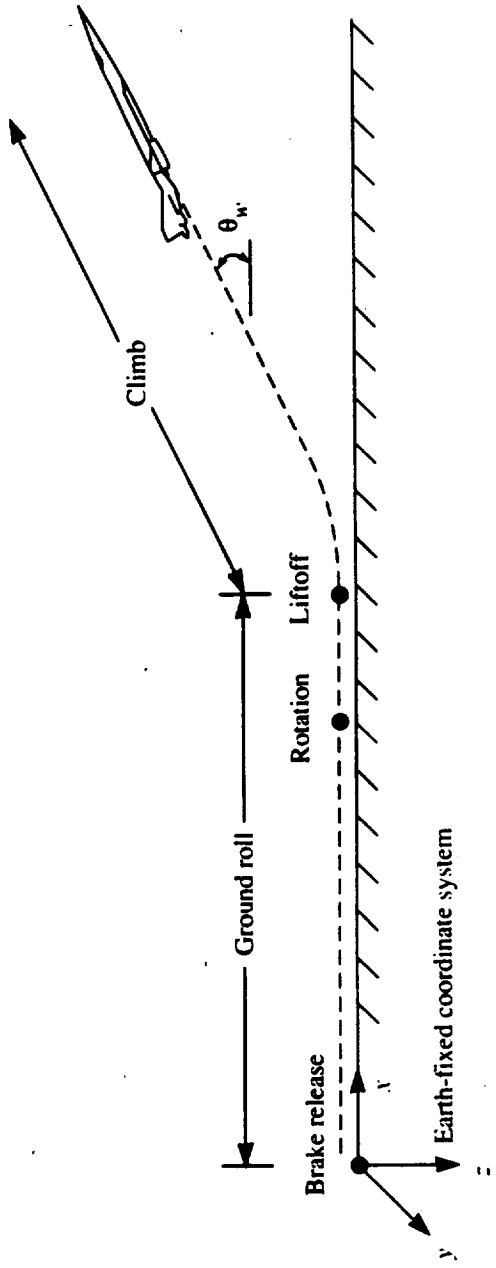

Figure 1. Basic takeoff profile.

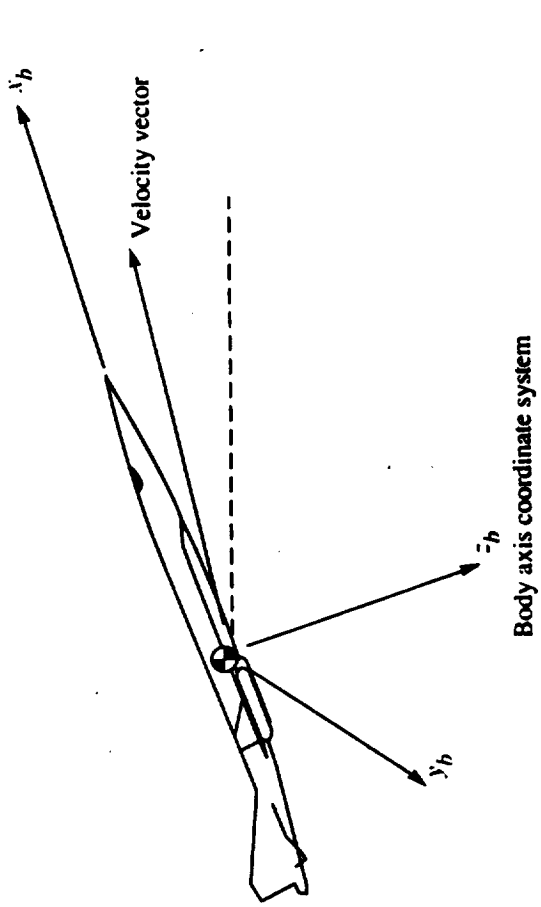

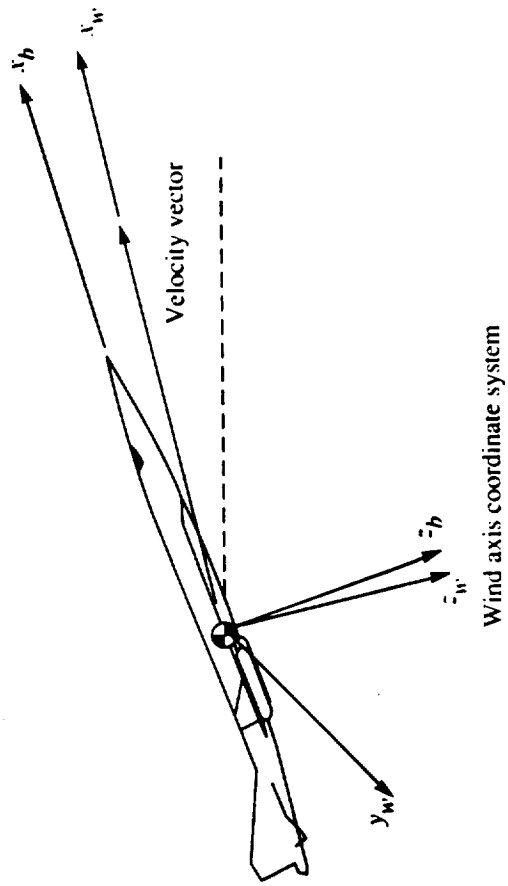

Figure 2. Body and wind axis coordinate systems.

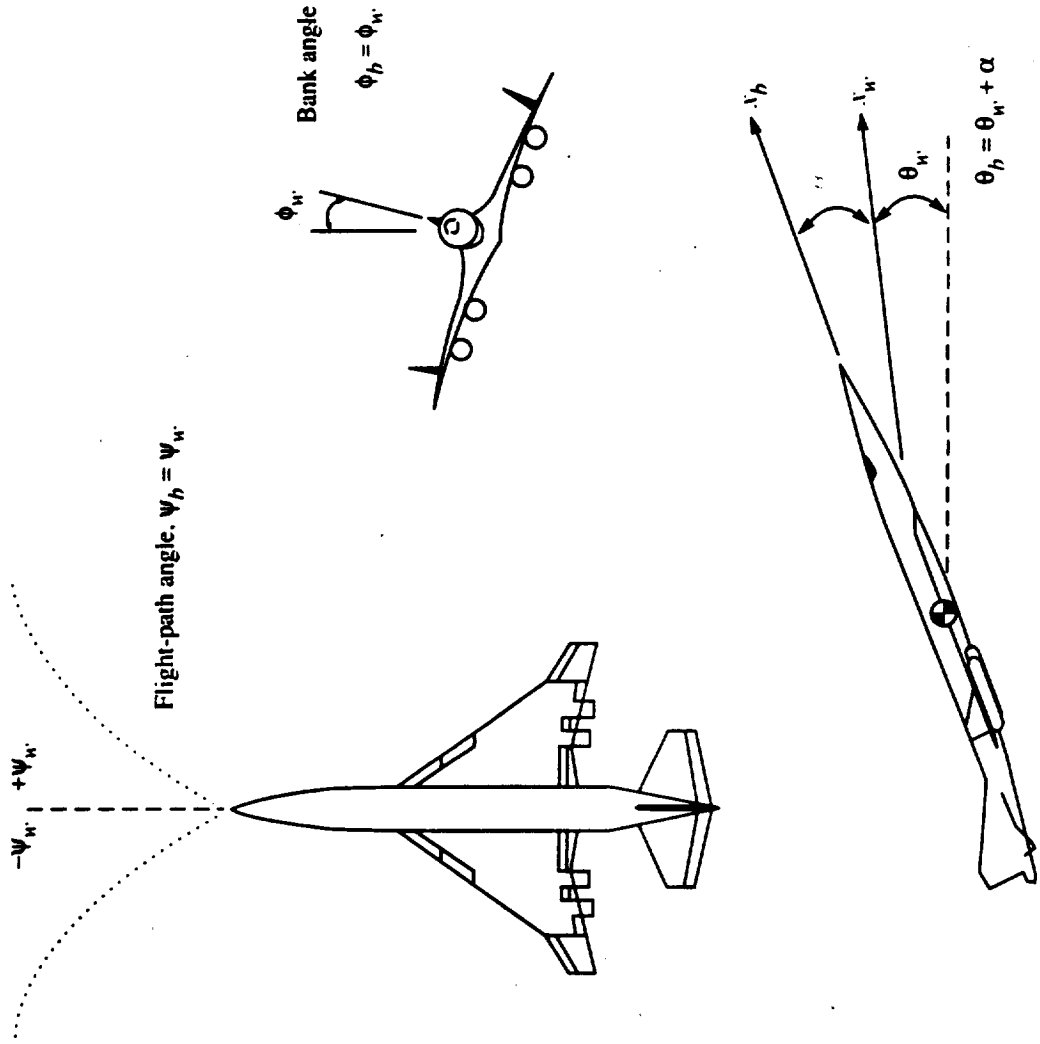

Figure 3. Euler angles in body axis and wind axis coordinate systems.

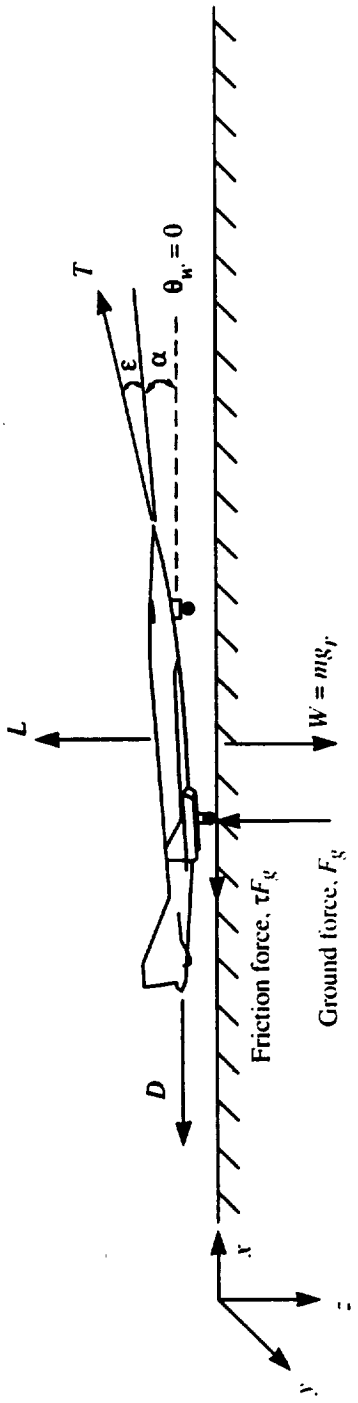

Figure 4. Forces acting on aircraft during ground roll.

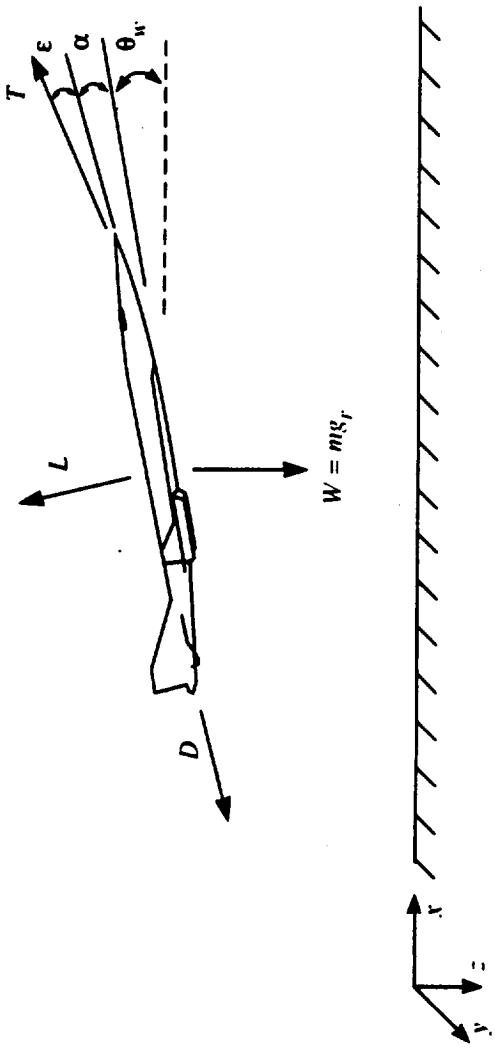

Figure 5. Forces acting on aircraft during climb.

2.5 Jet Landing (JLD) Module

Mark Wilson

Lockheed Engineering & Sciences Company

Introduction

The Jet Landing (JLD) Module computes the position of an aircraft during an approach to the runway based on the aircraft performance characteristics. The landing procedure can be divided into as many as five segments. The basic landing profile consists of one segment with an approach angle of 3°. During each segment, the approach speed and flight-path angle are required to be constant. This constraint reduces the differential equations of motion to an algebraic form which is used to determine the angle of attack and thrust required to maintain the input approach speed and flight-path angle.

Symbols

A_w	aircraft wing reference area, m^2 (ft^2)
C_D	aerodynamic drag coefficient, $\frac{D}{\frac{1}{2}\rho_a V^2 A_w}$
$C_{D,\mathrm{Lg}}$	aerodynamic drag coefficient due to landing gear
C_L	aerodynamic lift coefficient, $\frac{L}{\frac{1}{2}\rho_a V^2 A_w}$
c	speed of sound, m/s (ft/s)
D	aerodynamic drag, N (lb)
F_g	ground force, N (lb)
g_r	gravitational constant, 9.8066 m/s^2 (32.1741 ft/s^2)
H	altitude, m (ft)
h_a	absolute humidity, percent mole fraction
L	aerodynamic lift, N (lb)
L_{Lg}	landing gear position, Up or Down
M	molecular weight of dry air, 28.9644
M_∞	aircraft Mach number, V/c
m	aircraft mass, W/g_r, kg (slugs)
N_{eng}	number of engines
N_{seg}	number of flight-path segments
$\overline{R}$	universal gas constant, 8314.32 $m^2/K\text{-}s^2$ (49 718.96 $ft^2/°R\text{-}s^2$)
T_e	thrust, N (lb)
T_r	standard sea level temperature, 288.15 K (518.67°R)
t	time, s
t_s	source time, s

Δt	incremental time step, s
V	aircraft velocity, m/s (ft/s)
W	aircraft weight, N (lb)
x	aircraft longitudinal distance from origin, m (ft)
y	aircraft lateral distance from origin, m (ft)
z	aircraft altitude above runway, m (ft)
α	aircraft angle of attack, deg
δ_f	flap control variable, deg
ϵ	engine inclination angle, deg
μ	dynamic viscosity, kg/m-s (slugs/ft-s)
Π	engine power setting, percent maximum thrust
Π_{RV}	thrust reverse power setting, percent maximum thrust
ρ	air density, kg/m^3 (slugs/ft^3)
τ	coefficient of rolling friction
$(\psi_b, \theta_b, \phi_b)$	body axis Euler angles, deg
$(\psi_w, \theta_w, \phi_w)$	wind axis Euler angles, deg
$(\psi_{wb}, \theta_{wb}, \phi_{wb})$	Euler angles relative to body axis, deg

Subscripts:

a	ambient
b	body axis
f	final
H	runway threshold
i	initial
Lg	landing gear
n	counter
w	wind axis
1	first segment
2	second segment

Superscript:

*	nondimensional

Input

A description of the aircraft geometry is required. The Aerodynamic Lift and Drag Coefficient Table and an Engine Performance Table describe the characteristics of the airframe and engine. The atmosphere is described by the Atmospheric Properties Table. Input parameters are used to define the number of landing segments and other altitude dependent variables such as the altitude for landing gear extension. An array of altitudes,

flight-path angles, and approach velocities for each segment of the landing profile are defined in the Landing Profile Table.

Input Parameters

N_{seg}	number of segments
Π_{RV}	thrust reverser power setting, percent maximum net thrust
Δt	time increment, s
V_f	final aircraft velocity, m/s (ft/s)
W	aircraft weight, N (lb)
z_{Lg}	altitude for flap and landing gear extension, m (ft)
z_H	altitude for end of runway crossing, m (ft)
δ_f	landing configuration flap setting, deg

Landing Profile Table

z_i	array of approach altitudes, m (ft)
$\theta_{w,i}$	array of approach flight-path angles, deg
V_i	array of approach velocities, m/s (ft/s)

Aircraft Configuration Parameters

A_w	aircraft wing reference area, m^2 (ft^2)
N_{eng}	number of engines
ϵ	engine inclination angle, deg
τ	coefficient of rolling friction

Aerodynamic Lift and Drag Coefficient Table

α	aircraft angle of attack, deg
δ_f	flap control variable, deg
$C_L(\alpha, \delta_f)$	aerodynamic lift coefficient, $\frac{L}{\frac{1}{2}\rho_a V^2 A_w}$
$C_D(\alpha, \delta_f)$	aerodynamic drag coefficient, $\frac{D}{\frac{1}{2}\rho_a V^2 A_w}$

Landing Gear Drag Coefficient Table

C_L	aerodynamic lift coefficient, $\frac{L}{\frac{1}{2}\rho_a V^2 A_w}$
$C_{D,Lg}(C_L)$	aerodynamic drag coefficient due to landing gear extension

Atmospheric Properties Table (ATM)

H^*	altitude, re $\frac{\overline{R}T_r}{Mg_r}$
$c^*(H^*)$	speed of sound, re c_a
$\rho^*(H^*)$	air density, re ρ_a
$\mu^*(H^*)$	dynamic viscosity, re μ_a
$h_a(H^*)$	absolute humidity, percent mole fraction

Engine Performance Table

Π	engine power setting, percent maximum net thrust
M_∞	aircraft Mach number
$T_e(\Pi, M_\infty)$	net thrust per engine, N (lb)

Output

Two output tables are created by this module. The Flight-Path Table gives the aircraft ground coordinates and Euler angles in both the body axis and the wind axis coordinates systems. The Source Variables Table is a function of source time with eight dependent variables including Mach number, engine power setting, flap setting, landing gear position, and ambient atmospheric conditions. A new source time is added to the Source Variables Table whenever one of the eight dependent quantities changes value.

Flight-Path Table

t	flight time, s
$(x(t), 0, z(t))$	aircraft ground coordinates, m (ft)
$(0, \theta_b(t), 0)$	aircraft body axis Euler angles, deg
$(0, \theta_{wb}(t), 0)$	aircraft wind axis Euler angles relative to body axis, deg

Source Variables Table

t_s	source time, s
$M_\infty(t_s)$	Mach number
$\Pi(t_s)$	engine power setting, percent maximum thrust
$\delta_f(t_s)$	flap setting, deg
$L_{\mathrm{Lg}}(t_s)$	landing gear position, Up or Down
$\rho_a(t_s)$	ambient air density, kg/m^3 (slugs/ft^3)
$c_a(t_s)$	ambient speed of sound, m/s (ft/s)
$\mu_a(t_s)$	ambient dynamic viscosity, kg/m-s (slugs/ft-s)
$h_a(t_s)$	absolute humidity, percent mole fraction

Method

The flight trajectory generated by this module is based on balancing the forces in the horizontal direction by

$$-\tau F_g + \sum_{e=1}^{N_{\text{eng}}} T_e \cos(\alpha + \varepsilon) - W \sin\theta_w - D = m\frac{dV}{dt} \tag{1}$$

and in the vertical direction by

$$F_g + \sum_{e=1}^{N_{\text{eng}}} T_e \sin(\alpha + \varepsilon) - W \cos\theta_w + L = mV\frac{d\theta_w}{dt} \tag{2}$$

These equations (refs. 1 and 2) are defined in the wind axis coordinate system shown in figure 1. The ground force term F_g is defined by

$$F_g = \begin{cases} W - L - \sum_{e=1}^{N_{\text{eng}}} T_e \sin(\alpha + \varepsilon) & (z = 0) \\ 0 & (z > 0) \end{cases} \tag{3}$$

and remains zero until the moment of touchdown. The coefficient of rolling friction τ is a function of landing gear and surface characteristics.

The aircraft lift L and drag D are computed by

$$L = \frac{1}{2}\rho_a V^2 A_w \left[C_L(\alpha, \delta_f)\right] \tag{4}$$

and

$$D = \frac{1}{2}\rho_a V^2 A_w \left[C_D(\alpha, \delta_f) + C_{D,\text{Lg}}(C_L)\right] \tag{5}$$

where the lift and drag coefficients are obtained from the Aerodynamic Lift and Drag Coefficient Table and the Landing Gear Drag Coefficient Table.

The position of the aircraft as a function of time is given by

$$\frac{dx}{dt} = V\cos\theta_w \tag{6}$$

and

$$\frac{dz}{dt} = V\sin\theta_w \tag{7}$$

This module divides the landing procedure into segments defined by the parameter N_{seg}. An array of altitudes, flight-path angles, and approach velocities are specified in the Landing Profile Table. The arrays are defined such that the first value corresponds to the outermost segment. Figure 2 shows an example of a two-segment landing profile. Note that the flight-path angles are defined to be negative down. The origin of x is defined at the end of the runway. The initial distance of the aircraft from the end of the runway is computed from the array of altitudes and flight-path angles by

$$x_i = \sum_{n=1}^{N_{\text{seg}}} \frac{z_n - z_{n+1}}{\tan\theta_{w,n}} \tag{8}$$

where the last altitude in the summation corresponds to the altitude at the end of the runway; that is,

$$z_{N_{\text{seg}}+1} = z_H - \tag{9}$$

By maintaining a constant approach speed and flight-path angle, the derivatives in equations (1) and (2) are zero. This allows the use of the following algebraic equations (assuming the aircraft is not on the ground; i.e., $F_g = 0$):

$$\sum_{e=1}^{N_{\text{eng}}} T_e \cos(\alpha + \varepsilon) - W \sin\theta_w - D = 0 \tag{10}$$

and

$$\sum_{e=1}^{N_{\text{eng}}} T_e \sin(\alpha + \varepsilon) - W \cos\theta_w + L = 0 \tag{11}$$

To calculate the aircraft angle of attack α required to maintain the desired approach speed, a small angle approximation is made for $\alpha + \varepsilon$ in equation (11). Assume that $\sin(\alpha + \varepsilon) \approx 0$ and equation (11) becomes

$$L = W \cos\theta_w \tag{12}$$

which can be written in terms of the lift coefficient as

$$C_L = \frac{W \cos\theta_w}{\frac{1}{2}\rho_a V^2 A_w} \tag{13}$$

The angle of attack that satisfies equation (13) is found by interpolating the Aerodynamic Lift and Drag Coefficient Table.

The thrust required to maintain the desired flight-path angle is obtained from

$$\sum_{e=1}^{N_{\text{eng}}} T_e = \frac{W\left[\cos\theta_w + (L/D)\sin\theta_w\right]}{(L/D)\cos(\alpha + \varepsilon) + \sin(\alpha + \varepsilon)} \tag{14}$$

During the airborne segments of the landing trajectory, the approach velocity remains constant so that the aircraft coordinates are

$$x_j = s_{j-1} + V \cos\theta_w \, \Delta t \tag{15}$$

and

$$z_j = z_{j-1} - V \sin\theta_w \, \Delta t \tag{16}$$

where j indicates segment number. After touchdown, the aircraft velocity becomes a function of time due to the ground force term. The velocity then becomes

$$V_j = V_{j-1} + \Delta V \tag{17}$$

where the reduction in velocity is given by

$$\Delta V = \frac{1}{m}\left[-\tau F_g - D - m g_r \sin\theta_w + \sum_{e=1}^{N_{\text{eng}}} T_e \cos(\alpha + \varepsilon)\right] \Delta t \tag{18}$$

Thrust T_e is calculated by using the Engine Performance Table where engine power setting and aircraft Mach number are used as inputs. After touchdown, thrust reversing may be employed to rapidly decelerate the aircraft. The engine power set is replaced by the thrust reverser parameter as input to the Engine Performance Table. Thrust is reversed by assigning a negative value to the thrust reverser parameter Π_{RV}. For example, a value of $\Pi_{RV} = -0.5$ would provide thrust reversing at a power setting of one half full power.

The aircraft Euler angles are also required as output (fig. 3). Since the two-degree-of-freedom assumption has been made, the landing profile takes place only in the vertical plane (i.e., no yaw or roll motion). This assumption implies that the values of the Euler angles ψ_b and ϕ_b are both zero. The aircraft body axis Euler angle θ_b can be calculated by the following relation between angle of attack and flight-path angle:

$$\theta_b = \alpha + \theta_w \tag{19}$$

The body axis Euler angle θ_b is transformed to the wind axis by using the following equation:

$$\theta_{wb} = -\alpha \tag{20}$$

References

1. Etkin, Bernard: *Dynamics of Atmospheric Flight.* John Wiley & Sons, Inc., c.1972.
2. Dommasch, Daniel O.; Sherby, Sydney S.; and Connolly, Thomas F.: *Airplane Aerodynamics.* Fourth ed. Pitman Publ. Corp., c.1967.

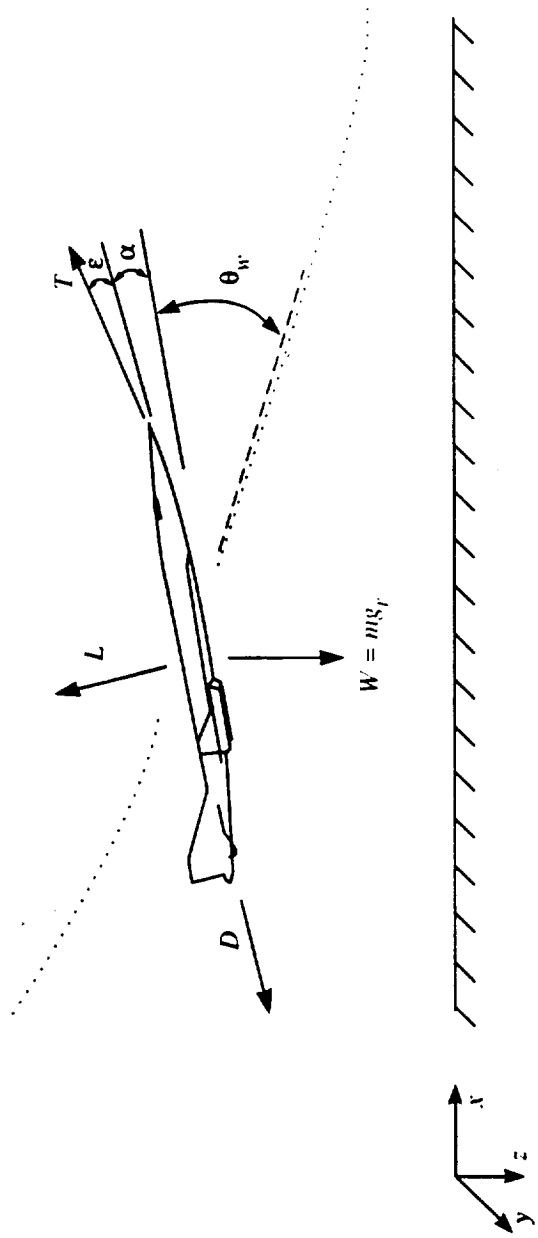

Figure 1. Forces acting on aircraft during descent.

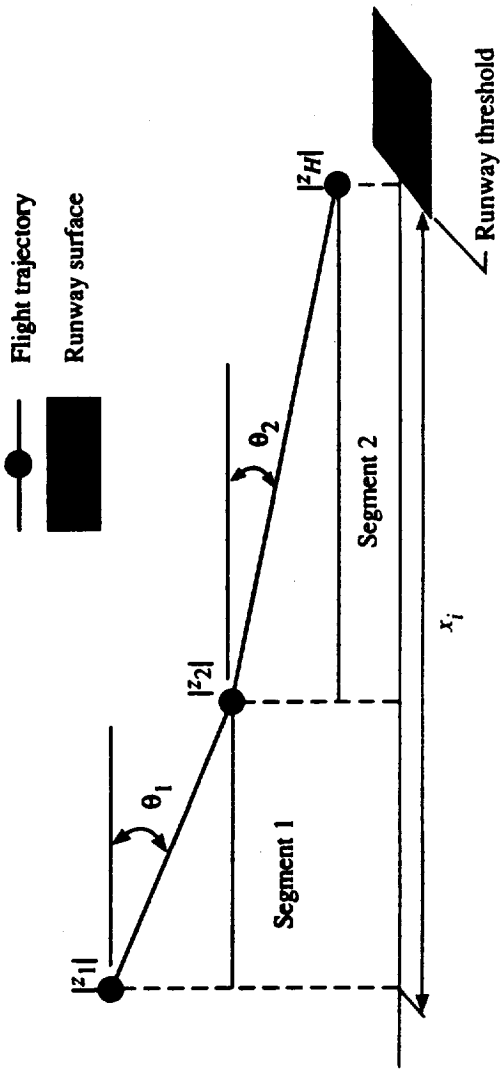

Figure 2. Schematic of two-segment landing profile.

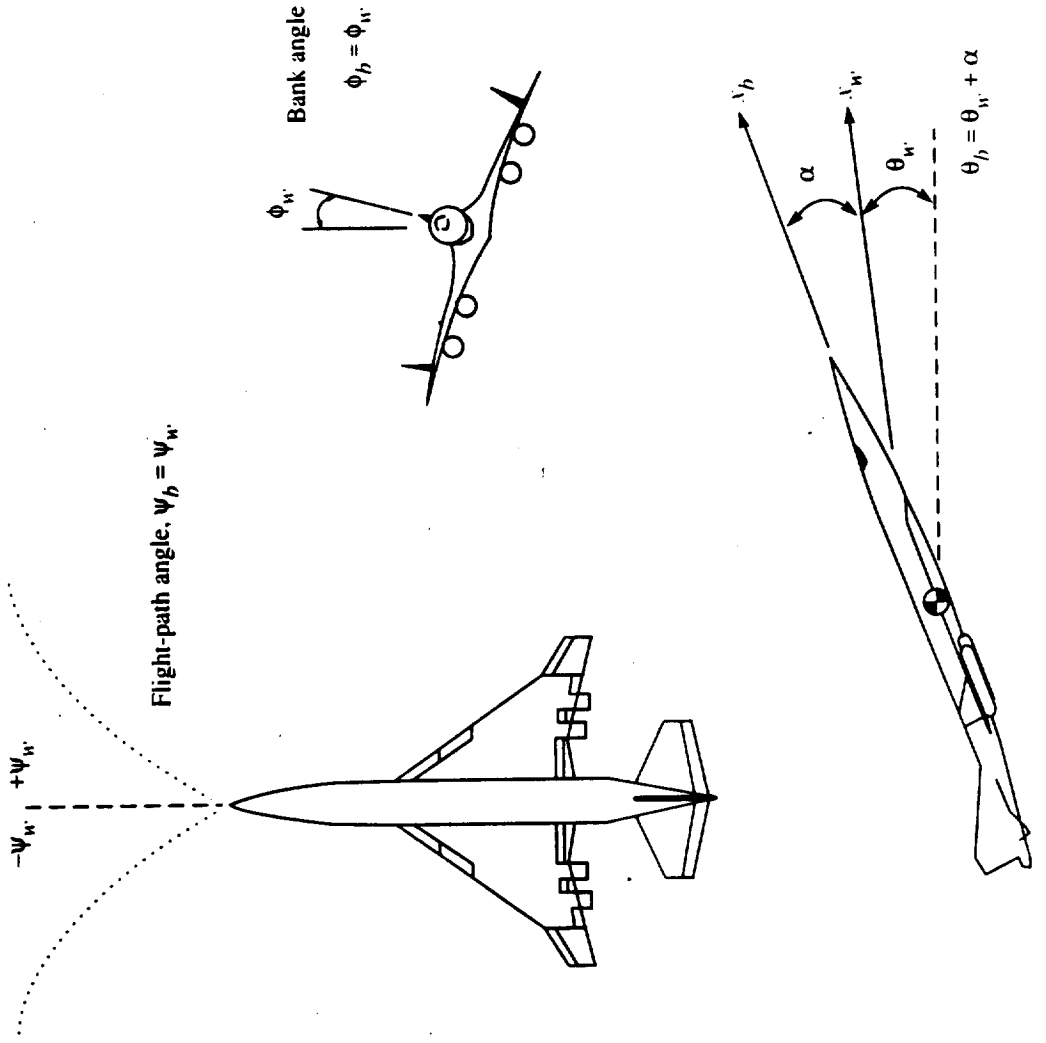

Figure 3. Euler angles in body axis and wind axis coordinate systems.

2.6 Steady Flyover (SFO) Module

John Rawls, Jr.

Lockheed Engineering & Sciences Company

Introduction

The Steady Flyover (SFO) Module defines the position of an aircraft based on kinematics (ref. 1). This approach enables flight paths to be defined without requiring engine and aircraft performance data as input. Aircraft motion is restricted to constant velocity or uniform acceleration along a rectilinear flight path. Flight paths that do not conform to this restriction may be divided into segments. A segmented flight path is constructed by executing this module once for each segment.

Input to the SFO Module consists of parameters that define a single flight-path segment. Output consists of parameters that allow repeated executions of the module, and two tables that are used by other ANOPP (Aircraft Noise Prediction Program) modules to predict noise produced by a moving source. One table defines the position of the aircraft as a function of time, and the other identifies changes in the noise source characteristics.

Symbols

a	aircraft acceleration, m/s^2 (ft/s^2)
c	speed of sound, m/s (ft/s)
d	distance, m (ft)
g_r	gravitational constant, 9.8066 m/s^2 (32.1741 ft/s^2)
H	altitude, m (ft)
h_a	absolute humidity, percent mole fraction
L_{Lg}	landing gear position, Up or Down
M	molecular weight of dry air, 28.9644
M_∞	aircraft Mach number, V/c
N	number of incremental time steps
$\overline{R}$	universal gas constant, 8314.32 m^2/k-s^2 (49 718.96 ft^2/°R-s^2)
T_r	standard sea level temperature, 288.15 K (518.67°R)
t	time, s
t_{Lg}	landing gear reset time, s
t_s	source time, s
Δt	incremental time step, s
V	aircraft velocity, m/s (ft/s)
x	aircraft longitudinal distance from origin, m (ft)
y	aircraft lateral distance from origin, m (ft)
z	aircraft altitude above runway, m (ft)

α	aircraft angle of attack. deg
δ_f	flap control variable. deg
μ	dynamic viscosity. kg/m-s (slugs/ft-s)
Π	engine power setting. percent maximum thrust
ρ	air density. kg/m^3 (slugs/ft^3)
$(\psi_b, \theta_b, \phi_b)$	body axis Euler angles. deg
$(\psi_w, \theta_w, \phi_w)$	wind axis Euler angles. deg
$(\psi_{wb}, \theta_{wb}, \phi_{wb})$	Euler angles relative to body axis. deg

Subscripts:

a	ambient
b	body axis
f	final
i	initial
ref	reference
w	wind axis
1	first segment
2	second segment

Superscript:

*	nondimensional

Input

A flight profile may consist of as many segments as the user desires. Each flight-path segment requires one execution of the SFO Module. To create a multiple segment flight profile. the APPEND parameter must be set to TRUE. This causes the data created for the Flight-Path Table and the Source Variables Table to be appended to the output created by the previous execution of the SFO Module. Therefore. it is important that each segment be created in the appropriate order. If the APPEND parameter is FALSE. each execution of the SFO Module creates a new flight profile.

The Mach number update criterion parameter ΔM_x identifies when the flight speed has altered the noise source characteristics sufficiently to warrant updating the Source Variables Table. If the aircraft velocity is not constant and $\Delta M_x = 0$. the Source Variables Table contains an entry for every incremental change in the aircraft velocity. A large number of noise predictions may result that may not be warranted considering the approximations required to define the flight path. The user can limit the number of source noise predictions and. as a result. reduce the total computation time by setting the Mach number update criterion parameter. Generally. $\Delta M_x = 0.05$ is adequate.

The computational option flag ZOPT allows the final z position of the aircraft to be specified directly by the input parameter z_f or to be computed by using the inclination angle θ_w. Sometimes the inclination angle is a more convenient parameter for constructing a flight-path segment.

The position of an aircraft is calculated with the initial and final condition parameters. The Aircraft Configuration Parameters do not affect the flight profile but are required as output by the Source Variables Table. Information from the Source Variables Table is used by other ANOPP modules to predict the noise characteristics of the engine and the airframe. With the exception of the landing gear, the Aircraft Configuration Parameters remain constant throughout a flight segment. The Earth-fixed coordinated system is defined such that z is positive down as shown in figure 1. For convenience, the z coordinates (corresponding to altitude) are input as positive values and converted to negative values within the module. In order to compute the aircraft Mach number, the speed of sound is provided by the Atmospheric Properties Table.

Input Parameters

APPEND	multiple segment flight-path flag, True or False
J_i	initial step number
ΔM_∞	Mach number update criterion
Δt	time step increment, s
z_{ref}	altitude of runway above reference level, m (ft)
ZOPT	computational option flag, for ZOPT = 1, input z_f and disregard θ_w and for ZOPT = 2, input θ_w and disregard z_f
θ_w	inclination angle of flight vector with respect to horizontal, positive for climb and negative for descent, deg

Initial Condition Parameters

t_i	initial time, s
V_i	initial velocity, m/s (ft/s)
x_i	initial longitudinal position from origin, m (ft)
y_i	initial lateral position from origin, m (ft)
z_i	initial altitude above runway, m (ft)

Final Condition Parameters

t_f	final time, s
V_f	final velocity, m/s (ft/s)
x_f	final longitudinal distance from origin, m (ft)
y_f	final lateral position from origin, m (ft)
z_f	final altitude above runway, m (ft)

Aircraft Configuration Parameters

$L_{Lg,i}$	initial landing gear position, Up or Down
t_{Lg}	landing gear reset time, s
Π	engine power setting, percent maximum thrust
δ_f	flap setting, deg
α	angle of attack, deg

Atmospheric Properties Table (ATM)

H^*	altitude, re $\frac{\overline{R}T_r}{Mg_r}$
$c^*(H^*)$	speed of sound, re c_a
$\rho^*(H^*)$	air density, re ρ_a
$\mu^*(H^*)$	dynamic viscosity, re μ_a
$h_a(H^*)$	absolute humidity, percent mole fraction

Output

The Final Condition Parameters provide pertinent information necessary for a repeat execution of the Steady Flyover Module. When a multiple-segment flight profile is created, the final conditions are used as the initial conditions for the next segment. Two output tables are created by this module. The Flight-Path Table gives the aircraft ground coordinates and Euler angles in both the body axis and the wind axis coordinates systems. The Source Variables Table is a function of source time with eight dependent variables including Mach number, engine power setting, flap setting landing gear position, and ambient atmospheric conditions. A new source time is added to the Source Variables Table whenever one of the eight dependent quantities changes value.

Final Condition Parameters

If the SFO Module is executed with APPEND = TRUE, the following parameters become the input parameters for the next execution of the SFO Module:

J_f	final step number
$L_{Lg,f}$	final landing gear position, Up or Down
t_f	final time, s
V_f	actual final velocity, m/s (ft/s)
x_f	actual final longitudinal position from origin, m (ft)
y_f	actual final lateral position from origin, m (ft)
z_f	actual final altitude above runway, m (ft)

Flight-Path Table

t	flight time, s
$(x(t), y(t), z(t))$	aircraft position coordinates, m (ft)
$(\psi_b(t), \theta_b(t), 0)$	aircraft body axis Euler angles, deg
$(0, \theta_{wb}(t), 0)$	aircraft wind axis Euler angles relative to body axis, deg

Source Variables Table

t_s	source time, s
$M_\infty(t_s)$	Mach number
$\Pi(t_s)$	engine power setting, percent maximum thrus
$\delta_f(t_s)$	flap setting, deg
$L_{Lg}(t_s)$	landing gear position, Up or Down
$\rho_a(t_s)$	ambient air density, kg/m^3 (slugs/ft^3)
$c_a(t_s)$	ambient speed of sound, m/s (ft/s)
$\mu_a(t_s)$	ambient dynamic viscosity, kg/m-s (slugs/ft-s)
$h_a(t_s)$	ambient absolute humidity, percent mole fraction

Method

The SFO Module computes the position of an aircraft based on kinematics. This approach is useful when aircraft performance data are not available or when simple flight profiles are required. Figures 2 through 4 illustrate three examples of flight profiles that can be constructed by using the SFO Module.

Figure 2 illustrates a single-segment flight path where the velocity and the altitude remain constant. A flight-path segment is defined by the initial and final position of the aircraft and by the initial and final velocity. At the beginning of each segment, the angle of attack, the flap setting, and the power setting are provided as input. As long as the flight path can be defined between two points, the motion of the aircraft may be climbing, descending, accelerating, or decelerating. The aircraft motion may also be stationary; therefore, a flight profile may be created for a hovering aircraft.

The flight profiles shown in figures 3 and 4 are constructed by repeated executions of the module. The landing profile shown in figure 3 is divided into two segments, representing approach and ground roll. The final position and velocity for the approach segment becomes the initial conditions for the ground roll segment.

Figure 4 illustrates a takeoff profile that has been divided into four segments: ground roll, first climb segment, second climb segment, and cutback. During ground roll and the first climb segment, the aircraft is accelerating. The landing gear may be retracted during the first climb segment by specifying the new gear position and the reset time which is measured from the beginning of the first climb segment. During the last two segments, the aircraft velocity is constant, but the two segments differ in climb angle and in power setting.

The position coordinates of the aircraft are computed by the following equations:

$$x_{k+1} = x_k + \left(V_k\ \Delta t + \frac{1}{2} a\ \Delta t^2\right) \cos\theta_w \cos\psi_w \tag{1}$$

$$y_{k+1} = y_k + \left(V_k\ \Delta t + \frac{1}{2} a\ \Delta t^2\right) \cos\theta_w \sin\psi_w \tag{2}$$

$$z_{k+1} = z_k - \left(V_k\ \Delta t + \frac{1}{2} a\ \Delta t^2\right) \sin\theta_w \tag{3}$$

Equations (1), (2), and (3) are solved iteratively for $k = J$ to N, where N is the integer part of

$$N = J_i + \frac{t}{\Delta t} \tag{4}$$

In equation (4), J_i is the initial step number, t is the total time required to complete the flight-path segment, and Δt is the incremental time step. The aircraft velocity at time step k is

$$V_k = V_{k-1} + a\ \Delta t \tag{5}$$

where V_{k-1} is the velocity from the previous time step and a is the acceleration. The acceleration of the aircraft given by

$$a = \frac{V_f^2 - V_i^2}{2d} \tag{6}$$

and is computed from the initial and final velocities and the distance traveled during the segment, which is

$$d = \sqrt{\Delta x^2 + \Delta y^2 + \Delta z^2} \tag{7}$$

The incremental distances Δx, Δy, and Δz are

$$\Delta x = x_f - x_i \tag{8}$$

$$\Delta y = y_f - y_i \tag{9}$$

$$\Delta z = z_f - z_i \tag{10}$$

The total time required to complete a segment is

$$t = \begin{cases} t_f - t_i & (V_i = V_f = 0) \\ \dfrac{2d}{V_i + V_f} & (|a| \geq 0) \end{cases} \tag{11}$$

The flight-path heading ψ_w and the climb angle θ_w remain constant during a segment. The flight-path heading is given by

$$\psi_w = \tan^{-1} \frac{\Delta y}{\Delta x} \tag{12}$$

An option is provided which allows either the final altitude z_f or the climb angle to be specified as input. If z_f is specified, the climb angle is computed by

$$\theta_w = \tan^{-1} \frac{\Delta z}{\Delta x} \tag{13}$$

If θ_{fp} is specified, Δz is computed by

$$\Delta z = \Delta x \tan \theta_{fp} \tag{14}$$

The aircraft body axis Euler angles θ_b and ψ_b are calculated by using the following relationship between angle of attack, flight-path angle, and flight-path heading. (See fig. 5.) The climb angle in the body axis is

$$\theta_b = \alpha - \theta \tag{15}$$

and the flight-path heading in the body axis is

$$\psi_b = \psi \tag{16}$$

The body axis Euler angle θ_b is transformed to the wind axis with the following relation:

$$\theta_{wb} = -\alpha \tag{17}$$

This module creates two output tables. One is the Flight-Path Table, which defines the aircraft position and Euler angles for each time increment Δt. The other is the Source Variables Table, which identifies times during the flight when the characteristics of the source noise are altered by changes in engine power setting, aircraft configuration, ambient conditions or aircraft velocity. The Source Variables Table always contains an entry corresponding to the start of a new flight-path segment.

The flight Mach number, given by

$$M_\infty(t_n) = \frac{V(t_n)}{c(H^*)} \tag{18}$$

is evaluated from the aircraft velocity and the ambient sound speed. The sound speed $c(H^*)$ is obtained from the Atmospheric Properties Table as a function of the nondimensional altitude H^* given by

$$H^* = \frac{z_i - z_{ref}}{\bar{R}T_r / Mg_r} \tag{19}$$

The parameter z_{ref} is the height of the runway above the reference level (usually sea level) specified in the Atmospheric Properties Table.

Reference

1. Beer, Ferdinand P.; and Johnston, E. Russell, Jr.: *Vector Mechanics for Engineers—Statics and Dynamics*. McGraw-Hill Book Co., 1962.

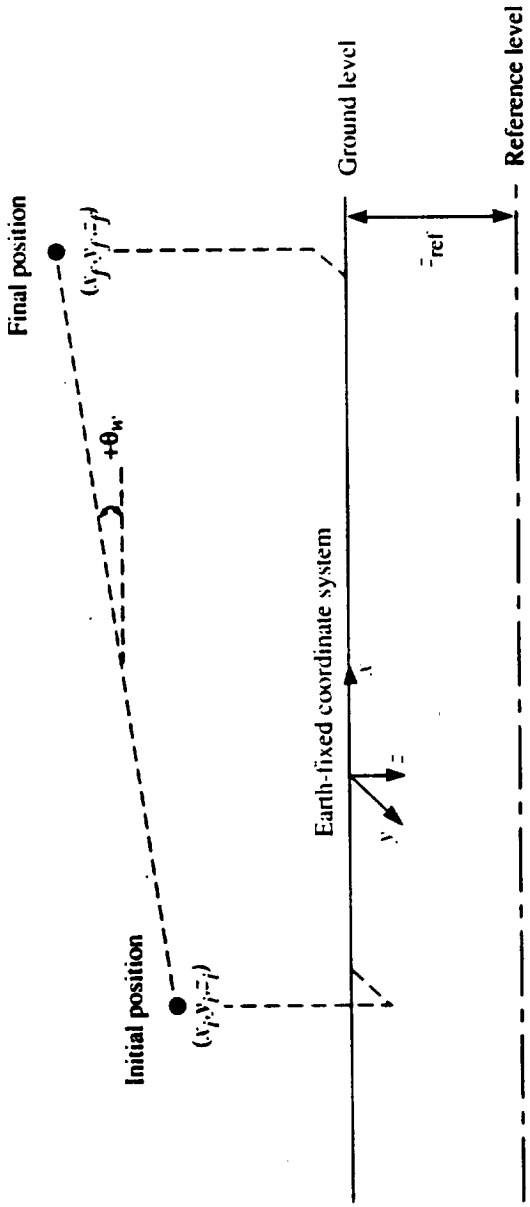

Figure 1. Coordinate system for Steady Flyover Module.

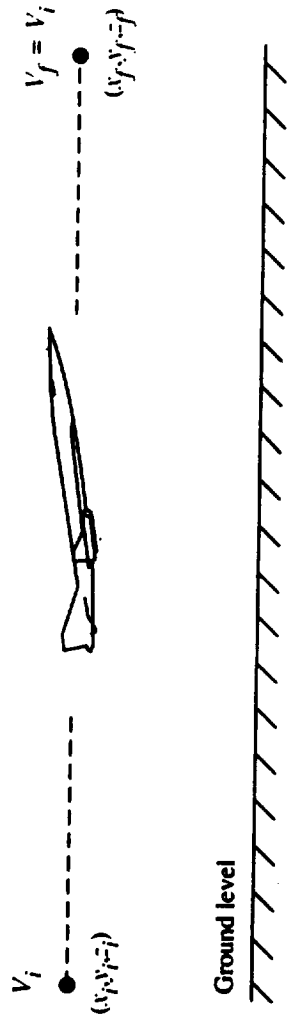

Figure 2. Constant velocity level flyover.

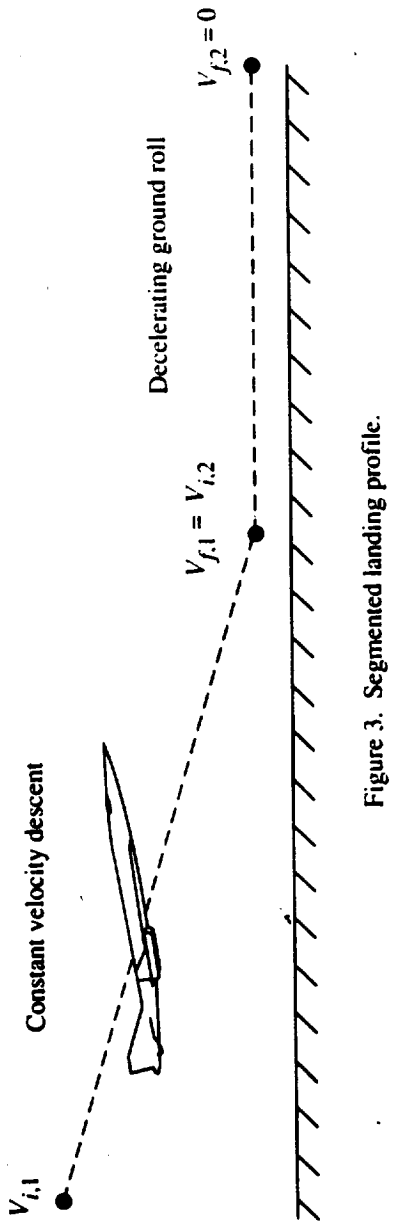

Figure 3. Segmented landing profile.

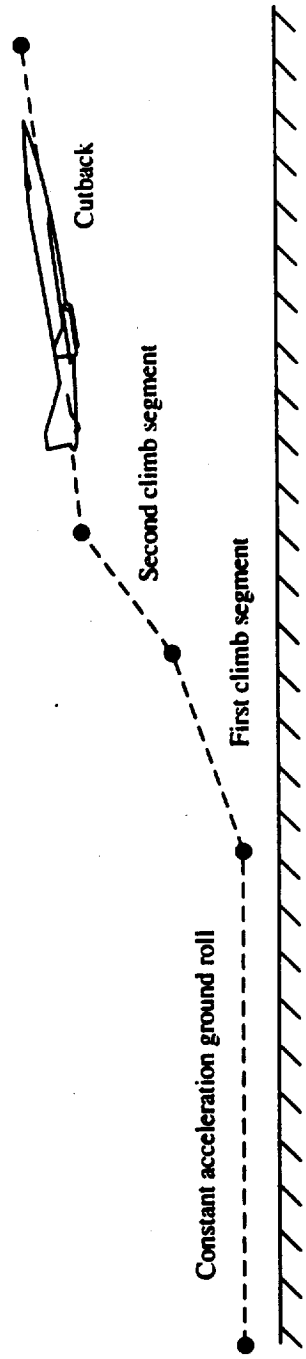

Figure 4. Segmented takeoff profile.

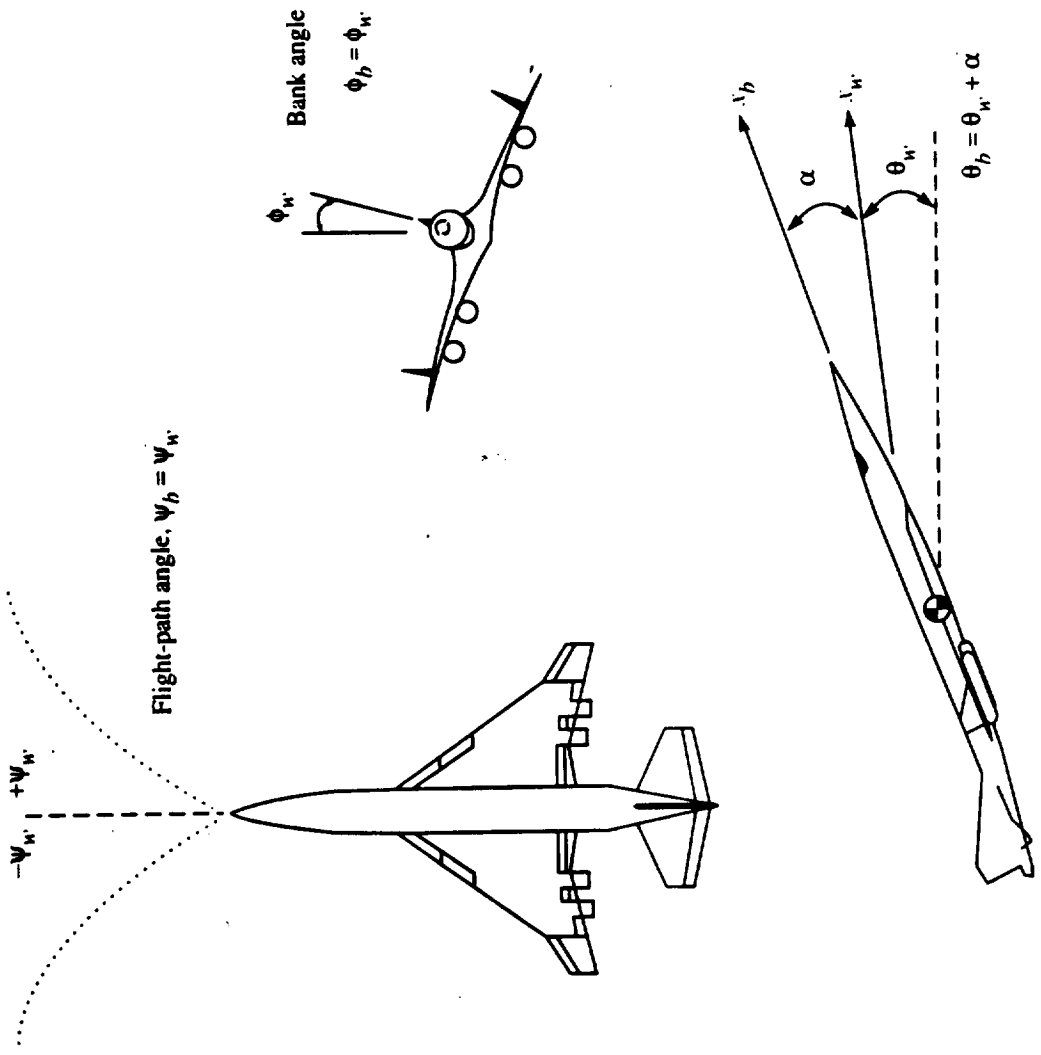

Figure 5. Euler angles in body axis and wind axis coordinate systems.

3. PROPAGATION EFFECTS

3.1 ATMOSPHERIC ABSORPTION MODULE

INTRODUCTION

As sound waves propagate from the source to the observer, they are attenuated due to atmospheric absorption. The Atmospheric Absorption Module accounts for the decrease in noise intensity produced by the atmosphere. This sound attenuation is expressed as an absorption coefficient which depends on frequency, temperature, pressure, and humidity.

The temperature, pressure, and humidity are assumed in ANOPP to be functions of altitude only. Therefore, the absorption coefficient is expressed as a function of altitude and frequency. It is shown that a mean absorption coefficient, which is the average value from ground level to a given altitude, can be applied to the sound intensity.

The atmospheric absorption occurs due to four basic causes. First is the classical loss due to thermal and viscous effects. Second is the molecular loss due to the rotational relaxation of nitrogen and oxygen molecules. Third is the molecular loss due to the vibrational relaxation of nitrogen molecules. Fourth is the molecular loss due to the vibrational relaxation of oxygen molecules. The total absorption coefficient is the sum of the coefficients for each of the four effects.

This module computes a table of the atmospheric-absorption coefficient in dimensionless form as a function of frequency and dimensionless altitude. This table is then available to be used with the Propagation Module to correct sound intensities for the atmospheric-absorption effect.

SYMBOLS

c	speed of sound, m/s (ft/s)
f	frequency, Hz
f_{rl}	relaxation frequency, Hz
g_r	acceleration due to gravity, m/s^2 (ft/s^2)
H	altitude, m (ft)
H_l	ground level altitude, m (ft)
h	absolute humidity, percent mole fraction
M	molecular weight of air
p	pressure, Pa (lb/ft^2)

$\langle p^2 \rangle$ mean-square pressure, Pa^2 (lb^2/ft^4)

$\bar{R}$ universal gas constant, $m^2/K\text{-}s^2$ ($ft^2/^oR\text{-}s^2$)

r distance, m (ft)

T temperature, K (^oR)

X fractional molar concentration

y dimensionless altitude, $Mg_r(H - H_1)/\bar{R}T_r$

α absorption coefficient, nepers/m (nepers/ft)

θ characteristic vibrational temperature, K (^oR)

$\bar{\mu}$ dimensionless absorption coefficient, $\bar{\alpha}c_r/f$, nepers

ρ reference density, kg/m^3 ($slugs/ft^3$)

Subscripts:

cl classical

n nitrogen

o oxygen

r standard sea level value

rot rotational

s source

vib vibrational

Superscript:

* dimensionless value

INPUT

The two basic independent variables for the module are frequency and altitude. Center-frequency values for 1/3-octave bands and the altitude values in the Atmospheric Module (ATM) define the independent-variable inputs. In addition, the module requires several of the atmospheric properties produced by the ATM.

f 1/3-octave-band center frequency, Hz

Atmospheric-Properties Table

y	dimensionless altitude, $Mg_r(H - H_1)/\bar{R}T_r$
h(y)	humidity, percent mole fraction
$p^*(y)$	pressure, re p_r
$T^*(y)$	temperature, re T_r

OUTPUT

The output is a table of the dimensionless absorption coefficient as a function of frequency and altitude.

Absorption-Coefficient Table

f	frequency, Hz
y	dimensionless altitude, $Mg_r(H - H_1)/\bar{R}T_r$
$\bar{\mu}(f,y)$	dimensionless absorption coefficient, $\bar{\alpha}c_r/f$, nepers

METHOD

The sound intensity lost due to atmospheric absorption is expressed as an atmospheric-absorption coefficient. This coefficient is defined by the relation

$$\langle p^2(r)\rangle = \left(\frac{r_s^2}{r^2}\right)\left[\langle p^2(r_s)\rangle\right] \exp\left[-2\alpha(r - r_s)\right] \tag{1}$$

where $\langle p^2(r)\rangle$ is the mean-square acoustic pressure at some distance r from the source, $\langle p^2(r_s)\rangle$ is the mean-square acoustic pressure at the source, and α is the absorption coefficient. The absorption coefficient is expressed as a sum of four components as

$$\alpha = \alpha_{cl} + \alpha_{rot} + \alpha_{vib,o} + \alpha_{vib,n} \tag{2}$$

where α_{cl} is the classical loss due to thermal and viscous effects, α_{rot} is the molecular-absorption loss due to the rotational relaxation of oxygen and nitrogen molecules, $\alpha_{vib,o}$ is the molecular-absorption loss due to the vibrational relaxation of oxygen molecules, and $\alpha_{vib,n}$ is the molecular-absorption loss due to the vibrational relaxation of nitrogen molecules. Additional sources of atmospheric attenuation are assumed to be negligible.

As a result of extensive theoretical and experimental effort, expressions have been developed for each of the terms in equation (2). Sutherland (ref. 1) presents the theoretical development and all existing experimental data. Reference 2 further refines that work. All of the empirical equations used in this module are results of the work in these references.

An important parameter in the vibrational-relaxation absorption loss of a gas is the relaxation frequency. The relaxation frequency is defined as that frequency at which the maximum vibrational absorption loss per unit wavelength occurs. In general, the relaxation frequency is a function of temperature, pressure, and humidity for a given gas. Air is assumed to be composed of nitrogen and oxygen, neglecting the absorption of the other components. Therefore, the following empirical expressions for the relaxation frequencies are used:

$$f_{rl,n} = (p/p_r)(293.15/T)^{1/2}\left(9 + 350h \exp\left\{-6.142\left[(293.15/T)^{1/3} - 1\right]\right\}\right) \quad (3)$$

and

$$f_{rl,o} = (p/p_r)\left\{24 + 44100h\left[(0.05 + h)/(0.391 + h)\right]\right\} \quad (4)$$

In equations (3) and (4), $f_{rl,n}$ is the relaxation frequency of nitrogen in hertz, $f_{rl,o}$ is the relaxation frequency of oxygen in hertz, p is the ambient pressure, T is the ambient temperature in Kelvin, and h is the absolute humidity in percent mole fraction. Rewriting equations (3) and (4) in terms of dimensionless variables yields

$$f_{rl,n} = p^*/(T^*)^{1/2}\left(9.08 + 340.65h \exp\left\{-6.178\left[(T^*)^{-1/3} - 1\right]\right\}\right) \quad (5)$$

and

$$f_{rl,o} = p^*\left\{24 + 44100h\left[(0.05 + h)/(0.391 + h)\right]\right\} \quad (6)$$

where $T^* = T/T_r$ and $p^* = p/p_r$. A graph of the relaxation frequency as a function of temperature and humidity at standard sea level pressure is presented in figure 1 for nitrogen. Relaxation frequency as a function of humidity at standard sea level pressure is presented in figure 2 for oxygen. It is interesting to note that the value of the oxygen relaxation frequency is always much greater than the nitrogen relaxation frequency and that the value of the relaxation frequency is highly dependent on the value of the absolute humidity.

The four terms on the right-hand side of equation (2) are now computed. The classical and rotational terms are combined and expressed as a function of temperature, pressure, and frequency as follows:

$$\alpha_{cl} + \alpha_{rot} = (1.84 \times 10^{-11})(T/293.15)^{1/2} f^2/(p/p_r) \tag{7}$$

Each of the two vibrational loss terms are written in the following form:

$$\alpha_{vib,i} = \frac{2\pi X_i}{35}\left(\frac{\theta_i}{T}\right)^2 \frac{\exp(-\theta_i/T)(f/c)}{\left[1 - \exp(-\theta_i/T)\right]^2} \frac{2ff_{rl,i}}{f^2 + f_{rl,i}^2} \tag{8}$$

where θ_i is the characteristic vibrational temperature and X_i is the fractional molar concentration. In equation (8), i is defined such that $i = o$ for oxygen and $i = n$ for nitrogen. Since the value of θ_i/T is large, the term in square brackets can be replaced by unity. Expressing equations (7) and (8) in terms of dimensionless variables, substituting the values for the physical constants given in table I, and using the relation

$$c = c_r(T^*)^{1/2} \tag{9}$$

yields the following:

$$\alpha_{cl} + \alpha_{rot} = (6.207 \times 10^{-9})(f/c_r)(T^*)^{1/2}(f/p^*) \tag{10}$$

$$\alpha_{vib,o} = (9.555 \times 10^{-4})(f/c_r)(T^*)^{-5/2} \times \exp\left[7.771(T^* - 1)/T^*\right]\left[2ff_{rl,o}/\left(f^2 + f_{rl,o}^2\right)\right] \tag{11}$$

and

$$\alpha_{vib,n} = (1.683 \times 10^{-4})(f/c_r)(T^*)^{-5/2} \times \exp\left[11.633(T^* - 1)/T^*\right]\left[2ff_{rl,n}/\left(f^2 + f_{rl,n}^2\right)\right] \tag{12}$$

The total absorption coefficient is the sum of equations (10), (11), and (12). The absorption coefficients in these equations are expressed in the units of nepers per meter. To convert to decibels per meter, it is necessary to multiply the right-hand side of each equation by 8.69.

Figure 3 shows a typical graph of the total absorption coefficient as a function of frequency with $h = 0.2$, $T^* = 1.0$, and $p^* = 1.0$. The three distinct regimes for the absorption coefficient are readily apparent from the figure. The first regime, where the frequency is less than the relaxation frequency of nitrogen, is dominated by the vibrational absorption of nitrogen. The second regime includes values of frequency between the nitrogen relaxation frequency and the oxygen relaxation frequency and is dominated by the oxygen vibrational absorption. The classical and rotational losses dominate in the third regime for frequencies above the oxygen relaxation frequency.

The data in figure 3 include a wide range of frequencies. For aircraft noise problems, the frequency range of interest is normally limited to less than 10 000 Hz. To further demonstrate the properties of the absorption coefficient, the classical and rotational, nitrogen vibrational, oxygen vibrational, and total coefficients are plotted as functions of frequency in figures 4 to 7. The effect of changing relaxation frequency is shown by the lines of constant humidity in figures 5 to 7. All data are for standard sea level temperature and pressure, and all four figures are plotted to the same scale to allow direct comparisons between the figures. Finally, the relaxation frequencies which correspond to each constant humidity line are shown in figures 5 to 7.

The total absorption-coefficient curves on figure 7 demonstrate how the characteristics of the absorption coefficient dramatically change as a result of changing relaxation frequency. As the values of the atmospheric properties change, the dominant absorption term that falls within the frequency range of interest changes. Comparison of figure 7 with figure 3 can assist in identifying the dominant term.

The atmospheric-absorption coefficient is dimensional. To express the coefficient in dimensionless form, a dimensionless absorption coefficient $\bar{\mu}$ is defined as

$$\bar{\mu} = \bar{\alpha} c_r / f \tag{13}$$

where $\bar{\alpha}$ is the average absorption coefficient from the ground to a given height. The dimensionless absorption coefficient expresses the absorption loss in terms of nepers per unit wavelength under standard conditions. In general, $\bar{\mu}$ is a function of temperature, pressure, humidity, and frequency. For the Atmospheric Module used in ANOPP (ATM), the temperature, pressure, and humidity are a function of altitude only. The dimensionless altitude y, as discussed in the ATM, is defined as

$$y = M g_r (H - H_1) \Big/ \bar{R} T_r \tag{14}$$

The Atmospheric-Properties Table from ATM gives temperature T^*, pressure p^*, and humidity h as functions of y. Therefore, the absorption coefficient is expressed as a function of y and f.

The total change in sound intensity due to atmospheric absorption is an integral over the length of the conical ray tube from the source to the observer. An average absorption coefficient is defined as this integral divided by the length. Since the absorption coefficient is a function of y and f only, the average dimensionless absorption coefficient from ground level to some value y is given by

$$\bar{\mu}(f,y) = \frac{1}{y}\int_0^y (\alpha c_r/f)\, dy \tag{15}$$

Equation (15) is also valid for each component of the absorption coefficient. Equations (10), (11), and (12) are then rewritten as

$$\bar{\mu}_{cl} + \bar{\mu}_{rot} = (6.207 \times 10^{-9})\frac{f}{y}\int_0^y (T^*)^{1/2}/p^*\, dy \tag{16}$$

$$\bar{\mu}_{vib,o} = (9.555 \times 10^{-4})\frac{1}{y}\int_0^y (T^*)^{-5/2}\, \frac{2ff_{rl,o}}{f^2 + f_{rl,o}^2} \times \exp\left[7.771(T^* - 1)/T^*\right] dy \tag{17}$$

and

$$\bar{\mu}_{vib,n} = (1.683 \times 10^{-4})\frac{1}{y}\int_0^y (T^*)^{-5/2}\, \frac{2ff_{rl,n}}{f^2 + f_{rl,n}^2} \times \exp\left[11.633(T^* - 1)/T^*\right] dy \tag{18}$$

The temperature T^*, pressure p^*, and relaxation frequencies are functions of y. The total average dimensionless absorption coefficient is

$$\bar{\mu}(f,y) = \bar{\mu}_{cl} + \bar{\mu}_{rot} + \bar{\mu}_{vib,o} + \bar{\mu}_{vib,n} \tag{19}$$

This module produces a table of $\bar{\mu}(f,y)$ for a range of values of the altitude H and frequency f for use by the Propagation Module. The Propagation Module corrects the sound intensity values for atmospheric-absorption effects.

REFERENCES

1. Sutherland, Louis C.: Review of Experimental Data in Support of a Proposed New Method for Computing Atmospheric Absorption Losses. DOT-TST-75-87, U.S. Dep. Transp., May 1975.

2. American National Standard Method for the Calculation of the Absorption of Sound by the Atmosphere. ANSI S1.26-1978 (ASA 23-1978), American Natl. Stand. Inst., Inc., June 23, 1978.

TABLE I.- STORED PRIMARY CONSTANTS

Constant	SI Units	U.S. Customary Units
c_r	340.294 m/s	1116.45 ft/s
g_r	9.806 65 m/s^2	32.1741 ft/s^2
M	28.9644	28.9644
ρ_r	1.225 kg/m^3	0.002 377 $slug/ft^3$
$\bar{R}$	8314.32 $m^2/K\text{-}s^2$	49 718.96 $ft^2/^oR\text{-}s^2$
T_r	288.15 K	518.67^oR
X_n	0.781	0.781
X_o	0.209	0.209
θ_n	3352.0 K	6033.6^oR
θ_o	2239.1 K	4030.38^oR

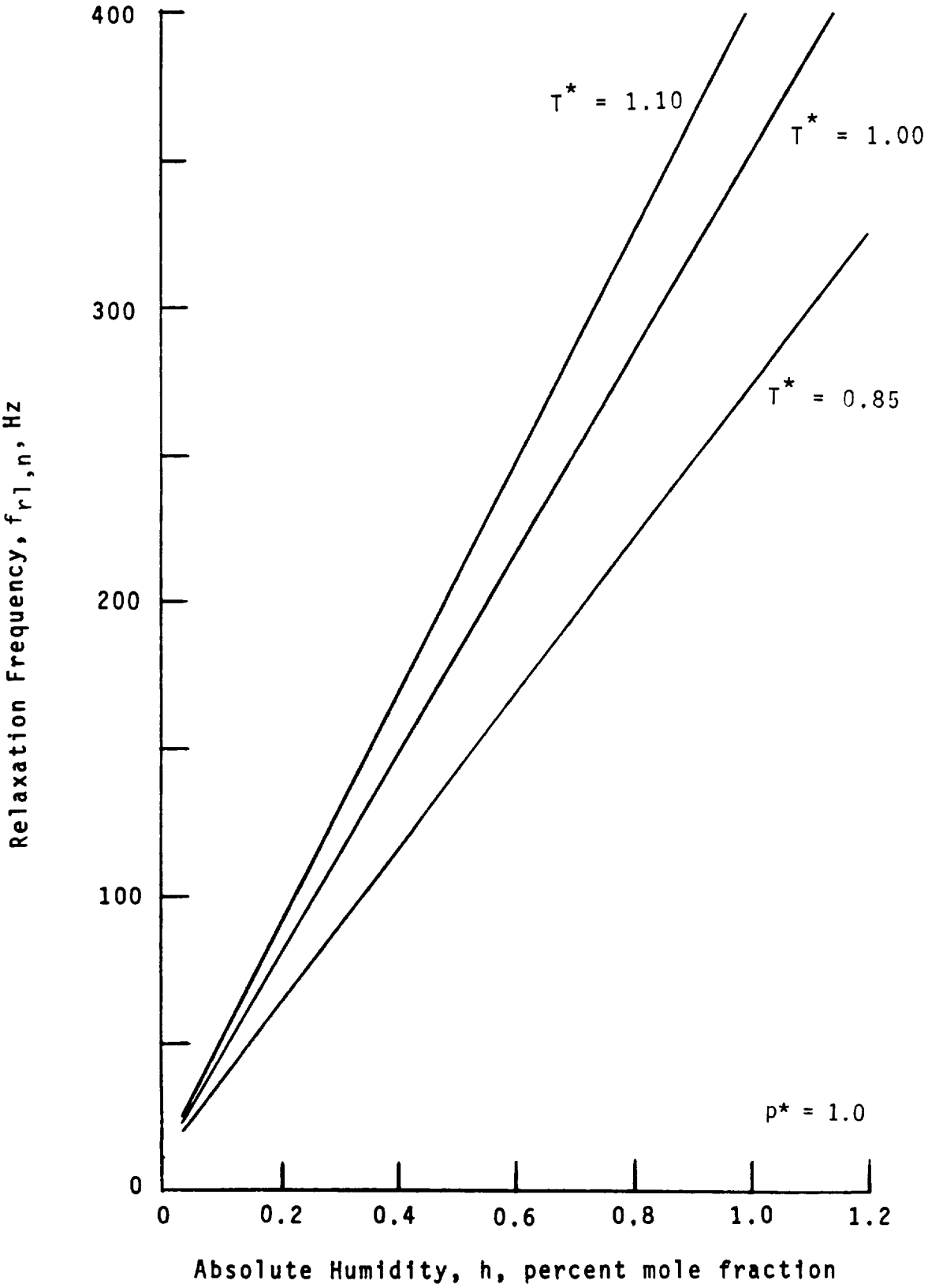

Figure 1.- Relaxation frequency for nitrogen.

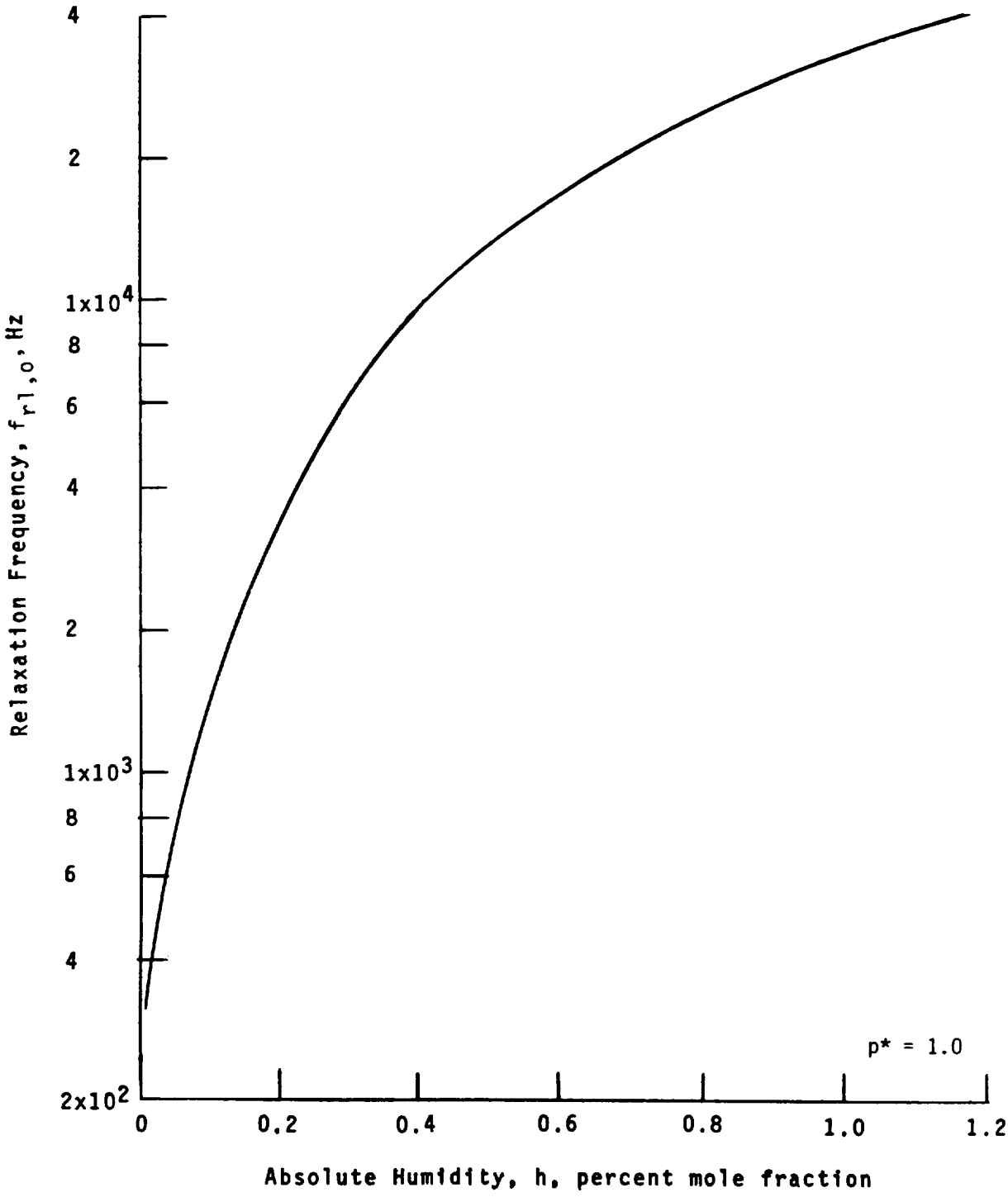

Figure 2.- Relaxation frequency for oxygen.

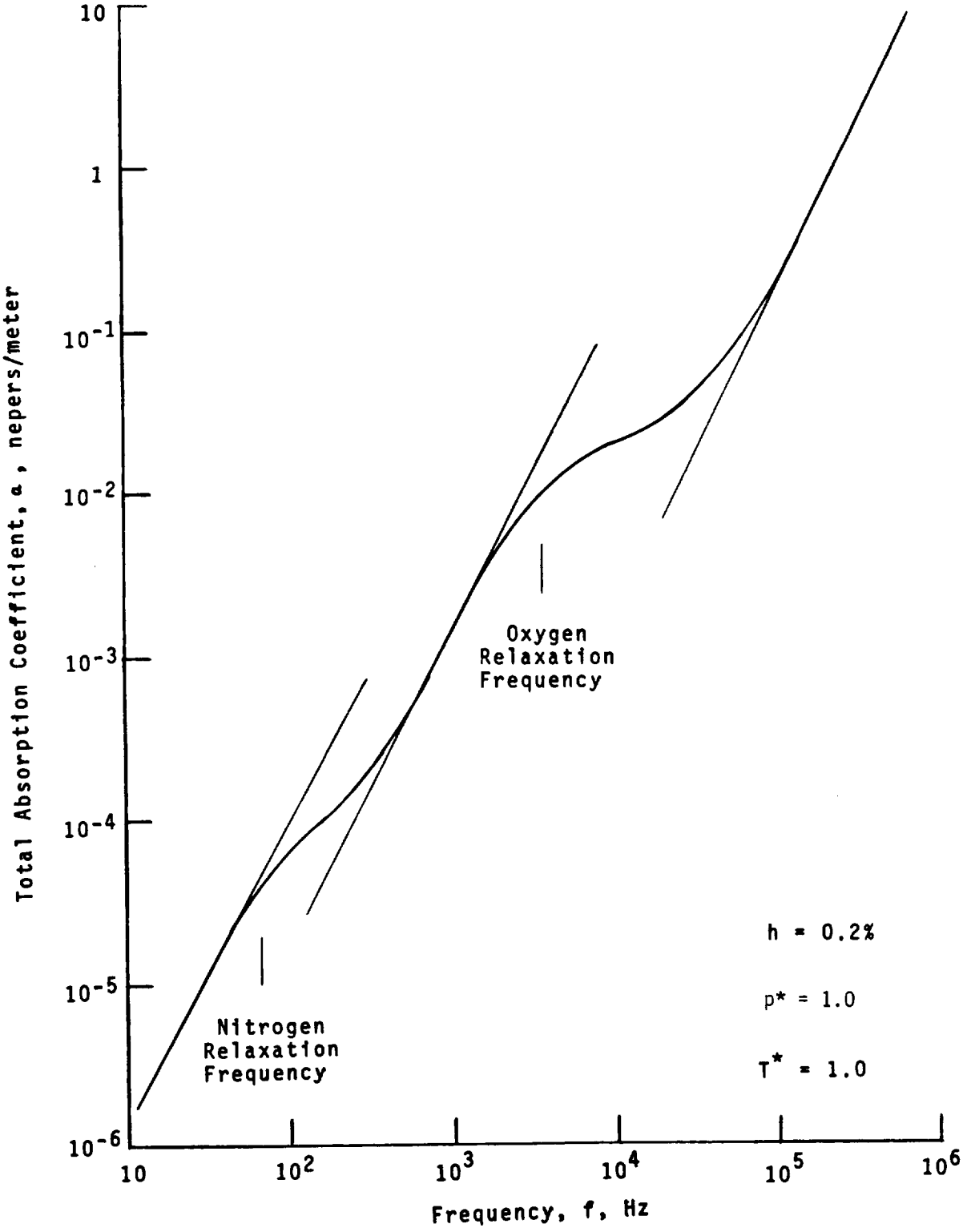

Figure 3.- Typical total absorption coefficient for standard sea level temperature and pressure.

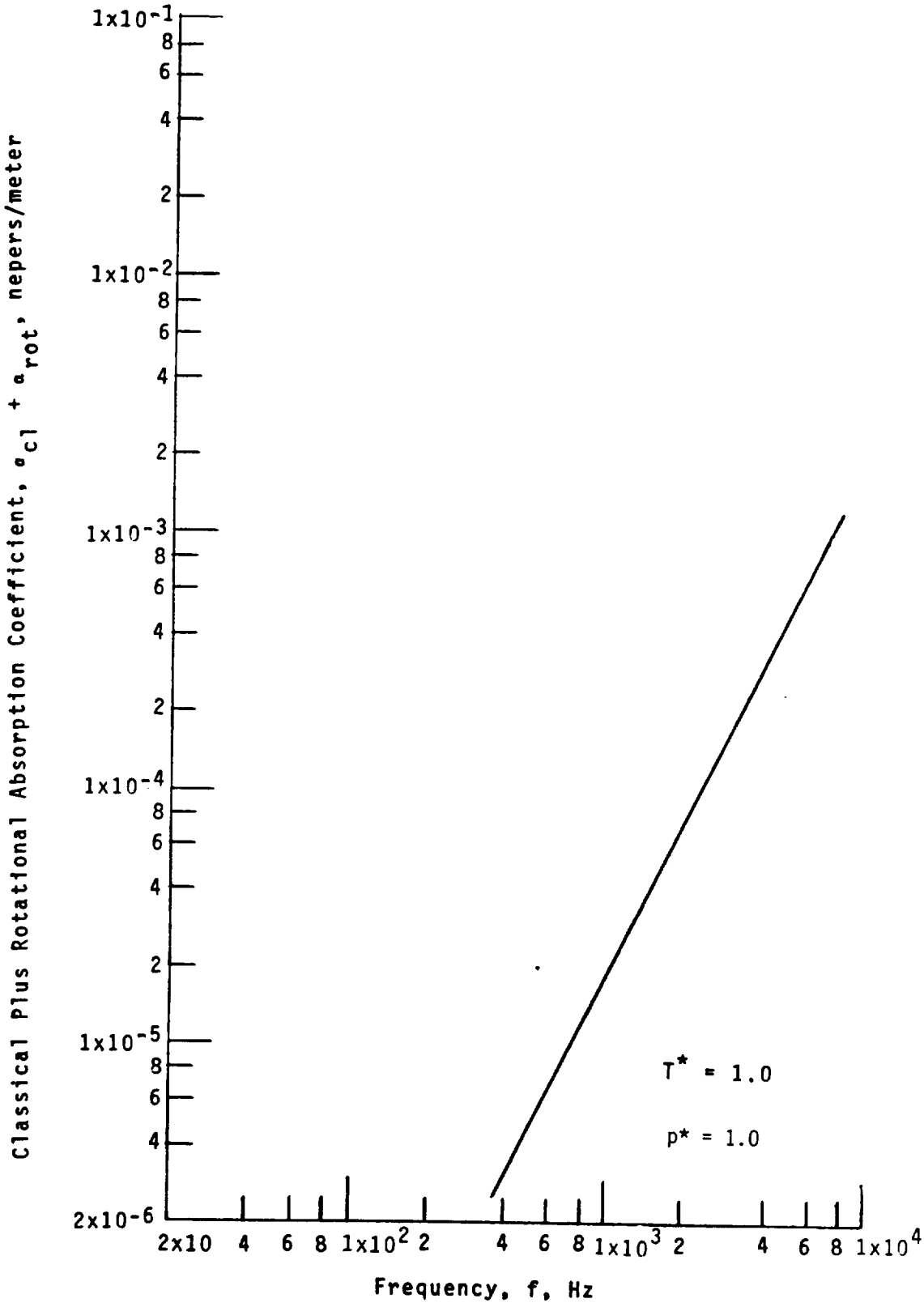

Figure 4.- Classical plus rotational absorption coefficient for standard sea level temperature and pressure.

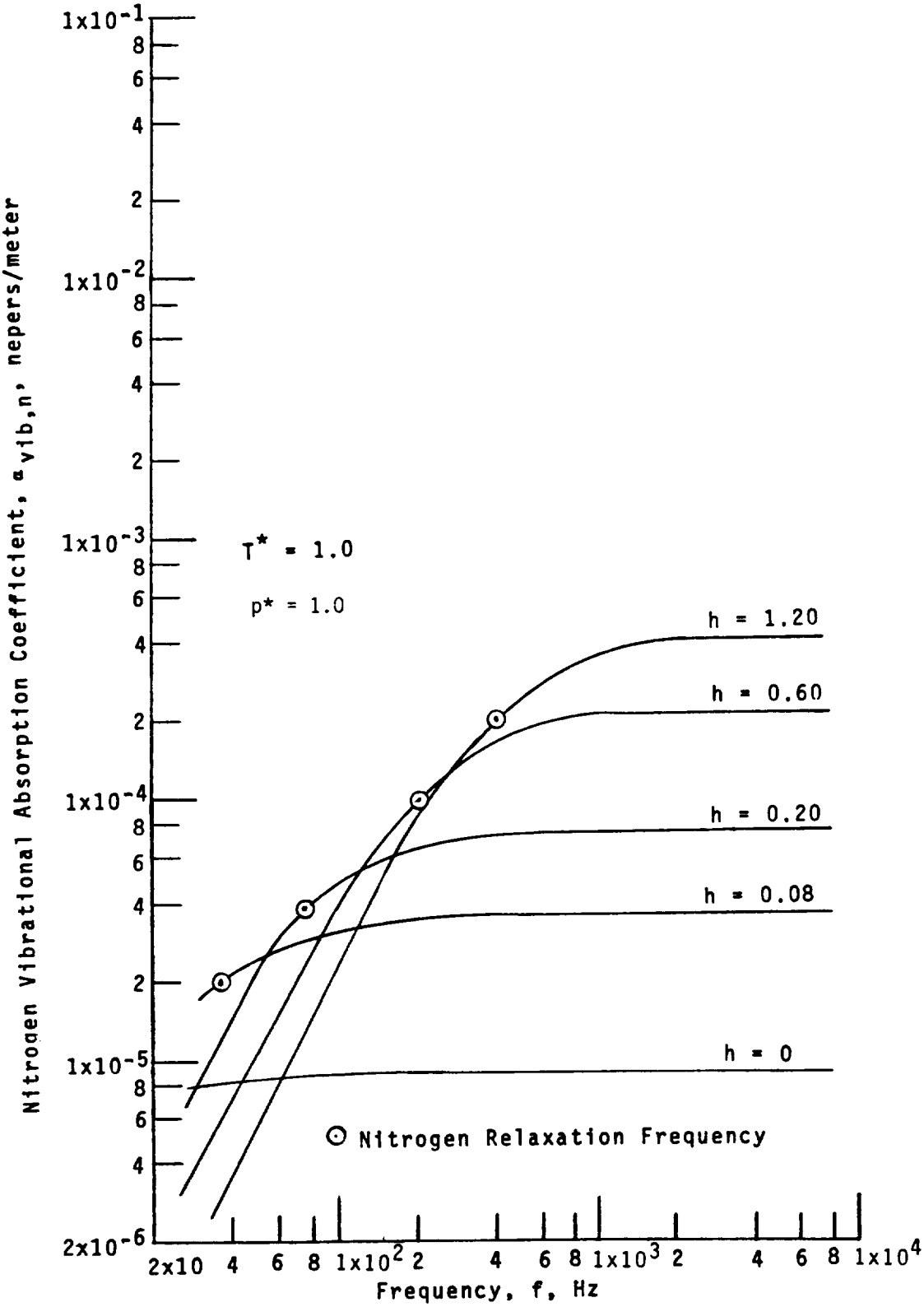

Figure 5.- Nitrogen vibrational absorption coefficient for standard sea level temperature and pressure.

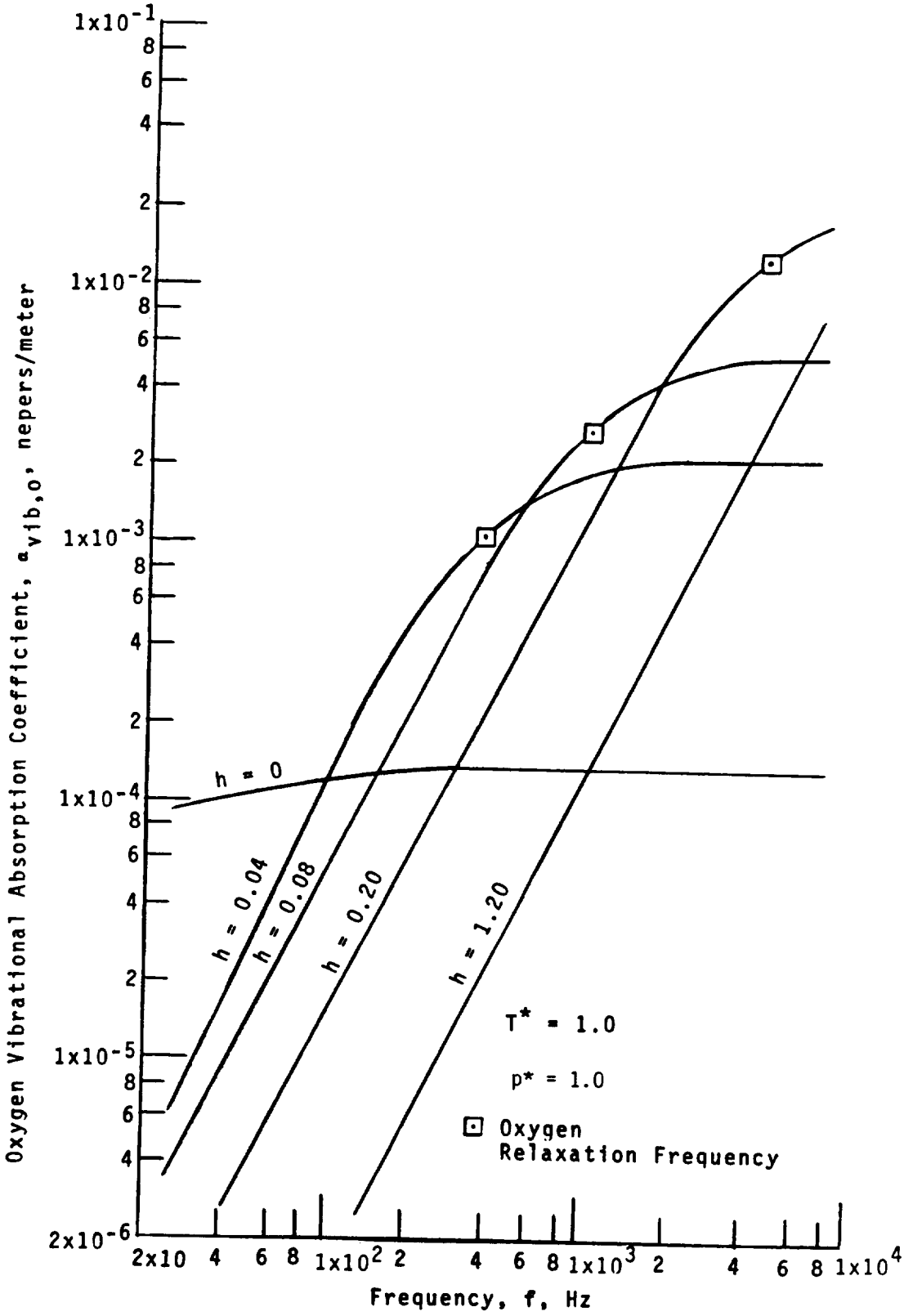

Figure 6.- Oxygen vibrational absorption coefficient for standard sea level temperature and pressure.

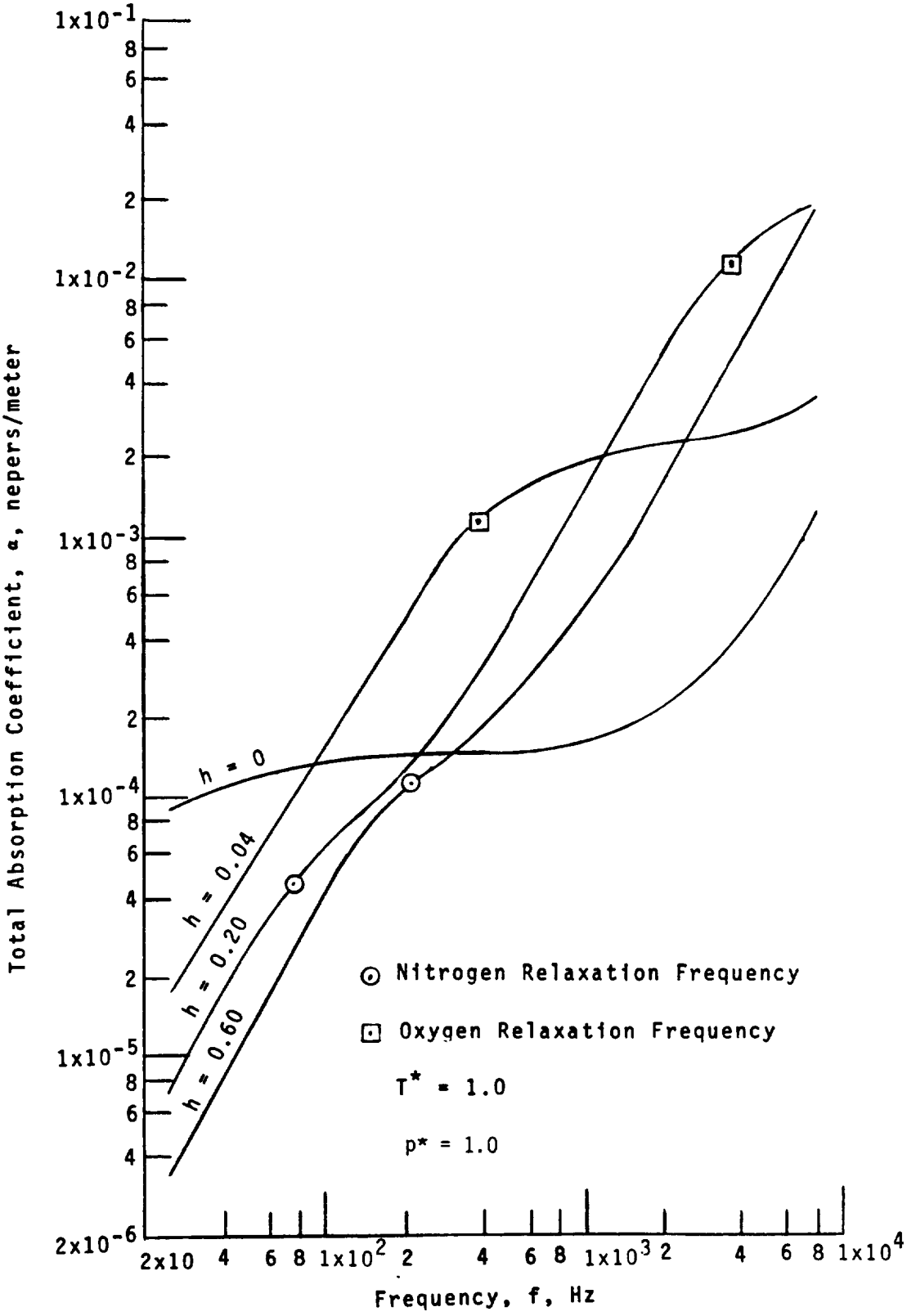

Figure 7.- Total absorption coefficient for standard sea level temperature and pressure.

3.2 GROUND REFLECTION AND ATTENUATION MODULE

INTRODUCTION

The noise produced by aircraft is of most concern during take-off and landing, when the observer and the aircraft are both close to the ground. The ground reflection and attenuation effects are a significant influence on the propagation of sound waves under these conditions. The presence of the Earth's surface causes a change in the sound spectrum due to the reflection and attenuation of the sound waves and the creation of surface waves. The ground reflection and attenuation must be properly accounted for in order to accurately predict the aircraft noise at the observer.

Sound waves which propagate nearly parallel to the Earth's surface may be attenuated by the absorption of the ground. The amount of attenuation is greatly dependent on the surface characteristics. A surface is characterized by a complex acoustic impedance. The sound waves can also be reflected by the ground and can either enhance or diminish the sound intensity received directly, depending on the phase-angle shift. Finally, surface waves can be produced in addition to the normal free-field spherical acoustic waves due to the ground influence. All of these effects must be accounted for to produce a complete model.

The ground-effects model chosen for ANOPP (ref. 1) is the Chien-Soroka theory (ref. 2). This theory, with the Delany and Bazley impedance function (ref. 3), assumes that the ground is a locally reacting uniform plane and that the source is a point source. This model has been validated (ref. 4) with the data of Parkin and Scholes (refs. 5 and 6).

The Ground Reflection and Attenuation Module computes a table of the ground-effects factor, which is a dimensionless coefficient incorporating the effects of reflection, attenuation, and surface waves. The ground-effects factor is tabulated in dimensionless form as a function of path-length difference, incidence angle, frequency, and source-to-observer distance.

SYMBOLS

a	incoherence constant
C	coherence coefficient
c	speed of sound, m/s (ft/s)
F	spherical-wave shape function
f	frequency, Hz

G ground-effects factor

H source altitude, m (ft)

h observer altitude, m (ft)

i unit imaginary number

K constant, $2^{1/(6N_b)}$

k wave number, $2\pi f/c$

N_b number of subbands per 1/3-octave band

N_d number of ground dips

$\langle p^2 \rangle$ mean-square pressure, Pa^2 (lb^2/ft^4)

R magnitude of complex spherical-wave reflection coefficient

r distance, m (ft)

U unit step function

α argument of complex spherical-wave reflection coefficient

Γ complex plane-wave reflection coefficient

Δr path-length difference, m (ft)

ε constant, $K - 1$

η $= 2\pi\rho f/\sigma$

θ incidence angle, deg

ν complex specific ground admittance

ρ density, kg/m^3 ($slugs/ft^3$)

σ specific flow resistance of ground, $kg/s\text{-}m^3$ ($lb/s\text{-}ft^3$)

τ $= (kr_2/2i)^{1/2}(\cos\theta + \nu)$

Subscripts:

c center band value

ff free field

gr ground effect

ℓ lower limit

u	upper limit
l	direct
2	reflected

INPUT

The basic independent variables for the model are path-length difference, incidence angle, frequency, and source-to-observer distance. The range of path-length differences is computed within the program based on the user-specified number of ground dips. The ranges for other variables are specified by upper and lower limits. The atmospheric properties of density and speed of sound and the specific flow resistance of the ground are also required. These values are assumed to be constant throughout the model. The number of 1/3-octave subband intervals adjusts the predicted effect for bandwidth. The incoherence constant is an empirical quantity which limits cancellation effects. The range and default values of each input are given in table I.

a	incoherence coefficient
c	speed of sound at the observer, m/s (ft/s)
(f_ℓ, f_u)	frequency lower and upper limits, Hz
N_b	number of subbands per 1/3-octave band
N_d	number of ground dips to be included
(r_ℓ, r_u)	source-to-observer distance lower and upper limits, m (ft)
(θ_ℓ, θ_u)	incidence angle lower and upper limits, deg
ρ	air density at the observer, kg/m^3 ($slugs/ft^3$)
σ	specific flow resistance of the ground, $kg/s\text{-}m^3$ ($slugs/s\text{-}ft^3$)

OUTPUT

The module produces a table of the ground-effects factor as a function of four dimensionless parameters: path-length difference, cosine of incidence angle, frequency, and source-image-to-observer distance.

Ground Effects Table

$k\Delta r$	path-length difference
$\cos\theta$	cosine of incidence angle

η $= 2\pi\rho f/\sigma$

kr_2 image distance

$G(k\Delta r, \cos\theta, \eta, kr_2)$ ground-effects factor

METHOD

The ground-effects geometry is shown in figure 1. A source is located at an altitude H over a ground plane. Sound arrives at the receiver at a height h from the direct path r_1 and from a reflected path r_2, which appears to the observer to be from an image source. The incidence angle of the reflected wave is θ. The path-length difference $\Delta r = r_2 - r_1$ is the most significant parameter of ground effects. As shown in figure 2, the path-length difference can be approximated in terms of the observer height and the incidence angle as

$$\Delta r \approx 2h \cos\theta \tag{1}$$

The Chien-Soroka theory is derived from a solution to the wave equation in the half space of figure 1. The derivation of the theory is presented in references 1 and 2. The resulting expression for the mean-square pressure with ground effect $\langle p^2 \rangle_{gr}$ is

$$\langle p^2 \rangle_{gr} = \langle p^2 \rangle_{ff} \left[1 + R^2 + 2RC \cos(\alpha + k\Delta r)\right] \tag{2}$$

where $\langle p^2 \rangle_{ff}$ is the free-field mean-square pressure, C is the coherence coefficient, k is the wave number, R is the magnitude, and α is the argument of the complex spherical-wave reflection coefficient. The term in brackets in equation (2) is referred to as the ground-effects factor G and is defined as follows:

$$G = \langle p^2 \rangle_{gr} / \langle p^2 \rangle_{ff} \tag{3}$$

The coherence coefficient C is the fraction of the initial acoustic energy in which phase relation is maintained throughout the propagation process. A reasonable approximation for the coherence coefficient is made by assuming a Gaussian distribution of the form

$$C = \exp\left[-(ak\Delta r)^2\right] \tag{4}$$

where a is the incoherence constant and exp denotes the exponential function. The incoherence constant is normally given a value of 0.01,

which corresponds to a value of C of 0.37 at a Δr value of 16 wavelengths. After substitution of equation (4), the ground-effects factor becomes the following:

$$G = 1 + R^2 + 2R \exp\left[-(ak\Delta r)^2\right] \cos(\alpha + k\Delta r) \tag{5}$$

The Chien-Soroka theory (ref. 2) shows that the complex spherical-wave reflection coefficient can be expressed as follows:

$$Re^{i\alpha} = \Gamma + (1 - \Gamma)F(\tau) \tag{6}$$

where Γ is the complex plane-wave reflection coefficient given as

$$\Gamma = (\cos\theta - \nu)/(\cos\theta + \nu) \tag{7}$$

and $F(\tau)$ accounts for the spherical-wave shape. In this equation ν is the complex specific ground admittance. The function $F(\tau)$ in equation (6) is

$$F(\tau) = 1 - \sqrt{\pi}\,\tau\, W(i\tau) \tag{8}$$

where

$$\tau = (kr_2/2i)^{1/2}(\cos\theta + \nu) \tag{9}$$

and W is the following complex error function:

$$W(z) = \frac{i}{\pi}\int_{-\infty}^{\infty} \frac{e^{-t^2}}{z - t}\,dt \qquad (\mathrm{Im}(z) > 0) \tag{10}$$

For any value of $|\tau| > 10$, an asymptotic approximation for the complex error function is used. This allows $F(\tau)$ to be expressed as the following:

$$F(\tau) = -2\sqrt{\pi}\,U\left[-\mathrm{Re}(\tau)\right]\tau e^{\tau^2} + \frac{1}{2\tau^2} - \frac{3}{(2\tau^2)^2} \tag{11}$$

where U is the unit step function defined as follows:

$$\left.\begin{aligned} U(S) &= 1 && (S > 0) \\ U(S) &= 1/2 && (S = 0) \\ U(S) &= 0 && (S < 0) \end{aligned}\right\} \qquad (12)$$

The remaining parameter to be determined is the complex specific ground admittance ν. Delaney and Bazley (ref. 3) developed the following empirical equation for ν:

$$\nu = \left[1 + (6.86\eta)^{-0.75} + i(4.36\eta)^{-0.73}\right]^{-1} \qquad (13)$$

where the dimensionless frequency η is

$$\eta = 2\pi\rho f/\sigma \qquad (14)$$

A graph of the ground admittance is shown in figure 3.

For an acoustically hard surface ($\eta = 0$), the theory is greatly simplified since $\eta = 0$, $\Gamma = 1$, $R = 1$, and $\alpha = 0$. The expression for the ground-effects factor reduces to

$$G = 2 + 2\exp\left[-(ak\Delta r)^2\right]\cos(k\Delta r) \qquad (15)$$

which is a function of $k\Delta r$ only.

Actual noise predictions are given for finite-frequency bandwidths. In order to approximate the effect of finite bandwidth, the ground-effects factor is integrated over the band, but only the variation of the term $\cos(\alpha + k\Delta r)$ is included as a variable in the integration. It is assumed that the variation of the other terms in the width of 1 band is small. This approximation is acceptable for 1/3-octave or narrower bands (ref. 4).

For purposes of analyzing attenuation and reflection effects, the standard 1/3-octave bands of sound are subdivided into N_b subbands, where N_b is an odd number. Using an odd number gives a center subband which has a center frequency equal to the center frequency of the original 1/3-octave band.

The ratio of the subband limit frequencies is $2^{1/(3N_b)}$, so that the integral for averaging the cosine term over the subband is the following:

$$\langle \cos\ (\alpha + k\Delta r) \rangle = \frac{1}{\Delta f} \int_{f_c/K}^{Kf_c} \cos\ (\alpha + k\Delta r)\ df \tag{16}$$

where $K = 2^{1/(6N_b)}$, $\Delta f = (K - K^{-1})f_c$, and f_c is the center frequency of the subband. Assuming that α remains constant throughout the subband, an approximation for equation (16) is expressed as

$$\langle \cos\ (\alpha + k\Delta r) \rangle = \cos\ (\alpha + k_c\Delta r)\ \frac{\sin\ (\varepsilon k_c \Delta r)}{\varepsilon k_c \Delta r} \tag{17}$$

where k_c is the subband center wave number and $\varepsilon = K - 1$. This produces the following final expression for the ground-effects factor:

$$G = 1 + R^2 + 2R\left\{\exp\left[-(ak\Delta r)^2\right]\right\} \cos\ (\alpha + k\Delta r)\ \frac{\sin\ (\varepsilon k\Delta r)}{\varepsilon k\Delta r} \tag{18}$$

where it is understood that k refers to the subband center wave number. For an acoustically hard surface, the averaged expression for the final band is

$$G = 2 + 2\left\{\exp\left[-(ak\Delta r)^2\right]\right\} \cos\ (k\Delta r)\ \frac{\sin\ (\varepsilon k\Delta r)}{\varepsilon k\Delta r} \tag{19}$$

A plot of G as a function of $k\Delta r$ is presented in figure 4 for the case of an acoustically hard surface.

It is apparent from figure 4 that the ground-effects factor has a series of nodes occurring at values of $k\Delta r$ of $(2n - 1)\pi$, where $n = 1, 2, \ldots, n + 1$. These nodes are caused by the cancellation of sound intensity between the direct and reflected waves and are commonly referred to as ground dips. It is imperative that the value of G at the minimum of each ground dip as well as at intermediate points be evaluated to adequately define the function; however, after the fifth dip ($N_d = 5$) the variation in G for increasing values of $k\Delta r$ is so small that it can be assumed to be constant. If this condition is not met, the user can provide a different value for N_d. In addition, the frequency, source-to-observer distance, and incidence-angle range of interest are user inputs. These three variable ranges are divided into equally spaced intervals.

For most conditions of interest for which the noise-generation models are valid, the source and observer separation is large. This means that h/r is much less than unity. Under this condition it can be assumed that $r_2 \approx r_1$ and $\Delta r \simeq 2h \cos\theta \approx 2hH/r_1$.

The output of the module is a table of the ground-effects-factor values as functions of four dimensionless variables: $k\Delta r$, $\cos \theta$, η, and kr_2. For a hard surface, the last three variables do not affect the ground-effects factor. In this case, the module output is a four-dimensional table with only one entry in each of the dimensions $\cos \theta$, η, and kr_2. The interpolation logic produces the same result for this table as it would for a one-dimensional table in $k\Delta r$.

In reference 4, the ground effects predicted by this method have been compared to the ground-to-ground propagation data from references 5 and 6. The predictions and data are in fair to good agreement in this case. Recent comparisons of this method with T-38A flyover data given in reference 7 and Boeing 747 flyover data given in reference 8 show that the predicted frequency of maximum ground attenuation agrees very well with the measured frequency. The amplitudes of the predicted attenuation are generally smaller than the measured amplitudes, indicating that the Chien-Soroka method may be a conservative estimate of the effects of ground reflection and attenuation.

REFERENCES

1. Pao, S. Paul; Wenzel, Alan R.; and Oncley, Paul B.: Prediction of Ground Effects on Aircraft Noise. NASA TP-1104, 1978.

2. Chien, C. F.; and Soroka, W. W.: Sound Propagation Along an Impedance Plane. J. Sound & Vib., vol. 43, no. 1, Nov. 8, 1975, pp. 9-20.

3. Delany, M. E.; and Bazley, E. N.: Acoustical Properties of Fibrous Absorbent Materials. Appl. Acoust., vol. 3, no. 2, Apr. 1970, pp. 105-116.

4. Zorumski, William E.: Prediction of Aircraft Sideline Noise Attenuation. NASA TM-78717, 1978.

5. Parkin, P. H.; and Scholes, W. E.: The Horizontal Propagation of Sound From a Jet Engine Close to the Ground, at Radlett. J. Sound & Vib., vol. 1, no. 1, Jan. 1964, pp. 1-13.

6. Parkin, P. H.; and Scholes, W. E.: The Horizontal Propagation of Sound From a Jet Engine Close to the Ground, at Hatfield. J. Sound & Vib., vol. 2, no. 4, Oct. 1965, pp. 353-374.

7. Willshire, William L., Jr.: Assessment of Ground Effects on the Propagation of Aircraft Noise: The T-38A Flight Experiment. NASA TP-1747, 1980.

8. Willshire, William L., Jr.: Lateral Attenuation of High-By-Pass Ratio Engined Aircraft Noise. NASA TM-81968, 1981.

TABLE I.- RECOMMENDED RANGES FOR INPUT PARAMETERS

Input	Minimum	Default	Maximum
a	0.001	0.010	0.100
c, m/s	300	340.294	400
f_ℓ, Hz	13	50	
f_u, Hz		2000	4000
N_b	1	5	9
N_d	2	5	10
r_ℓ, m	10	10	
r_u, km		10	10
θ_ℓ, deg	0	0	
θ_u, deg		89	89
ρ, kg/m^3	1.0	1.225	1.5
σ, $kg/s\text{-}m^3$	1.0×10^5	2.5×10^5	5.0×10^5

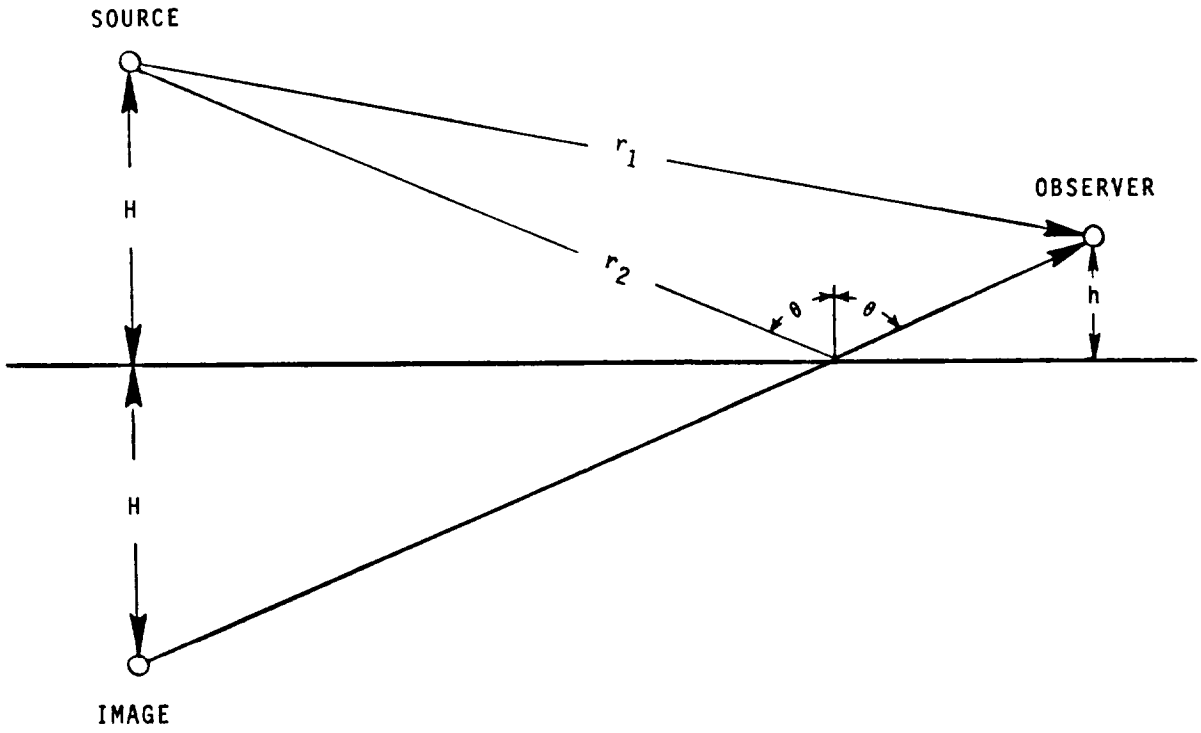

Figure 1.- Ground-effects geometry.

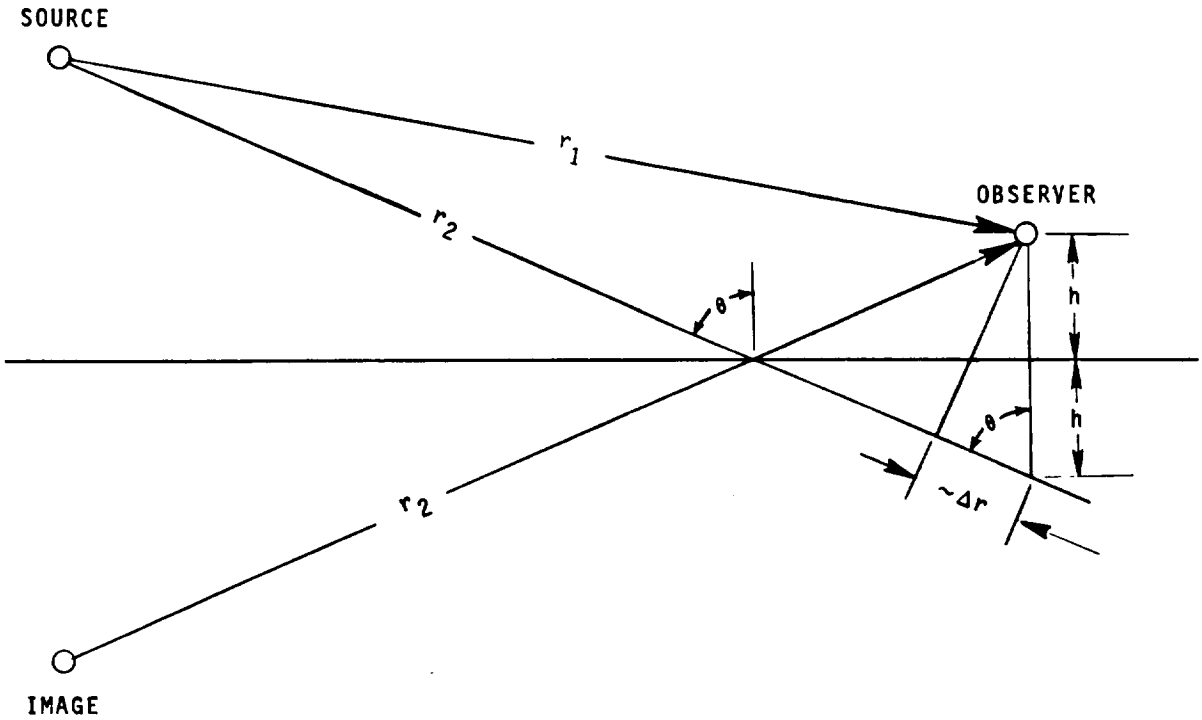

Figure 2.- Derivation of path-length difference.

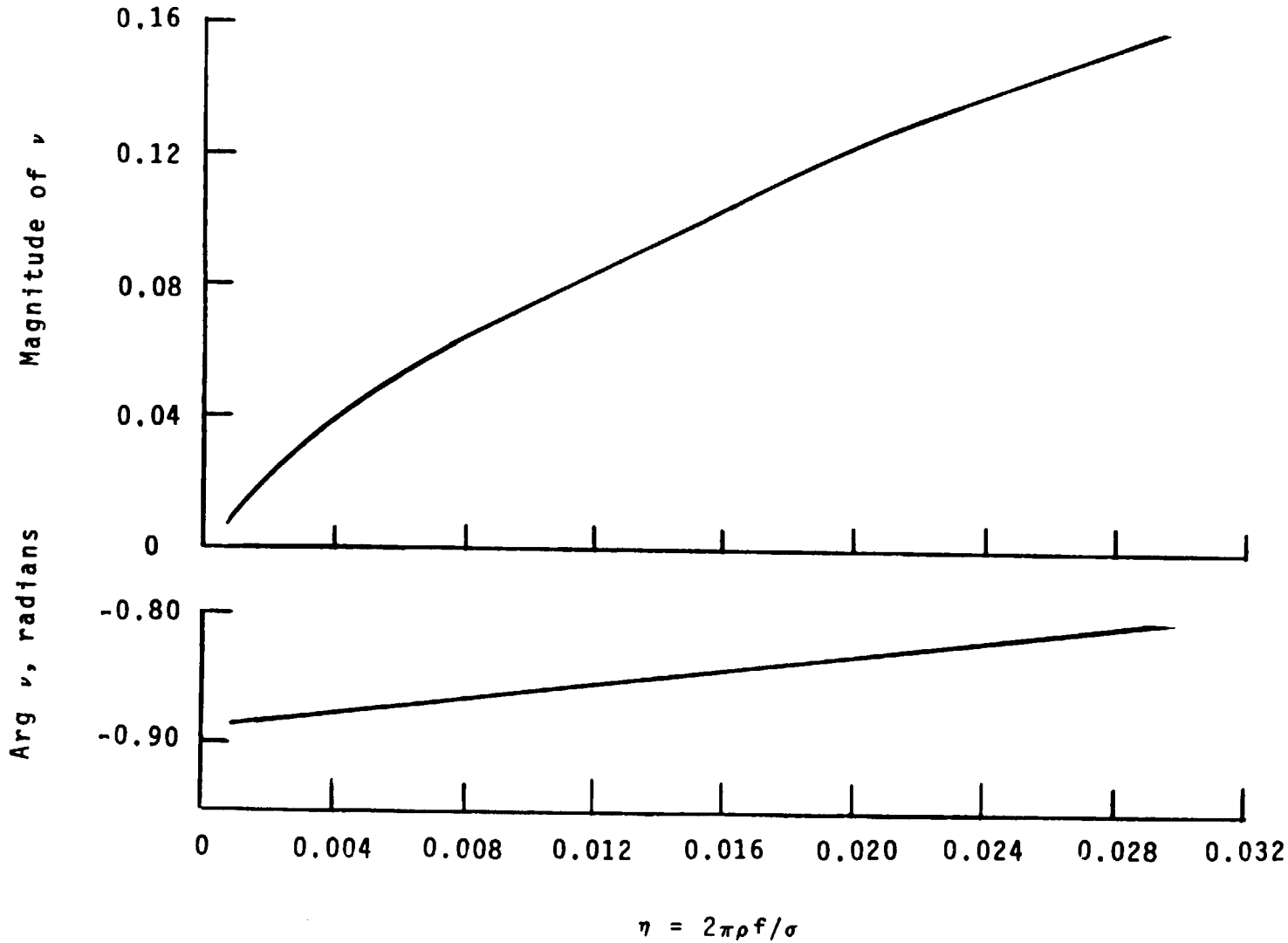

Figure 3.- Empirical function for normalized ground admittance.

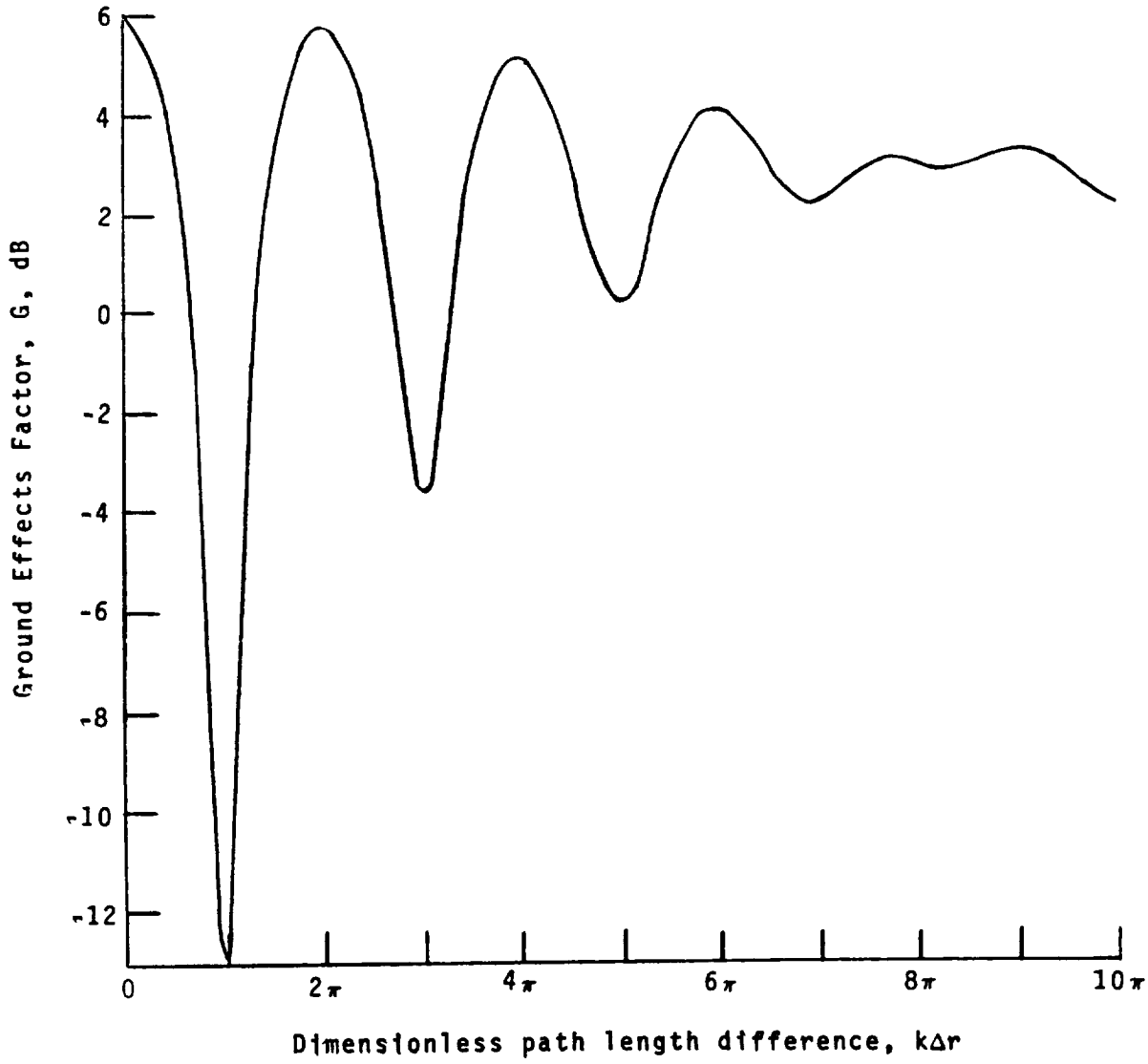

Figure 4.- Ground-effects factor for acoustically hard surface.

4. SOURCE NOISE PARAMETERS

4.1 FAN NOISE PARAMETERS MODULE

INTRODUCTION

Fan noise is a significant part of the total noise produced by turbojet and turbofan engines. Fan noise prediction methods are included in ANOPP. The purpose of the Fan Noise Parameters Module is to generate the physical parameters required by Heidmann's method (ref. 1) for fan noise prediction for turbojet and turbofan engines.

The fan entrance and exit flow states are provided by the user. These engine-state data are first converted to a function of time, using data from the flight-path characteristics. The required fan parameters for fan noise prediction are then computed.

SYMBOLS

A	area, m^2 (ft^2)
c	speed of sound, m/s (ft/s)
D	fan diameter, m (ft)
M_∞	aircraft Mach number
$\dot{m}$	mass flow rate, kg/s (slugs/s)
N	rotational speed, Hz
n	number of source times
p	pressure, Pa (lb/ft^2)
R	dry-air gas constant, $m^2/K\text{-}s^2$ ($ft^2/{}^oR\text{-}s^2$)
T	temperature, K (^oR)
t	time, s
γ	ratio of specific heats
π	power setting
ρ	density, kg/m^3 ($slugs/ft^3$)

Subscripts:

e	engine
i	entrance
j	exit
t	total
∞	ambient

Superscript:

*	dimensionless quantity

INPUT

This module provides the parameters for a typical axial-flow fan as shown in figure 1. The entrance and exit flow states for the fan are required from the user. The engine power setting, aircraft Mach number, and ambient density and speed of sound are provided by the engine variable table.

Fan Entrance Flow State

π	engine power setting
M_∞	aircraft Mach number
$\dot{m}_i^*(\pi, M_\infty)$	mass flow rate, re $A_e p_\infty / \sqrt{RT_\infty}$
$N^*(\pi, M_\infty)$	rotational speed, re $\sqrt{RT_\infty}/D$
$T_{t,i}^*(\pi, M_\infty)$	total temperature, re T_∞

Fan Exit Flow State

π	engine power setting
M_∞	aircraft Mach number
$\dot{m}_j^*(\pi, M_\infty)$	mass flow rate, re $\rho_\infty A_e p_\infty / \sqrt{RT_\infty}$
$T_{t,j}^*(\pi, M_\infty)$	total temperature, re T_∞

Engine Variable Table

t	source time, s
$M_\infty(t)$	aircraft Mach number

$\pi(t)$ engine power setting

$c_\infty(t)$ ambient speed of sound, m/s (ft/s)

$\rho_\infty(t)$ ambient density, kg/m^3 (slugs/ft^3)

OUTPUT

The outputs to this module are the physical parameters required for execution of the fan noise modules as a function of source time.

Fan Noise Parameters

n number of source time values

t source time, s

$\dot{m}_i^*(t)$ entrance mass flow rate, re $\rho_\infty c_\infty A_e$

$\dot{m}_j^*(t)$ exit mass flow rate, re $\rho_\infty c_\infty A_e$

$N^*(t)$ rotational speed, re c_∞/D

$\Delta T^*(t)$ total temperature rise across fan, re T_∞

Ambient Conditions

$c_\infty(t)$ ambient speed of sound, m/s (ft/s)

$M_\infty(t)$ aircraft Mach number

$\rho_\infty(t)$ ambient density, kg/m^3 (slugs/ft^3)

METHOD

The fan entrance and exit flow states are expressed as a function of the engine power setting π and the aircraft Mach number M_∞. These tables must be provided directly by the user. These data are converted to a function of source time. The engine variable table gives M_∞ and π as a function of source time as provided by the Flight Dynamics Module or the user.

The fan entrance and exit mass flow rate and the fan rotational speed must be converted to the referred variables used by the Fan Noise Module by the relations

$$\dot{m}^*(t) = \frac{\dot{m}^*}{\sqrt{\gamma}} \tag{1}$$

and

$$N^*(t) = \frac{N^*}{\sqrt{\gamma}} \tag{2}$$

where the ambient value of the ratio of specific heats γ is 1.4. Finally, the temperature rise across the fan ΔT^* is the difference in total temperature,

$$\Delta T^* = T^*_{t,j} - T^*_{t,i} \tag{3}$$

REFERENCE

1. Heidmann, M. F.: Interim Prediction Method for Fan and Compressor Source Noise. NASA TM X-71763, 1975.

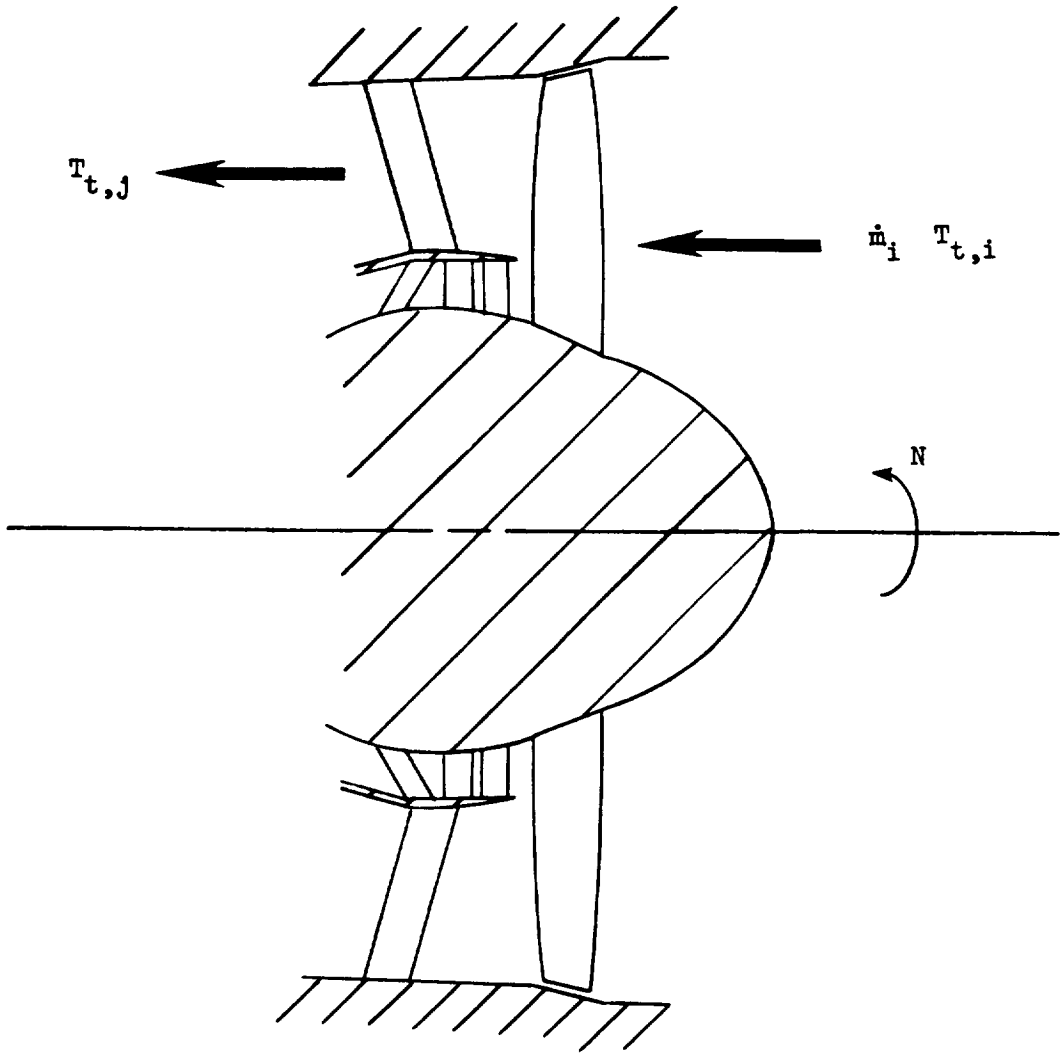

Figure 1.- Schematic diagram of a typical axial-flow fan.

4.2 CORE NOISE PARAMETERS MODULE

INTRODUCTION

Core noise is a significant part of the total noise produced by turboprop, turbofan, and turbojet engines. Core noise prediction methods are included in ANOPP. The purpose of the Core Noise Parameters Module is to generate the physical parameters required for a core noise prediction module.

The core entrance and exit flow states are provided by the user. These engine-state data are first converted to a function of time, using data from the flight-path characteristics. The required core parameters for core noise prediction are then computed.

SYMBOLS

A	area, m^2 (ft^2)
c_∞	ambient speed of sound, m/s (ft/s)
M_∞	aircraft Mach number
$\dot{m}$	mass flow rate, kg/s (slugs/s)
n	number of source times
p	pressure, Pa (lb/ft^2)
R	dry-air gas constant, $m^2/K\text{-}s^2$ ($ft^2/{}^\circ R\text{-}s^2$)
T	temperature, K ($^\circ R$)
t	time, s
π	engine power setting
ρ	density, kg/m^3 ($slugs/ft^3$)

Subscripts:

e	engine
i	entrance
j	exit

t total

∞ ambient

Superscript:

$*$ dimensionless quantity

INPUT

The entrance and exit combustor flow states are required from the user. The engine power settings and aircraft Mach numbers in the engine variable table are provided by the Flight Dynamics Module or the user.

Core Entrance Flow State

π engine power setting

M_∞ aircraft Mach number

$\dot{m}_i^*(\pi, M_\infty)$ mass flow rate, re $A_e p_\infty / \sqrt{RT_\infty}$

$p_{t,i}^*(\pi, M_\infty)$ total pressure, re p_∞

$T_{t,i}^*(\pi, M_\infty)$ total temperature, re T_∞

Core Exit Flow State

π engine power setting

M_∞ aircraft Mach number

$T_{t,j}^*(\pi, M_\infty)$ total temperature, re T_∞

Engine Variable Table

t source time, s

$M_\infty(t)$ aircraft Mach number

$\pi(t)$ engine power setting

$c_\infty(t)$ ambient speed of sound, m/s (ft/s)

$\rho_\infty(t)$ ambient density, kg/m^3 ($slugs/ft^3$)

OUTPUT

The outputs to this module are the physical parameters required for the execution of the core noise modules as a function of source time.

Core Noise Parameters

n	number of source time values
t	source time, s
$\dot{m}_i^*(t)$	combustor entrance mass flow rate, re $\rho_\infty c_\infty A_e$
$p_i^*(t)$	combustor entrance total pressure, re p_∞
$T_i^*(t)$	combustor entrance total temperature, re T_∞
$T_j^*(t)$	combustor exit total temperature, re T_∞

Ambient Conditions

$c_\infty(t)$	ambient speed of sound, m/s (ft/s)
$M_\infty(t)$	aircraft Mach number
$\rho_\infty(t)$	ambient density, kg/m^3 (slugs/ft^3)

METHOD

A schematic diagram of a typical combustor depicting the entrance and exit flow states is shown in figure 1. These flow states are a function of the engine power setting π and the aircraft Mach number M_∞. These data are converted to a function of source time by interpolating the core flow state tables with respect to $M_\infty(t)$ and $\pi(t)$ values from the engine variable table. In addition, the combustor entrance mass flow rate must be converted to the referred variables used by the Combustion Noise Module by the relation

$$\dot{m}_i^*(t) = \frac{\dot{m}_i^*}{\sqrt{\gamma}} \tag{1}$$

where the ambient value of the ratio of specific heats γ is 1.4.

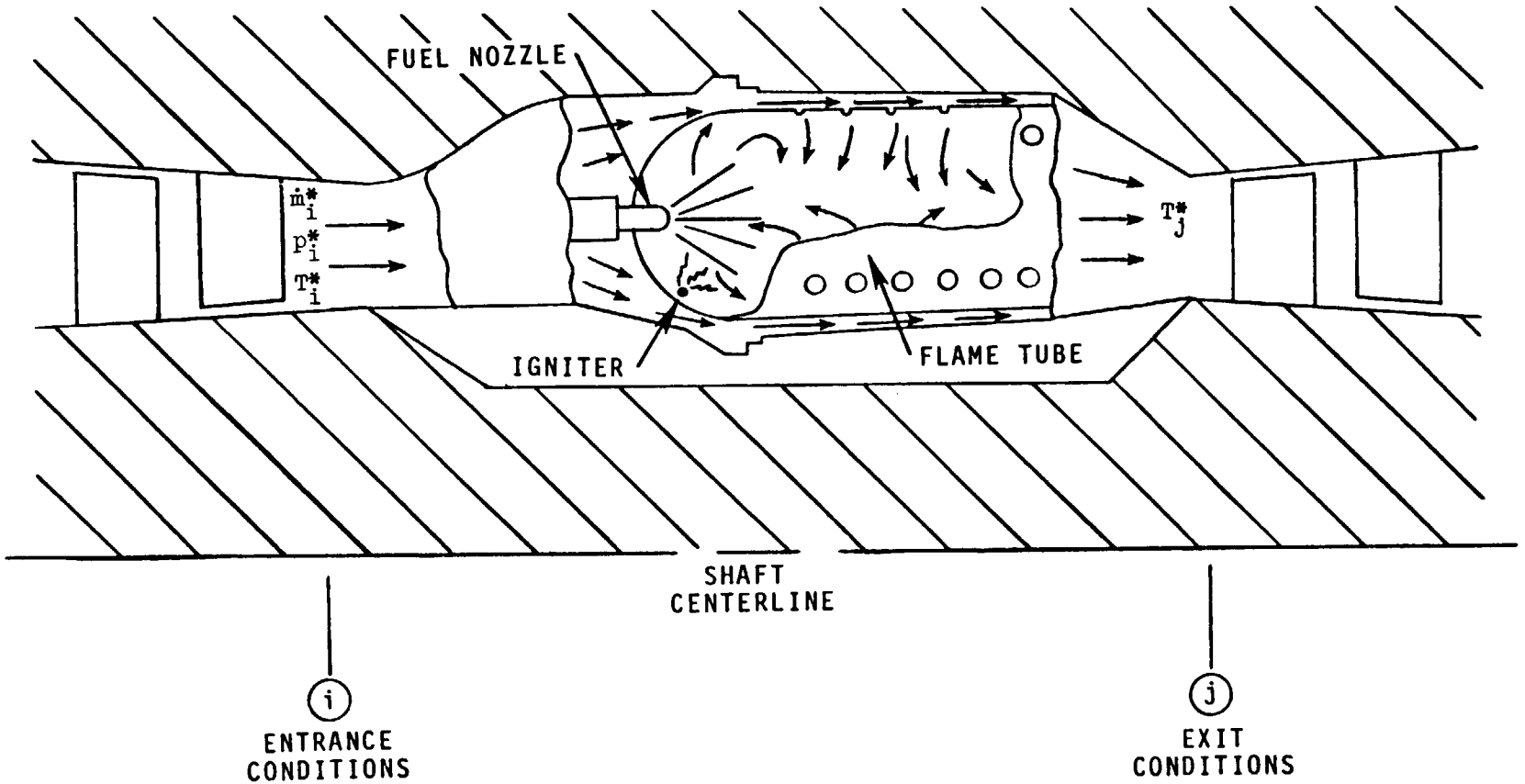

Figure 1.- Schematic diagram of can-type combustor.

4.3 TURBINE NOISE PARAMETERS MODULE

INTRODUCTION

Turbine noise is a significant part of the total noise produced by turbofan and turbojet engines during low-power operations. Turbine noise modules are included in ANOPP. The purpose of the Turbine Noise Parameters Module is to generate the physical parameters required for turbine noise prediction for turbojet and turbofan engines.

The turbine entrance and exit flow states are provided by the user. These engine-state data are first converted to a function of time, using data from the flight-path characteristics. The required turbine parameters for turbine noise prediction are then computed.

SYMBOLS

A	area, m^2 (ft^2)
c	speed of sound, m/s (ft/s)
D	turbine rotor diameter, m (ft)
f	fuel-to-air ratio
h^*	specific enthalpy, re $\mathcal{R}T_\infty$
h_a	absolute humidity, percent mole fraction
M	Mach number
M_∞	aircraft Mach number
$\dot{m}$	mass flow rate, kg/s (slugs/s)
N	rotational speed, Hz
n	number of source times
p	pressure, Pa (lb/ft^2)
R	dry-air gas constant, $m^2/K\text{-}s^2$ ($ft^2/{}^oR\text{-}s^2$)
$\mathcal{R}$	gas constant, $m^2/K\text{-}s^2$ ($ft^2/{}^oR\text{-}s^2$)
T	temperature, K (^oR)
t	time, s

γ ratio of specific heats

π engine power setting

ρ density, kg/m^3 ($slugs/ft^3$)

ϕ^* specific entropy function, re R

Subscripts:

e engine

i entrance

j exit

s static

t total

∞ ambient

Superscript:

* dimensionless quantity

INPUT

This module provides the parameters for a typical axial-flow turbine as shown in figure 1. The entrance and exit flow states for the turbine are required from the user for predicting the turbine noise. The engine power settings, aircraft Mach numbers, and ambient densities are provided by the engine variable tables.

Turbine Entrance Flow State

π engine power setting

M_∞ aircraft Mach number

$\dot{m}_i^*(\pi, M_\infty)$ mass flow rate, re $A_\infty p_\infty / \sqrt{RT_\infty}$

$N^*(\pi, M_\infty)$ rotational speed, re $\sqrt{RT_\infty}/D$

$T_{t,i}^*(\pi, M_\infty)$ total temperature, re T_∞

Turbine Exit Flow State

π engine power setting

M_∞ aircraft Mach number

$A_j^*(\pi,M_\infty)$	turbine exit area, re A_e
$f(\pi,M_\infty)$	fuel-to-air ratio
$\dot{m}_j^*(\pi,M_\infty)$	exit mass flow rate, re $A_e p_\infty / \sqrt{RT_\infty}$
$p_{t,j}^*(\pi,M_\infty)$	exit total pressure, re p_∞
$T_{t,j}^*(\pi,M_\infty)$	exit total temperature, re T_∞

Engine Variable Table

t	source time, s
$M_\infty(t)$	aircraft Mach number
$\pi(t)$	engine power setting
$c_\infty(t)$	ambient speed of sound, m/s (ft/s)
$\rho_\infty(t)$	ambient density, kg/m^3 ($slugs/ft^3$)
$h_a(t)$	absolute humidity, percent mole fraction

OUTPUT

The outputs of this module are the physical parameters required for the execution of the turbine noise modules as a function of source time.

Turbine Noise Parameters

n	number of source time values
t	source time, s
$f(t)$	fuel-to-air ratio
$\dot{m}^*(t)$	mass flow rate, re $\rho_\infty c_\infty A_e$
$N^*(t)$	rotational speed, re c_∞/D
$T_{t,i}^*(t)$	entrance total temperature, re T_∞
$T_{s,j}^*(t)$	exit static temperature, re T_∞

Ambient Conditions

$c_\infty(t)$	ambient speed of sound, m/s (ft/s)
$h_a(t)$	absolute humidity, percent mole fraction

$M_\infty(t)$ aircraft Mach number

$\rho_\infty(t)$ ambient density, kg/m^3 (slugs/ft^3)

METHOD

The turbine entrance and exit flow states are expressed as a function of the engine power setting π and the aircraft Mach number M_∞. These tables are provided directly by the user. These data are converted to a function of source time. The engine variable table gives M_∞ and π as a function of source time as provided by the Flight Dynamics Module or the user.

The turbine rotational speed and mass flow rate must be converted to the referred variables used by the turbine noise modules by the relation

$$N^*(t) = \frac{N^*}{\sqrt{\gamma}} \tag{1}$$

and

$$\dot{m}^*(t) = \frac{\dot{m}^*}{\sqrt{\gamma}} \tag{2}$$

where the ambient value of the ratio of specific heats γ is 1.4. The turbine exit static temperature $T^*_{s,j}$ is required by the turbine noise modules for the computation of the ideal work extraction. The exit static temperature can be computed assuming either constant specific heats or variable specific heats.

Constant Specific Heats

The ratio of specific heats at the turbine exit γ_t and the dimensionless gas constant $R^* = R/R$ are computed from the total temperature $T^*_{t,j}$, fuel-to-air ratio f, and absolute humidity h_a, using the appropriate thermodynamic utility. The turbine exit Mach number M_j can be computed by the relation

$$\frac{\dot{m}^*_j \sqrt{R^* T^*_{t,j}}}{A^*_j \, p^*_{t,j}} = \sqrt{\gamma_t}\, M_j \left(1 + \frac{\gamma_t - 1}{2} M^2\right)^{-\frac{1}{2}\frac{\gamma_t+1}{\gamma_t-1}} \tag{3}$$

as discussed in Thermodynamic Utilities. Then, the turbine exit static temperature $T^*_{s,j}$ is

$$T^*_{s,j} = T^*_{t,j}\left(1 + \frac{\gamma_t - 1}{2} M_j^2\right)^{-1} \tag{4}$$

Variable Specific Heats

As discussed in Thermodynamic Utilities, the static temperature $T^*_{s,j}$ can be computed from simultaneous solution of

$$\frac{p^*_{s,j}}{p^*_{t,j}} = e^{-\left(\phi^*_t - \phi^*_s\right)} \tag{5}$$

and

$$\frac{\dot{m}^*_j \sqrt{RT^*_{t,j}}}{A^*_j\, p^*_{t,j}} = \frac{\sqrt{T^*_{t,j}}}{T^*_{s,j}} \frac{p^*_{s,j}}{p^*_{t,j}} \sqrt{2\left(h^*_t - h^*_s\right)} \tag{6}$$

where ϕ^* is the dimensionless entropy function and h^* is the dimensionless enthalpy.

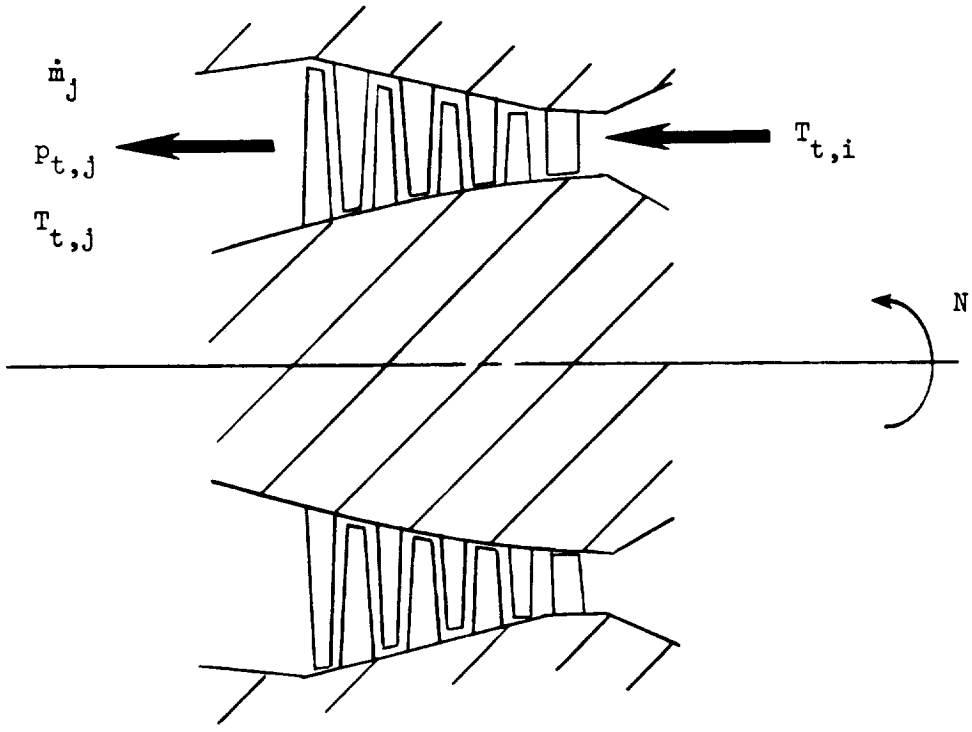

Figure 1.- Schematic diagram of typical axial-flow turbine.

4.4 JET NOISE PARAMETERS MODULE

INTRODUCTION

Exhaust jet noise is a significant part of the total noise produced by turbojet and turbofan engines. Several jet noise prediction methods are included in ANOPP. The purpose of the Jet Noise Parameters Module is to generate the physical parameters required for the exhaust jet noise prediction modules for turbojet and turbofan engines.

The engine nozzle exit flow state is provided by the user. These engine-state data are first converted to a function of time, using data from the flight path characteristics. The required jet parameters for jet noise prediction are then computed.

SYMBOLS

A	area, m^2 (ft^2)
c	speed of sound, m/s (ft/s)
D_e	equivalent circular nozzle diameter, m (ft)
D_h	hydraulic diameter, m (ft)
D_p	plug diameter, m (ft)
f	fuel-to-air ratio
h_a	absolute humidity, percent mole fraction
M	Mach number
M_∞	aircraft Mach number
$\dot{m}$	mass flow rate, kg/s (slugs/s)
n	number of source times
p	pressure, Pa (lb/ft^2)
R	dry-air gas constant, $m^2/K\text{-}s^2$ ($ft^2/{}^oR\text{-}s^2$)
$\mathcal{R}$	gas constant, $m^2/K\text{-}s^2$ ($ft^2/{}^oR\text{-}s^2$)
T	temperature, K (^oR)
t	time, s

V velocity, m/s (ft/s)

γ ratio of specific heats

π engine power setting

ρ density, kg/m^3 (slugs/ft^3)

ϕ^* specific entropy function, re R

Subscripts:

a aircraft

e engine

fe fully expanded

p plug

s static

t total

1 primary stream

2 secondary stream

∞ ambient

Superscript:

* dimensionless quantity

INPUT

This module provides the parameters which are used for the prediction of jet mixing and shock cell noise. The primary nozzle flow state is required for single-stream jets such as on turbojet engines. Both the primary and secondary nozzle flow states are required for dual-stream jets such as on turbofan engines. These jets and their associated state variables are illustrated in figure 1. The areas are included as state variables since the nozzle sizes may be functions of engine power setting. In addition to the areas A_1 and A_2, the primary nozzle may have a plug with area A_p, which must be specified, and the engine reference area A_e must be given since input data will usually be specified relative to it. It is assumed that the outer diameter of the inner nozzle is equal to the inner diameter of the outer nozzle as shown in figure 1. Local atmospheric conditions - density, speed of sound, and humidity - are used in evaluation of the static flow variables; however, humidity may be neglected without significant error if it is not available. The local density and speed of sound are used in computing decibel levels; however, they are not needed if only normalized mean-squared pressure is to be computed or if the SPL is corrected to standard conditions. Table I

gives the recommended ranges and the default values for the input parameters.

A_e engine reference area, m^2 (ft^2)

A_p^* primary nozzle plug area, re A_e

Primary-Nozzle Flow State

π engine power setting

M_∞ aircraft Mach number

$A_1^*(\pi)$ nozzle area, re A_e

$f_1(\pi, M_\infty)$ fuel-to-air ratio

$\dot{m}_1^*(\pi, M_\infty)$ mass flow rate, re $A_e p_\infty / \sqrt{RT_\infty}$

$p_{t,1}^*(\pi, M_\infty)$ total pressure, re p_∞

$T_{t,1}^*(\pi, M_\infty)$ total temperature, re T_∞

Secondary-Nozzle Flow State (Optional)

π engine power setting

M_∞ aircraft Mach number

$A_2^*(\pi)$ nozzle area, re A_e

$f_2(\pi, M_\infty)$ fuel-to-air ratio

$\dot{m}_2^*(\pi, M_\infty)$ mass flow rate, re $A_e p_\infty / \sqrt{RT_\infty}$

$p_{t,2}^*(\pi, M_\infty)$ total pressure, re p_∞

$T_{t,2}^*(\pi, M_\infty)$ total temperature, re T_∞

Engine Variable Table

t source time, s

$M_\infty(t)$ aircraft Mach number

$\pi(t)$ engine power setting

$c_\infty(t)$ ambient speed of sound, m/s (ft/s)

$\rho_\infty(t)$ ambient density, kg/m^3 ($slugs/ft^3$)

$h_a(t)$ absolute humidity, percent mole fraction

OUTPUT

The outputs to this module are the physical parameters required for execution of the exhaust jet noise modules as a function of source time. Unless otherwise stated, all parameters are computed for a hypothetical fully expanded jet which has a static pressure equal to ambient pressure.

Primary Jet Parameters

n	number of source time values
t	source time, s
$A^*_{fe,1}(t)$	primary jet area, re A_e
$D^*_{e,1}(t)$	actual primary jet equivalent diameter, re $\sqrt{A_e}$
$D^*_{h,1}(t)$	actual primary jet hydraulic diameter, re $\sqrt{A_e}$
$M_1(t)$	primary jet Mach number
$T^*_1(t)$	primary jet total temperature, re T_∞
$V^*_1(t)$	primary jet velocity, re c_∞
$\rho^*_1(t)$	primary jet density, re ρ_∞
$\gamma_1(t)$	ratio of specific heats for primary jet

Secondary Jet Parameters (Optional)

$A^*_{fe,2}(t)$	secondary jet area, re A_e
$D^*_{e,2}(t)$	actual secondary jet equivalent diameter, re $\sqrt{A_e}$
$D^*_{h,2}(t)$	actual secondary jet hydraulic diameter, re $\sqrt{A_e}$
$M_2(t)$	secondary jet Mach number
$T^*_2(t)$	secondary jet total temperature, re T_∞
$V^*_2(t)$	secondary jet velocity, re c_∞
$\rho^*_2(t)$	secondary jet density, re ρ_∞
$\gamma_2(t)$	ratio of specific heats for secondary jet

Ambient Conditions

$c_\infty(t)$ ambient speed of sound, m/s (ft/s)

$M_a(t)$ aircraft Mach number

$\rho_\infty(t)$ ambient density, kg/m^3 ($slugs/ft^3$)

METHOD

The user has two options for the method of this module. The first is the previously stated option of computing data for either a single-stream or dual-stream jet. The second is the selection of constant ratio of specific heats or variable ratio of specific heats for calculation of static state variables.

The input nozzle flow states as shown in figure 1 are expressed as a function of the engine power setting π and the aircraft Mach number M_a. These tables must be provided directly by the user. These data are converted to a function of source time. The engine variable table gives M_a and π as a function of source time as provided by the Flight Dynamics Module or the user.

Single-Stream Jet

The ratio of specific heats for the primary jet γ_1 is computed from the total temperature $T^*_{t,1}$, the fuel-to-air ratio f, and the absolute humidity h_a, as discussed in the Thermodynamic Utilities portion of this manual.

Constant specific heats.- The primary jet velocity and jet density may be estimated assuming constant specific heats. The jet Mach number M_1 is computed from the jet total pressure and ratio of specific heats by the relation

$$p^*_{s,1} = p^*_{t,1}\left(1 + \frac{\gamma_1 - 1}{2} M_1^2\right)^{-\gamma_1/(\gamma_1-1)} \tag{1}$$

where $p^*_{s,1} = 1$ for a fully expanded jet.

The primary jet static temperature is computed from the jet Mach number and specific heat ratio as

$$T^*_{s,1} = T^*_{t,1}\left(1 + \frac{\gamma_1 - 1}{2} M_1^2\right)^{-1} \tag{2}$$

as discussed in Thermodynamics Utilities. The jet density is then

$$\rho_1^*(t) = \frac{p_{s,1}^*}{R^* T_{s,1}^*} \tag{3}$$

where $R^* = R/R$ is the primary jet gas constant. Finally, the jet velocity is given by

$$V_1^* = M_1 \left(\frac{\gamma_s R^* T_{s,1}^*}{\gamma_\infty} \right)^{1/2} \tag{4}$$

where the ambient ratio of specific heats γ_∞ is 1.4.

Variable specific heats.- As discussed in Thermodynamic Utilities, the primary jet static temperature is evaluated from the relation

$$\frac{p_{s,1}^*}{p_{t,1}^*} = e^{-\left(\phi_t^* - \phi_s^*\right)} \tag{5}$$

where ϕ^* is the dimensionless entropy function and $p_{s,1}^* = 1$ for a fully expanded jet. The jet Mach number is then given by

$$M_1 = \sqrt{\frac{R^* T_{s,1}^*}{\gamma_s}} \frac{\dot{m}_1^*}{A_1^* p_{s,1}^*} \tag{6}$$

where γ_s is the ratio of specific heats evaluated at $T_{s,1}^*$. Finally, the jet density $\rho_1^*(t)$ and the jet velocity V_1^* are computed from equations (3) and (4), respectively.

Jet geometry.- The area of the fully expanded primary jet is

$$A_{fe,1}^* = \dot{m}_1^* / \rho_1^* V_1^* \tag{7}$$

The equivalent and hydraulic diameters, D_e^* and D_h^*, are based on actual geometric values for the nozzles instead of the fully expanded area, which may occur slightly away from the nozzle exit plane. The equivalent diameter is

$$D_{e,1}^* = \sqrt{4A_1^*/\pi} \tag{8}$$

and the hydraulic diameter is

$$D^*_{h,1} = \sqrt{\frac{4A^*_1}{\pi} + D^{*2}_p} - D^*_p \tag{9}$$

Secondary Jet

Computations for the secondary stream are identical to those for the primary, except that the secondary plug diameter is taken to be the first outer diameter of the inner nozzle. Therefore, the hydraulic diameter of the secondary jet is

$$D^*_{h,2} = \sqrt{\frac{4}{\pi}\left(A^*_1 + A^*_2\right) + D^2_p} - \sqrt{\frac{4}{\pi} A^*_1 + D^2_p} \tag{10}$$

TABLE I.- RANGE AND DEFAULT VALUES OF INPUT PARAMETERS

Input parameter	Minimum	Default	Maximum
A_e, m^2	0.01	$\pi/4$	10
A_p^*	0	0	1

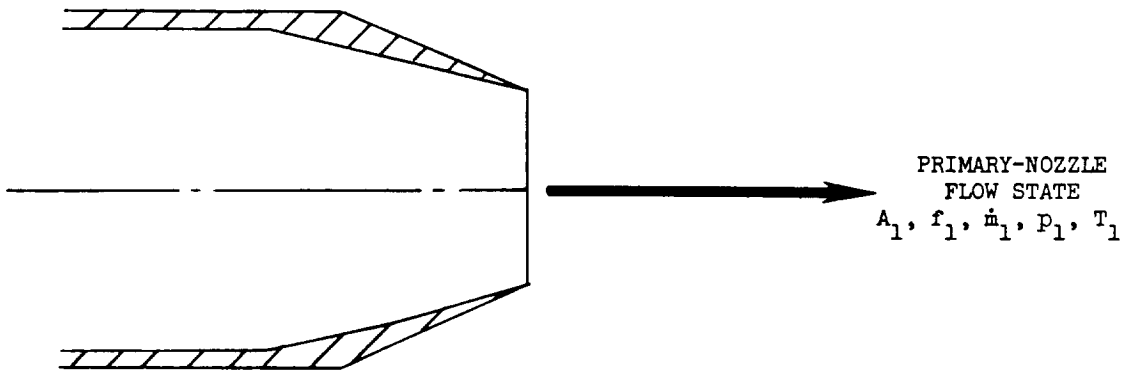

(a) Single-stream circular nozzle.

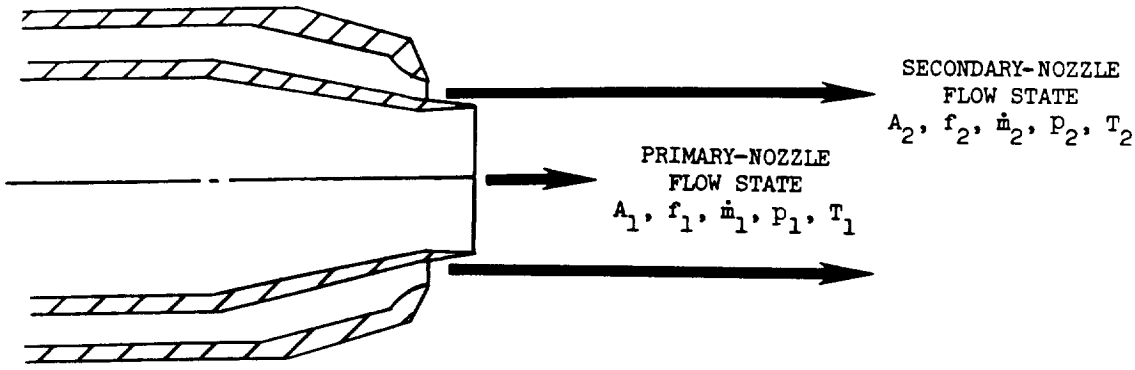

(b) Dual-stream coannular nozzle.

Figure 1.- Schematic diagram of a circular and coannular nozzle depicting the appropriate flow states.

4.5 AIRFRAME NOISE PARAMETERS MODULE

INTRODUCTION

Airframe noise is a significant part of the total noise of the aircraft during low-power operations. Airframe noise modules are included in ANOPP. The Airframe Noise Parameters Module generates the three time parameters needed for the execution of the airframe modules. The physical values output by the module are identical to the input; however, the input is in the form of a data member in ANOPP, whereas the prediction modules must have their input as parameters.

SYMBOLS

c_∞	ambient speed of sound, m/s (ft/s)
$I_{\ell g}$	landing-gear position
M_∞	aircraft Mach number
n	number of source times
t	time, s
δ_f	flap setting, deg
μ_∞	ambient dynamic viscosity, kg/m-s (slugs/ft-s)
ρ_∞	ambient density, kg/m^3 ($slugs/ft^3$)

INPUT

Input to this module is the engine variable table as provided by the Flight Dynamics Module or the user.

Engine Variable Table

t	source time, s
$I_{\ell g}(t)$	landing-gear position
$M_\infty(t)$	aircraft Mach number
$\delta_f(t)$	flap setting, deg

$c_\infty(t)$ ambient speed of sound, m/s (ft/s)

$\rho_\infty(t)$ ambient density, kg/m^3 (slugs/ft^3)

$\mu_\infty(t)$ ambient dynamic viscosity, kg/m-s (slugs/ft-s)

OUTPUT

The outputs to this module are the three time parameters required to execute the airframe noise modules as a function of source time.

Airframe Noise Parameters

n number of source time values

t source time, s

$I_{\ell g}(t)$ landing-gear position

$M_\infty(t)$ aircraft Mach number

$\delta_f(t)$ flap setting, deg

Ambient Conditions

$c_\infty(t)$ ambient speed of sound, m/s (ft/s)

$\rho_\infty(t)$ ambient density, kg/m^3 (slugs/ft^3)

$\mu_\infty(t)$ ambient dynamic viscosity, kg/m-s (slugs/ft-s)

METHOD

The engine variable table is read and the appropriate output parameters are generated.

5. PROPAGATION

5.1 PROPAGATION MODULE

INTRODUCTION

The Propagation Module (PRO) takes noise data which are generated by the noise modules in the source frame of reference and applies all of the appropriate computations to transfer them to the observer frame of reference. If a sum of two or more noise sources is desired in the same coordinate system, the sum is performed first. The required computations for propagation include the effects of spherical spreading, atmospheric absorption, ground reflection and attenuation, and retarded time. The data for some of the various propagation effects have been previously prepared by the Geometry Module (GEO), the Atmospheric Absorption Module (ABS), and the Atmospheric Module (ATM).

There are six steps necessary to propagate the sound to the observer. They are performed in the following order:

1. Interpolate the input source noise data as a function of emission time and observer directivity angles

2. Apply spherical spreading and characteristic impedance change effects

3. Divide the 1/3-octave frequency bands into subbands for more accurate absorption and ground effects modeling (ref. 1)

4. Apply the atmospheric absorption effect

5. Apply the ground reflection and attenuation effect

6. Combine frequency subbands into 1/3-octave bands

The resulting output table is the mean-square acoustic pressure at the observer position as a function of frequency, reception time, and observer.

SYMBOLS

A	subband amplitude adjusting factor
c	speed of sound, m/s (ft/s)
f	frequency, Hz
g_r	acceleration due to gravity, m/s^2 (ft/s^2)
H	altitude, m (ft)

h	observer height, m (ft)
k	wave number, $2\pi f/c_a$
M	molecular weight of air
N_b	number of subbands per 1/3-octave band
o	observer index
$\langle p^2 \rangle$	mean-square acoustic pressure, Pa^2 (lb^2/ft^4)
$\bar{R}$	universal gas constant, $m^2/K\text{-}s^2$ ($ft^2/^oR\text{-}s^2$)
r	distance, m (ft)
Δr	path-length difference, m (ft)
SPL	sound pressure level, dB
T	temperature, K (^oR)
t	time, s
u,v	spectrum slopes
w	ratio of subband center frequencies
y	dimensionless altitude, $Mg_r(H - H_1)/\bar{R}T_r$
γ	elevation angle, deg
η	$= 2\pi\rho_a f/\sigma$
Θ	incidence angle, deg
θ	polar directivity angle, deg
$\bar{\mu}$	average absorption coefficient, nepers per wavelength
ρ	density, kg/m^3 ($slugs/ft^3$)
σ	specific flow resistance of the ground, $kg/s\text{-}m^3$ ($slugs/s\text{-}ft^3$)
ϕ	azimuthal directivity angle, deg
Ω	solid angle for a ray cone, sr

Subscripts:

a	ambient
e	emission
o	observer

r standard sea-level reference value

s source

Superscript:

* dimensionless quantity

INPUT

The input to this module consists of one or more noise data tables computed for the same source coordinate system on the aircraft. When two or more source noise data tables are input, they are summed prior to being propagated to the observer. Additional tables are required which incorporate the various propagation effects. The range and default values of the required input parameters are given in table I.

N_b number of subbands per 1/3-octave band

r_s source radius, m (ft)

σ specific flow resistance of the ground, kg/s-m^3 (slugs/s-ft^3)

Source Noise Data Table

f frequency, Hz

θ polar directivity angle, deg

ϕ azimuthal directivity angle, deg

t_e emission time, s

$\langle p^2(f,\theta,\phi,t_e)\rangle^*$ mean-square acoustic pressure, re $\rho_a^2 c_a^4$

Geometry Table

t reception time, s

o observer index

r(t,o) distance, m (ft)

t_e(t,o) emission time, s

θ(t,o) polar directivity angle, deg

ϕ(t,o) azimuthal directivity angle, deg

γ(t,o) elevation angle, deg

h(o) observer height, m (ft)

Atmospheric Properties Table

y	altitude, $Mg_r(H - H_l)/\bar{R}T_r$
$c^*(y)$	speed of sound, re c_r
$\rho c^*(y)$	characteristic impedance, re $\rho_r c_r$
$\rho^*(y)$	density, re ρ_r

Absorption Coefficient Table

f	frequency, Hz
y	altitude, $Mg_r(H - H_l)/\bar{R}T_r$
$\bar{\mu}(f,y)$	average absorption coefficient, nepers per wavelength

OUTPUT

This module produces a table of mean-square acoustic pressures at the observer as a function of frequency, time, and observer.

Received Noise Data Table

f	frequency, Hz
t	reception time, s
o	observer index
$c_a^*(o)$	speed of sound at the observer, re c_r
$\rho_a^*(o)$	air density at the observer, re ρ_r
$\langle p^2(f,t,o)\rangle^*$	mean-square acoustic pressure, re $\rho_a^2 c_a^4$

METHOD

Noise Data Interpolation

If two or more noise data tables are input, the tables are summed to produce one data table. Since the input noise data are expressed in terms of mean-square pressure, the noise data summation is a simple element-by-element addition. This noise data table is a function of source time values and constant polar and azimuthal directivity angle increments (pseudo observers). Before these data can be propagated to the observer, they must be interpolated for the emission time values corresponding to reception time, polar directivity angles, and azimuthal directivity angles to the actual observers. This is accomplished by

using the polar directivity angle, azimuthal directivity angle, and emission time values from the geometry table. That is, using $\theta(t,o)$, $\phi(t,o)$, and $t_e(t,o)$, the input table $\langle p^2(f,\theta,\phi,t_e)\rangle^*$ is converted to $\langle p^2(f,t,o)\rangle^*$. Figure 1 is a graphic representation of the time scale mapping.

Spherical Spreading and Characteristic Impedance Effects

The table $\langle p^2(f,t,o)\rangle^*$ is now processed on a column-by-column basis throughout the remainder of the module for each value of received time and observer index. The next step is to apply spherical spreading and the characteristic impedance correction. These are derived from the condition of conservation of acoustic power within a conical ray tube.

Figure 2 is a schematic diagram of a conical ray tube of solid angle $d\Omega$ from a source to an observer. The acoustic power, which is the product of the intensity and the cross-sectional area, must be constant from a source radius r_s to an observer radius r_o. This is expressed in equation form as

$$\frac{\langle p^2(r_s)\rangle}{\rho c_s} r_s^2 \, d\Omega = \frac{\langle p^2(r_o)\rangle}{\rho c_o} r_o^2 \, d\Omega \tag{1}$$

Expressing equation (1) in dimensionless form yields

$$\langle p^2(r_o)\rangle^* = \frac{\rho c(y_o)^*}{\rho c(y_s)^*} \frac{r_s^2}{r_o^2} \langle p^2(r_s)\rangle^* \tag{2}$$

where ρc_o^* and ρc_s^* are determined from the atmospheric properties table for the observer height and source altitude, respectively. The dimensionless height at the source and observer are given by

$$y_o = Mg_r h / \bar{R} T_r \tag{3}$$

and

$$y_s = Mg_r (r \sin \gamma + h) / \bar{R} T_r \tag{4}$$

The observer distance r and observer height h are found from the geometry table. In equation (2), r_s^2/r_o^2 is the spherical spreading term and $\rho c(y_o)^*/\rho c(y_s)^*$ is the characteristic impedance correction.

Subband Division

The mean-square acoustic pressure $\langle p^2 \rangle_*^*$ is expressed as a function of the frequency f. The table $\langle p^2(f,t,o) \rangle$ has values of frequency corresponding to the ANSI standard 1/3-octave-band frequencies. As shown in the reference, the accurate application of atmospheric absorption and ground effects requires that the 1/3-octave bands be divided into $N_b = 2m + 1$ subbands, where m is an integer greater than 0. The default value of m is 2. The ratio of subband center frequencies is

$$\frac{f_{j+1}}{f_j} = w = 10^{1/10N_b} \tag{5}$$

where j is the index number of the subband center frequencies. The index number j is related to the index number of the original 1/3-octave center frequencies i by the relation

$$j = (i - 1)N_b + h \qquad (h = 1, 2, \ldots, N_b) \tag{6}$$

Then, each subband center frequency is expressed in terms of a 1/3-octave-band frequency as

$$f_j = w^{h-m-1} f_i \qquad (h = 1, 2, \ldots, N_b;\ i = 1, 2, \ldots, k) \tag{7}$$

where k is the total number of 1/3-octave bands. The 1/3-octave and subband frequencies for m = 2 are given in table II.

The value of the mean-square acoustic pressure for each subband is determined from the slopes of the 1/3-octave-band spectrum. For each 1/3-octave center frequency f_i, the slope of the spectrum in the lower half of the band is

$$u_i = \frac{\langle p^2 \rangle_i^*}{\langle p^2 \rangle_{i-1}^*} \tag{8}$$

and the slope for the upper half is

$$v_i = u_{i+1} \tag{9}$$

The term $\langle p^2 \rangle_i^*$ is the value of the mean-square acoustic pressure for f_i. The terms u_1 and v_k are not defined by equations (8) and (9);

therefore, the end slopes are established by setting $u_1 = v_1$ and $v_k = u_k$. Then the value of the mean-square pressure for each subband $\langle p^2 \rangle_j^*$ is given by

$$\langle p^2 \rangle_j^* = \begin{cases} \left(\langle p^2 \rangle_i^* / A_i \right) u_i^{h-m-1} & (h = 1, 2, \ldots, m) \\ \langle p^2 \rangle_i^* / A_i & (h = m + 1) \\ \left(\langle p^2 \rangle_i^* / A_i \right) v_i^{h-m-1} & (h = m + 2, \ldots, N_b) \end{cases} \quad (m > 0) \qquad (10)$$

The subband adjusting factor A_i is defined such that

$$\sum_{h=1}^{N_b} \langle p^2 \rangle_j^* = \langle p^2 \rangle_i^* \qquad (11)$$

Substituting equation (10) into equation (11) and solving for A_i yields

$$A_i = 1 + \sum_{h=1}^{m} \left(u_i^{h-m-1} + v_i^h \right) \qquad (12)$$

Defining the subband adjusting factor A_i in this manner ensures that the sum of the mean-square acoustic pressure for the subbands equals the total mean-square acoustic pressure of the 1/3-octave band.

Atmospheric Effects

The atmospheric absorption and the ground effects are now applied to the subband data. The atmospheric absorption coefficient $\bar{\mu}$ is a function of frequency f and altitude y as computed by the Atmospheric Absorption Module (ABS). The average absorption coefficient from the source to the observer is defined as

$$\bar{\mu}(f, y_s, y_o) = \frac{1}{y_s - y_o} \int_{y_s}^{y_o} \mu(y)\, dy = \frac{y_s\, \bar{\mu}(f, y_s) - y_o\, \bar{\mu}(f, y_o)}{y_s - y_o} \qquad (13)$$

where y_o and y_s are given by equations (3) and (4), respectively. Then, the mean-square pressure with the atmospheric absorption effect applied is

$$\langle p^2 \rangle^*_{j,abs} = \langle p^2 \rangle^*_j \, e^{-\left[2\bar{\mu}(f,y_s,y_o)f/c_r\right](r-r_s)} \tag{14}$$

The subscript abs indicates that the absorption has been included in the mean-square pressure.

Ground Effects

Similarly, the ground effects are applied to the subband data. The ground effects factor G is a function of path-length difference $k\Delta r$, cosine of the incidence angle $\cos\theta$, dimensionless frequency η, and source-to-image distance kr_2, as discussed in the Ground Reflection and Attenuation Module (GRA). Figure 3 shows the source-to-observer geometry for the ground effects computation. Referring to the figure, the quantities r, h, and γ are obtained from the geometry table. Then, from the Law of Cosines, the source-to-image distance is given by

$$r_2^2 = r^2 + (2h)^2 - (2r)(2h)\cos(90^\circ + \gamma) \tag{15}$$

or

$$r_2^2 = r^2 + 4h^2 + 4rh \sin\gamma \tag{16}$$

Then the path-length difference Δr is

$$\Delta r = r_2 - r \tag{17}$$

and the cosine of the incidence angle is

$$\cos\theta = \frac{r \sin\gamma + 2h}{r_2} \tag{18}$$

The dimensionless frequency η and the wave number k are given by

$$\eta = \frac{2\pi\rho_a f}{\sigma} \tag{19}$$

and

$$k = \frac{2\pi f}{c_a} \tag{20}$$

where ρ_a and c_a are evaluated from the atmospheric properties table at the observer altitude y_o. The value of G is now computed using the method presented for the Ground Reflection and Attenuation Module. The mean-square pressure with ground effects is then given by

$$\langle p^2 \rangle^*_{j,gr} = G \langle p^2 \rangle^*_j \tag{21}$$

The subscript gr indicates that the ground effect has been included in the mean-square pressure.

Subband Combination

The final step is to recombine the subbands into 1/3-octave bands. The mean-square pressure is summed over each 1/3-octave band by the relation

$$\langle p^2 \rangle^*_i = \sum_{h=1}^{N_b} \langle p^2 \rangle^*_j \tag{22}$$

where $j = m(i - 1) + h$. Once the processing of the mean-square pressure has been completed for all values of reception time and observer index, the received noise data table is complete.

The Propagation Module always performs the spherical spreading and characteristic impedance change. The user has four options concerning the application of atmospheric attenuation and ground effects:

1. No atmospheric attenuation or ground effects

2. Atmospheric attenuation effects only

3. Ground effects only

4. Both atmospheric attenuation and ground effects

The appropriate option is selected by the user depending on the nature of the problem.

The standard output form for the noise data at the observer is the dimensionless mean-square pressure $\langle p^2 \rangle^*$. The user may also request printed output of the sound pressure level SPL in decibels, defined as

$$SPL = 10 \log_{10} \langle p^2 \rangle^* + 20 \log_{10} \rho_a^* \left(c_a^*\right)^2 + 197 \qquad (23)$$

where ρ_a^* and c_a^* are determined from the atmospheric properties table at the observer altitude y_o.

REFERENCE

1. Montegani, Francis J.: Computation of Atmospheric Attenuation of Sound for Fractional-Octave Bands. NASA TP-1412, 1979.

TABLE I.- RANGE AND DEFAULT VALUES OF INPUT PARAMETERS

Input parameter	Minimum	Default	Maximum
N_b	1	5	9
r_s, m	0.1	1	100
σ, kg/s-m^3	5×10^4	2.5×10^5	1×10^6

TABLE II.- ANSI STANDARD OCTAVE AND 1/3-OCTAVE BANDS

WITH 1/15-OCTAVE-BAND FREQUENCIES

Octave	1/3 octave	1/15 octave	Octave	1/3 octave	1/15 octave	Octave	1/3 octave	1/15 octave
		45.7			288			1 820
		47.9			302			1 910
	50	50.0		315	315	2000	2 000	2 000
		52.5			331			2 090
		55.0			347			2 190
		57.5			363			2 290
		60.3			380			2 400
63	63	63.0		400	400		2 500	2 500
		66.1			417			2 630
		69.2			437			2 750
		72.4			457			2 880
		75.9			479			3 020
	80	80.0	500	500	500		3 150	3 150
		83.2			525			3 310
		87.1			550			3 470
		91.2			575			3 630
		95.5			603			3 800
	100	100		630	630	4000	4 000	4 000
		105			661			4 170
		110			692			4 370
		115			724			4 570
		120			759			4 790
125	125	125		800	800		5 000	5 000
		132			832			5 250
		138			871			5 500
		145			912			5 750
		151			955			6 030
	160	160	1000	1000	1000		6 300	6 300
		166			1050			6 610
		174			1100			6 920
		182			1150			7 240
		191			1200			7 590
	200	200		1250	1250	8000	8 000	8 000
		209			1320			8 320
		219			1380			8 710
		229			1450			9 120
		240			1510			9 550
250	250	250		1600	1600		10 000	10 000
		263			1660			10 500
		275			1740			11 000

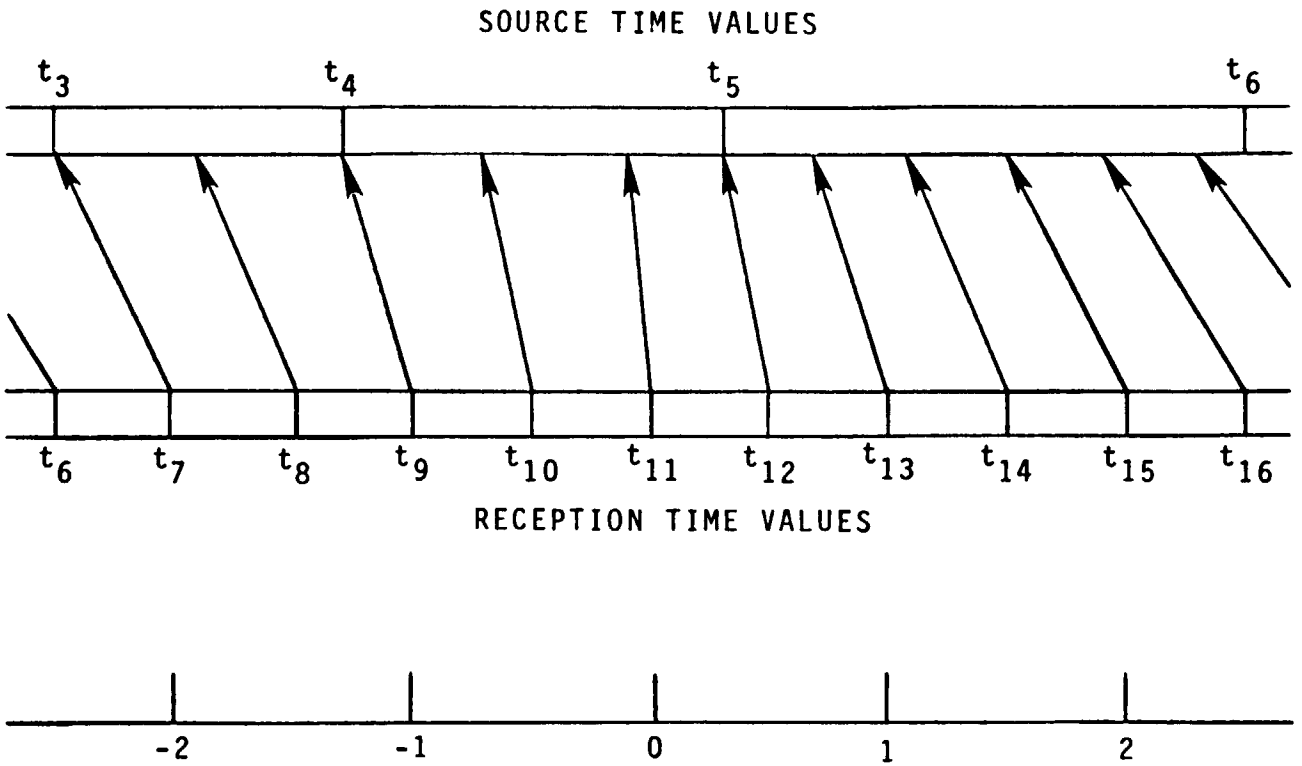

Figure 1.- Mapping of reception time values to source time line demonstrating retarded time effects.

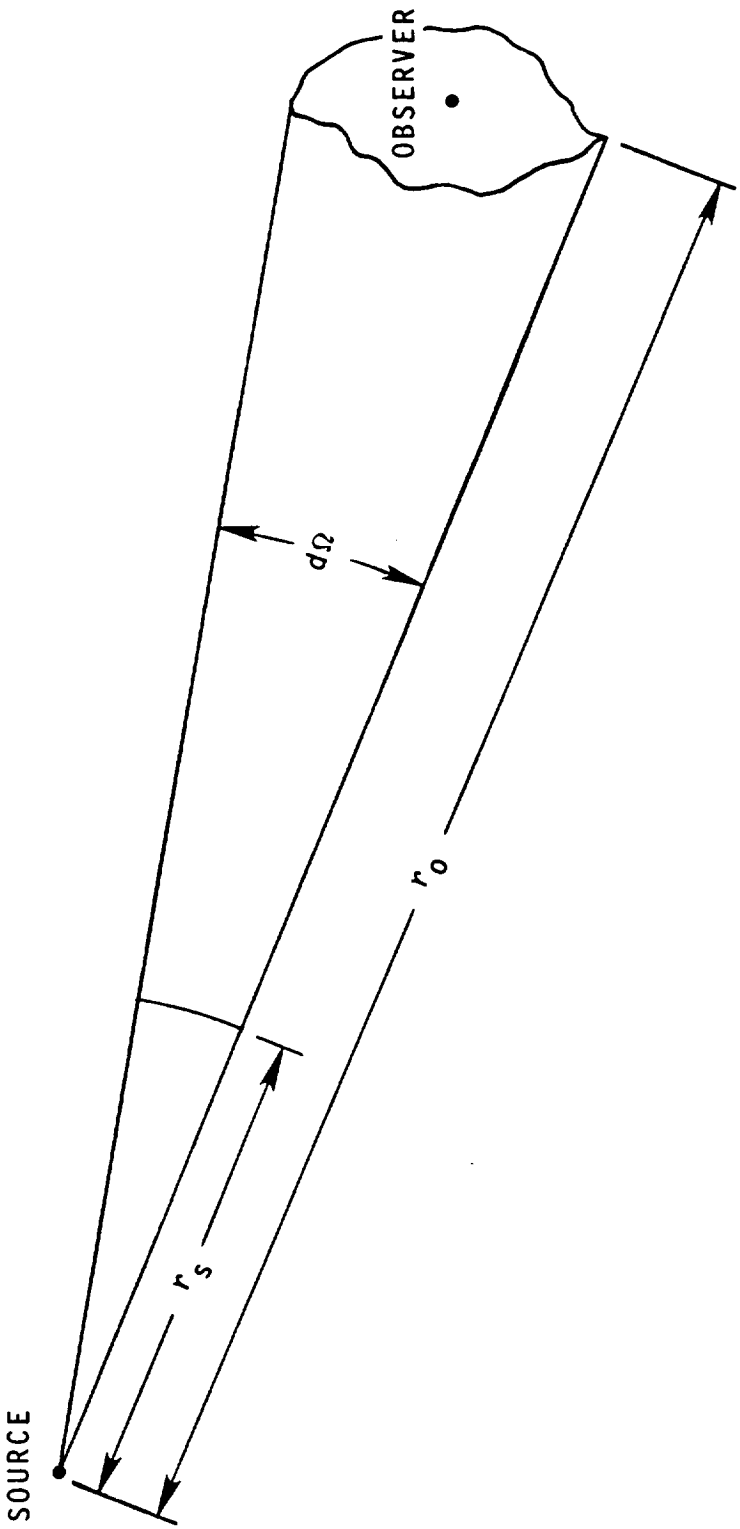

Figure 2.- Schematic diagram of ray tube from source to observer.

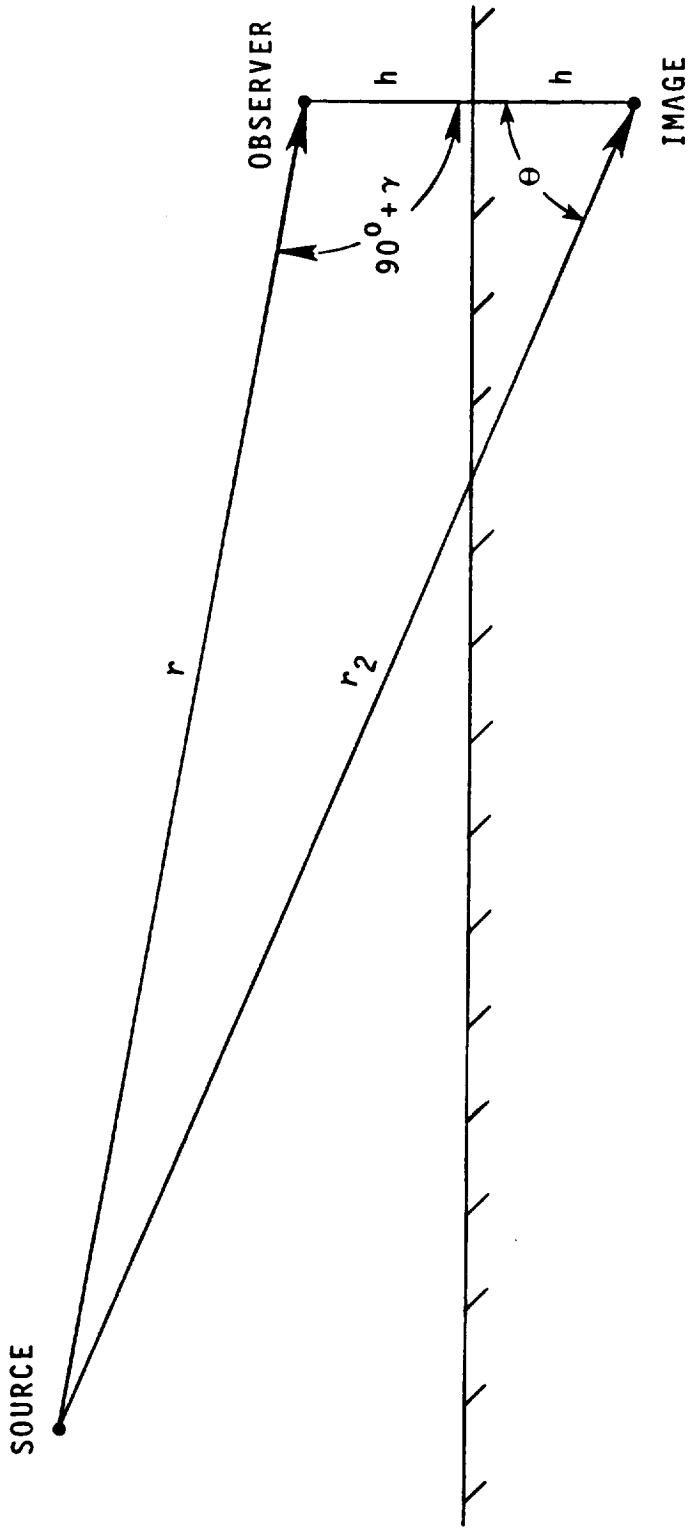

Figure 3.- Source-to-observer geometry for computation of ground effects.

5.2 GENERAL SUPPRESSION MODULE

INTRODUCTION

The General Suppression Module applies a noise suppression factor to a noise table produced by any ANOPP noise source module. The noise suppression factor is supplied by the user as a function of frequency, polar directivity angle, and azimuthal directivity angle. The output table of suppressed noise is in the same format as the input noise table.

SYMBOLS

c_∞	ambient speed of sound, m/s (ft/s)
f	frequency, Hz
$\langle p^2 \rangle^*$	mean-square acoustic pressure, re $\rho_\infty^2 c_\infty^4$
p_{ref}	reference pressure, 2×10^{-5} Pa (4.177×10^{-7} lb/ft^2)
S	suppression factor
θ	polar directivity angle, deg
ρ_∞	ambient density, kg/m^3 (slugs/ft^3)
ϕ	azimuthal directivity angle, deg

INPUT

A table of mean-square acoustic pressure and a suppression factor must be provided. In addition, ambient conditions are required for computation of sound pressure levels.

Noise Table

f	frequency, Hz
θ	polar directivity angle, deg
ϕ	azimuthal directivity angle, deg
$\langle p^2(f,\theta,\phi) \rangle$	mean-square acoustic pressure, re $\rho_\infty^2 c_\infty^4$

Ambient Conditions

c_∞	ambient speed of sound, m/s (ft/s)
ρ_∞	ambient density, kg/m^3 (slugs/ft^3)

Suppression Factor Table

f	frequency, Hz
θ	polar directivity angle, deg
ϕ	azimuthal directivity angle, deg
$S(f,\theta,\phi)$	suppression factor

OUTPUT

The output is the suppressed noise table.

Suppressed Noise Table

f	frequency, Hz
θ	polar directivity angle, deg
ϕ	azimuthal directivity angle, deg
$\langle p^2(f,\theta,\phi)\rangle^*$	suppressed mean-square acoustic pressure, re $\rho_\infty^2 c_\infty^4$

METHOD

The suppression factor is defined as

$$S = \frac{\langle p^2\rangle_s^*}{\langle p^2\rangle^*} \tag{1}$$

where $\langle p^2\rangle_s^*$ is the suppressed mean-square acoustic pressure and $\langle p^2\rangle^*$ is the unsuppressed mean-square acoustic pressure. The module multiplies each element of the input noise table by the appropriate value of the suppression factor to yield the suppressed noise table. In addition, printed output is available of the suppressed sound pressure level SPL defined as

$$SPL = 10 \log_{10} \langle p^2\rangle_s^* + 20 \log_{10} \frac{\rho_\infty c_\infty^2}{p_{ref}} \tag{2}$$

6. RECEIVED NOISE

6.1 NOISE LEVELS MODULE

INTRODUCTION

Previous modules within ANOPP have been concerned with Level III data; that is, data that have frequency, time, observer, and source as independent variables. In the Noise Levels Module (LEV), these Level III data are integrated over frequency to produce Level II data. Level II noise data are a function of time, observer, and source and are referred to as noise levels.

There are many varied scales that are used to describe noise levels. The overall sound pressure level (OASPL) is a simple integration of the spectrum. The A-weighted sound pressure level (L_A) and the D-weighted sound pressure level (L_D) add a weighting factor to account for the relative annoyance of the frequency bands. The perceived noise level (PNL) adds a weighting factor that is a function of frequency and mean-square acoustic pressure. The tone-corrected perceived noise level (PNLT) adds to PNL the impact of sounds which have pure tone characteristics.

The Noise Levels Module can produce tables of OASPL, L_A, L_D, PNL, or PNLT as a function of time and observer. One, some, or all of these noise level scales can be selected by the user. The PNLT table is required by the Effective Noise Module (EFF) to compute effective perceived noise level. This module can also sum the noise data from two or more sources prior to computation of noise levels.

SYMBOLS

A_k, B_k	constants
C	discrete frequency correction
c	speed of sound, m/s (ft/s)
ΔD_i	second difference of band sound pressure
F	tone correction difference
f	frequency, Hz
i	standard 1/3-octave-band number
L_A	A-weighted sound pressure level, dB(A)
L_D	D-weighted sound pressure level, dB(D)
N	noisiness index, noys

N_t	total noys value
OASPL	overall sound pressure level, dB
o	observer index
PNL	perceived noise level, PNdB
PNLT	tone-corrected perceived noise level, PNdB
$\langle p^2 \rangle$	mean-square acoustic pressure, Pa^2 (lb^2/ft^4)
SPL	sound pressure level, dB
t	time, s
W	weighting function
ρ	density, kg/m^3 ($slugs/ft^3$)

Subscripts:

a	ambient
r	standard sea level value

Superscript:

*	dimensionless quantity

INPUT

The input is a table of the mean-square acoustic pressure as prepared by the Propagation Module (PRO).

Received Noise Data Table

f	frequency, Hz
t	reception time, s
o	observer index
$c^*(o)$	speed of sound at observer, re c_r
$\rho^*(o)$	density at observer, re ρ_r
$\langle p^2(f,t,o) \rangle^*$	mean-square acoustic pressure, re $\rho_a^2 c_a^4$

OUTPUT

The output of this module is one or more of the following tables, depending on the desires of the user:

Overall Sound Pressure Level Table

t	reception time, s
o	observer index
OASPL(t,o)	overall sound pressure level, dB

A-Weighted Sound Pressure Level Table

t	reception time, s
o	observer index
$L_A(t,o)$	A-weighted sound pressure level, dB(A)

D-Weighted Sound Pressure Level Table

t	reception time, s
o	observer index
$L_D(t,o)$	D-weighted sound pressure level, dB(D)

Perceived Noise Level Table

t	reception time, s
o	observer index
PNL(t,o)	perceived noise level, PNdB

Tone-Corrected Perceived Noise Level Table

t	reception time, s
o	observer index
PNLT(t,o)	tone-corrected perceived noise level, PNdB

METHOD

The method for each noise level scale is presented as a separate section. Further details and a comparison of the noise level scales are

presented in reference 1. If two or more received noise data tables are input, they are summed element by element prior to the noise level computation.

Overall Sound Pressure Level (OASPL)

The overall sound pressure level is a simple integration of the frequency spectra. It is expressed in the units of decibels in the form

$$OASPL = 10 \log_{10} \sum_{i=1}^{n} \langle p^2 \rangle_i^* + 20 \log_{10} \rho_a^* \left(c_a^*\right)^2 + 197 \qquad (1)$$

where n is the number of frequency terms in the input table and $\langle p^2 \rangle_i^*$ is the dimensionless mean-square pressure for the ith frequency band.

A-Weighted Sound Pressure Level (L_A)

The A-weighted sound pressure level applies a weighting factor to each 1/3-octave band that is representative of the degree of annoyance of each frequency. The values of the A-weighting factors are given in table I and plotted in figure 1. The equation for L_A is

$$L_A = 10 \log_{10} \sum_{i=1}^{n} \left[\langle p^2 \rangle_i^* W(i,A)\right] + 20 \log_{10} \rho_a^* \left(c_a^*\right)^2 + 197 \qquad (2)$$

where $W(i,A)$ is the A-weighting factor.

D-Weighted Sound Pressure Level (L_D)

The D-weighted sound pressure level is similar to L_A except a different weighting factor is applied to the data. The values of the D-weighting factors are given in table II and plotted in figure 2. The equation for L_D is

$$L_D = 10 \log_{10} \sum_{i=1}^{n} \left[\langle p^2 \rangle_i^* W(i,D)\right] + 20 \log_{10} \rho_a^* \left(c_a^*\right)^2 + 197 \qquad (3)$$

where $W(i,D)$ is the D-weighting factor.

Perceived Noise Level (PNL)

The perceived noise level scale applies a weighting factor, which is a function of both frequency and sound intensity, to the mean-square acoustic pressure. This weighting is accomplished with the use of a

noisiness rating measured in noys. Figure 3 shows the values of the noisiness rating as a function of frequency and sound pressure level (SPL). The SPL is defined as

$$SPL = 10 \log_{10} \langle p^2 \rangle^* + 20 \log_{10} \rho_a^* \left(c_a^*\right)^2 + 197 \tag{4}$$

The noisiness rating has been expressed in functional form for ease of computation. The noisiness rating for a given value of frequency and sound pressure level is

$$N = \begin{cases} 0 & (SPL < A_1) \\ 10^{B_1(SPL-A_1)-1} & (A_1 \leq SPL \leq A_2) \\ 10^{B_2(SPL-A_3)} & (A_2 \leq SPL \leq A_3) \\ 10^{B_3(SPL-A_3)} & (A_3 \leq SPL \leq A_4) \\ 10^{B_5(SPL-A_5)} & (A_4 \leq SPL \leq 150) \end{cases} \tag{5}$$

The coefficients A_k and B_k are functions of frequency as given in table III.

The computation of PNL uses values of N. The process is

1. Determine the value of N, in noys, from equation (5) for each band

2. Determine the maximum noys value N_{max}

3. Compute the total noys value from the equation

$$N_t = N_{max} + 0.15 \left[\left(\sum_{i=1}^{24} N_i \right) - N_{max} \right] \tag{6}$$

for the 1/3-octave bands

4. Compute the perceived noise level in units of PNdB from

$$PNL = 40 + 33.22 \log_{10} N_t \tag{7}$$

Tone-Corrected Perceived Noise Level (PNLT)

The tone-corrected perceived noise level is perceived noise level modified for the impact of pure tone content of the noise spectra. Pure tones provide an additional irritation not found in broadband noise. The method provides for detection of pure tone content in 1/3-octave-band spectra and correction of the PNL for the impact of the pure tones.

The procedure may be illustrated with reference to figure 4, which shows an example spectrum, and table IV, which gives the spectrum in tabular form. The following steps are performed:

1. Compute the second difference ΔD_i of the SPL, which is

$$\Delta D_i = SPL_{i+1} - 2SPL_i + SPL_{i-1} \tag{8}$$

2. If $\Delta D_i < -5$, check to see if SPL_i is a local maximum, that is, if

$$SPL_i > SPL_{i-1} \quad \text{and} \quad SPL_i > SPL_{i+1} \tag{9}$$

3. If SPL_i is a local maximum, compute the average, or background, noise level $\overline{SPL_i}$ defined as

$$\overline{SPL_i} = \frac{SPL_{i+1} + SPL_{i-1}}{2} \tag{10}$$

These average values are given in table IV at frequencies of 250 and 2500 Hz. The background noise levels are shown as dashed lines in figure 4.

4. The difference between the local maximum and the background noise level F is

$$F = SPL_i - \overline{SPL_i} \tag{11}$$

5. The discrete frequency correction C(f,F) can now be determined. For frequencies in the range $500 < f_i < 5000$,

$$C(f,F) = \begin{cases} 0 & (F < 3) \\ F/3 & (3 \leq F < 20) \\ 6.7 & (20 \leq F) \end{cases} \tag{12}$$

and for frequencies in the range $f_i \leq 500$ or $f_i \geq 5000$,

$$C(f,F) = \begin{cases} 0 & (F < 3) \\ F/6 & (3 \leq F < 20) \\ 3.3 & (20 \leq F) \end{cases} \quad (13)$$

6. The tone correction is the maximum value of the discrete frequency correction C_{max} which in the example occurs at 2500 Hz with a value of 2. Then the tone-corrected perceived noise level PNLT is computed from the PNL as

$$PNLT = PNL + C_{max} \quad (14)$$

REFERENCE

1. Edge, Philip M., Jr.; and Cawthorn, Jimmy M.: Selected Methods for Quantification of Community Exposure to Aircraft Noise. NASA TN D-7977, 1976.

TABLE I.- WEIGHTING FUNCTION FOR A-WEIGHTED SOUND PRESSURE LEVEL

1/3-octave-band center frequency	W(i,A)	dB correction	1/3-octave-band center frequency	W(i,A)	dB correction
50	0.00096	-30.2	1 000	1.0	0
63	.0024	-26.2	1 250	1.148	.6
80	.0056	-22.5	1 600	1.259	1.0
100	.0123	-19.1	2 000	1.318	1.2
125	.0245	-16.1	2 500	1.349	1.3
160	.0457	-13.4	3 150	1.318	1.2
200	.0813	-10.9	4 000	1.259	1.0
250	.138	-8.6	5 000	1.112	.5
315	.219	-6.6	6 300	.977	-.1
400	.331	-4.8	8 000	.776	-1.1
500	.479	-3.2	10 000	.562	-2.5
630	.646	-1.9	12 500	.372	-4.3
800	.832	-.8			

TABLE II.- WEIGHTING FUNCTION FOR D-WEIGHTED SOUND PRESSURE LEVEL

1/3-octave-band center frequency	W(i,D)	dB correction	1/3-octave-band center frequency	W(i,D)	dB correction
50	0.0525	-12.8	1 000	1.0	0
63	.0813	-10.9	1 250	1.585	2.0
80	.126	-9.0	1 600	3.090	4.9
100	.191	-7.2	2 000	6.166	7.9
125	.282	-5.5	2 500	11.482	10.6
160	.398	-4.0	3 150	14.125	11.5
200	.550	-2.6	4 000	12.882	11.1
250	.692	-1.6	5 000	9.120	9.6
315	.832	-.8	6 300	5.754	7.6
400	.912	-.4	8 000	3.548	5.5
500	.933	-.3	10 000	2.188	3.4
630	.891	-.5	12 500	.724	-1.4
800	.871	-.6			

TABLE III.- CONSTANTS REQUIRED FOR COMPUTATION

OF PERCEIVED NOISE LEVEL

1/3-octave-band center frequency, Hz	A_1	B_1	A_2	B_2	A_3	B_3	A_4	B_5	A_5
50	49	0.079520	55	0.058098	64	0.043478	91.01	0.030103	52
63	44	.068160	51	.058098	60	.040570	85.88	.030103	51
80	39	.068160	46	.052288	56	.036831	87.32	.030103	49
100	34	.059640	42	.047534	53	.036831	79.85	.030103	47
125	30	.053013	39	.043573	51	.035336	79.76	.030103	46
160	27	.053013	36	.043573	48	.033333	75.96	.030103	45
200	24	.053013	33	.040221	46	.033333	73.96	.030103	43
250	21	.053013	30	.037349	44	.032051	74.91	.030103	42
315	18	.053013	27	.034859	42	.030675	94.63	.030103	41
400	16	.053013	25	.034859	40	.030103	100.00	.030103	40
500	16	.053013	25	.034859	40	.030103	100.00	.030103	40
630	16	.053013	25	.034859	40	.030103	100.00	.030103	40
800	16	.053013	25	.034859	40	.030103	100.00	.030103	40
1 000	16	.053013	25	.034859	40	.030103	100.00	.030103	40
1 250	15	.059640	23	.034859	38	.030103	100.00	.030103	38
1 600	12	.053013	21	.040221	34	.029960	100.00	.029960	34
2 000	9	.053013	18	.037349	32	.029960	100.00	.029960	32
2 500	5	.047712	15	.034859	30	.029960	100.00	.029960	30
3 150	4	.047712	14	.034859	29	.029960	100.00	.029960	29
4 000	5	.053013	14	.034859	29	.029960	100.00	.029960	29
5 000	6	.053013	15	.034859	30	.029960	100.00	.029960	30
6 300	10	.068160	17	.037349	31	.029960	100.00	.029960	31
8 000	17	.079520	23	.037349	37	.042285	44.29	.029960	34
10 000	21	.0596401	29	.043573	41	.042285	50.72	.029960	37

TABLE IV.- EXAMPLE PROBLEM FOR DETERMINATION

OF DISCRETE FREQUENCY CORRECTION

Band i	f_i	SPL_i	ΔD_i	$\overline{SPL_i}$	C(f,F)
19	80	70			
20	100	62	16		
21	125	70	2		
22	160	80	-8		
23	200	82	-1		
24	250	83	-8	79	2/3
25	315	76	11		
26	400	80	-4		
27	500	80	-1		
28	630	79	0		
29	800	78	3		
30	1 000	80	-4		
31	1 250	78	0		
32	1 600	76	5		
33	2 000	79	3		
34	2 500	85	-12	79	2
35	3 150	79	5		
36	4 000	78	-6		
37	5 000	71	-4		
38	6 300	60	-5		
39	8 000	54	-3		
40	10 000	45			

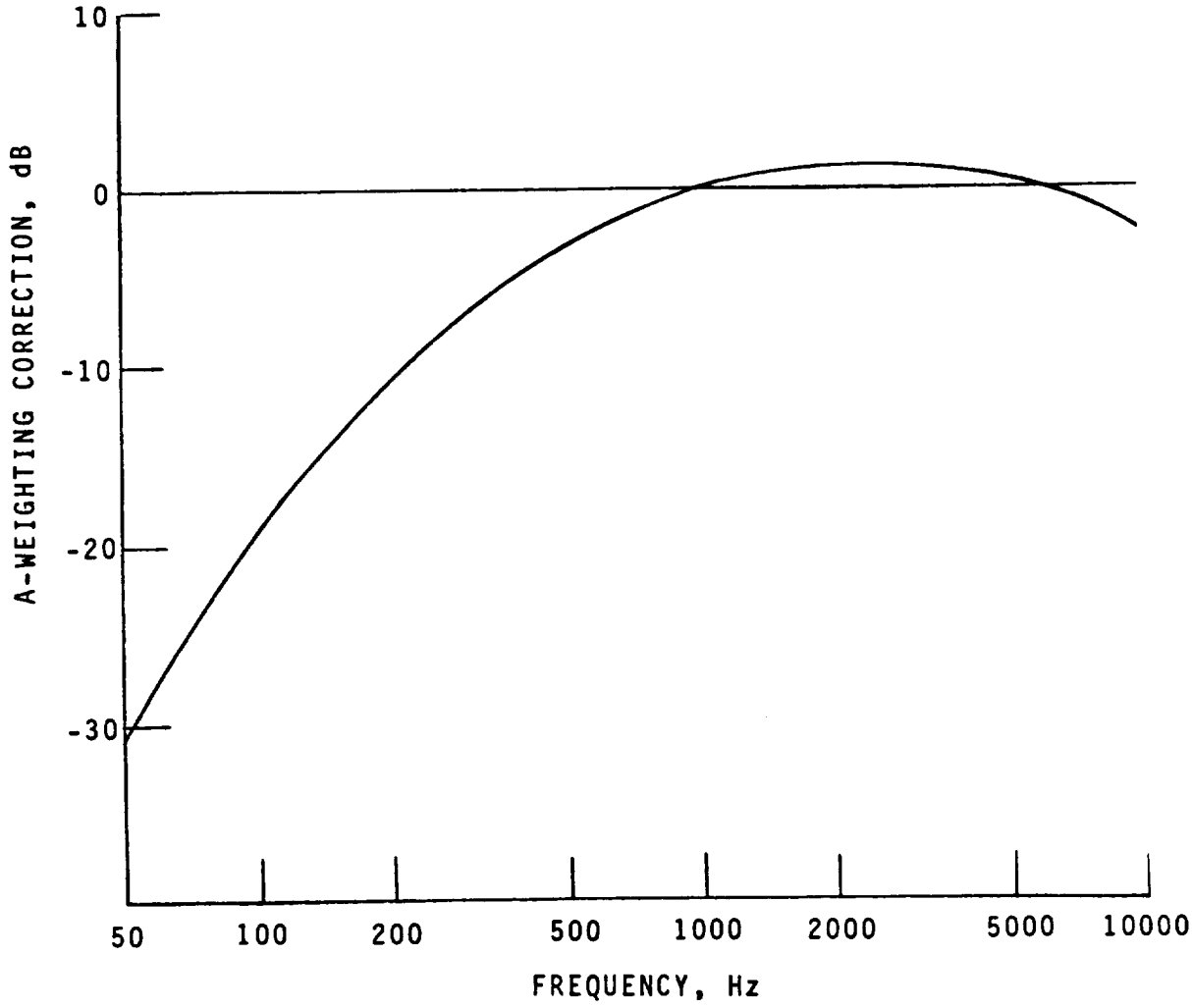

Figure 1.- Decibel correction for A-weighted sound pressure level.

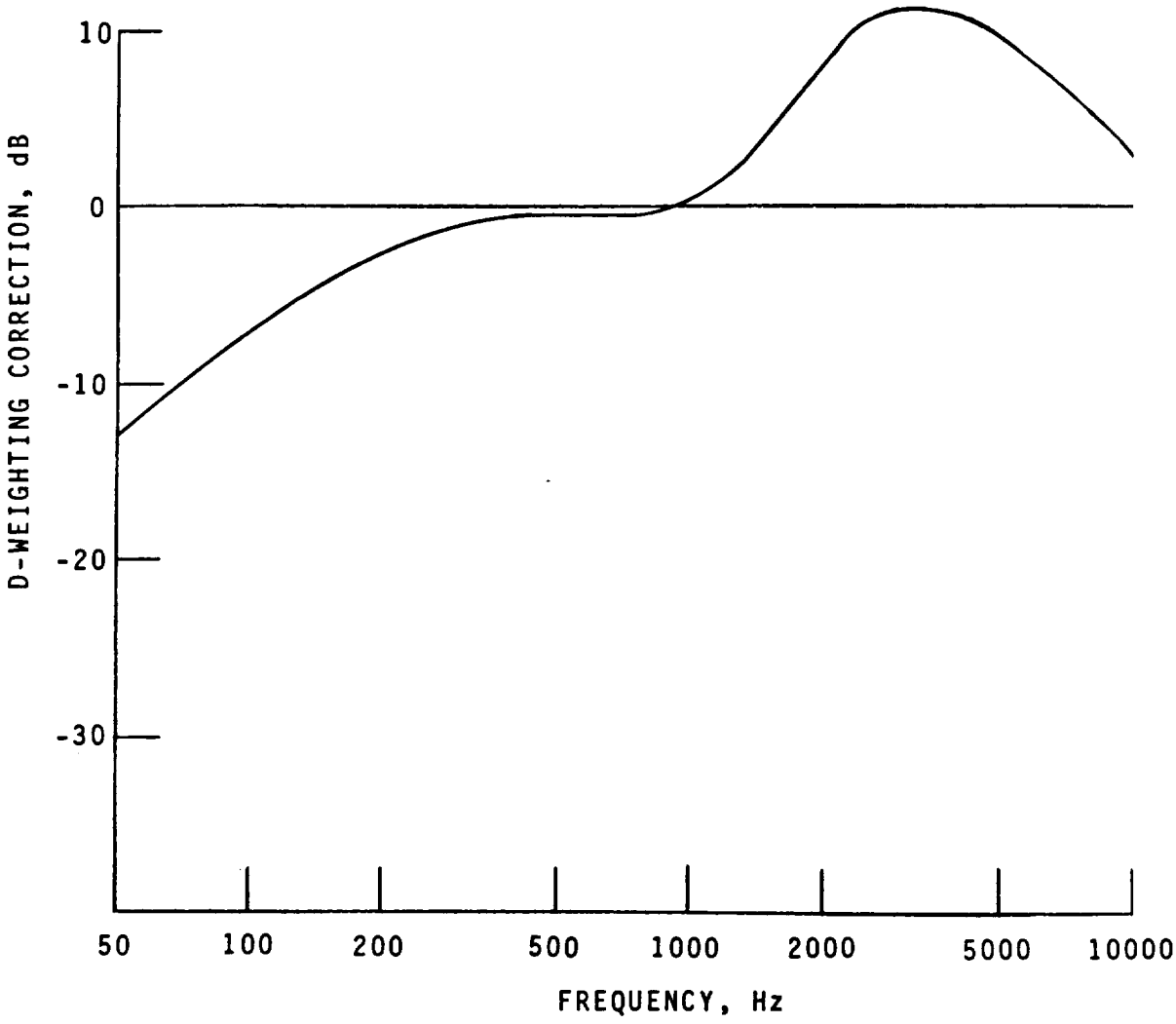

Figure 2.- Decibel correction for D-weighted sound pressure level.

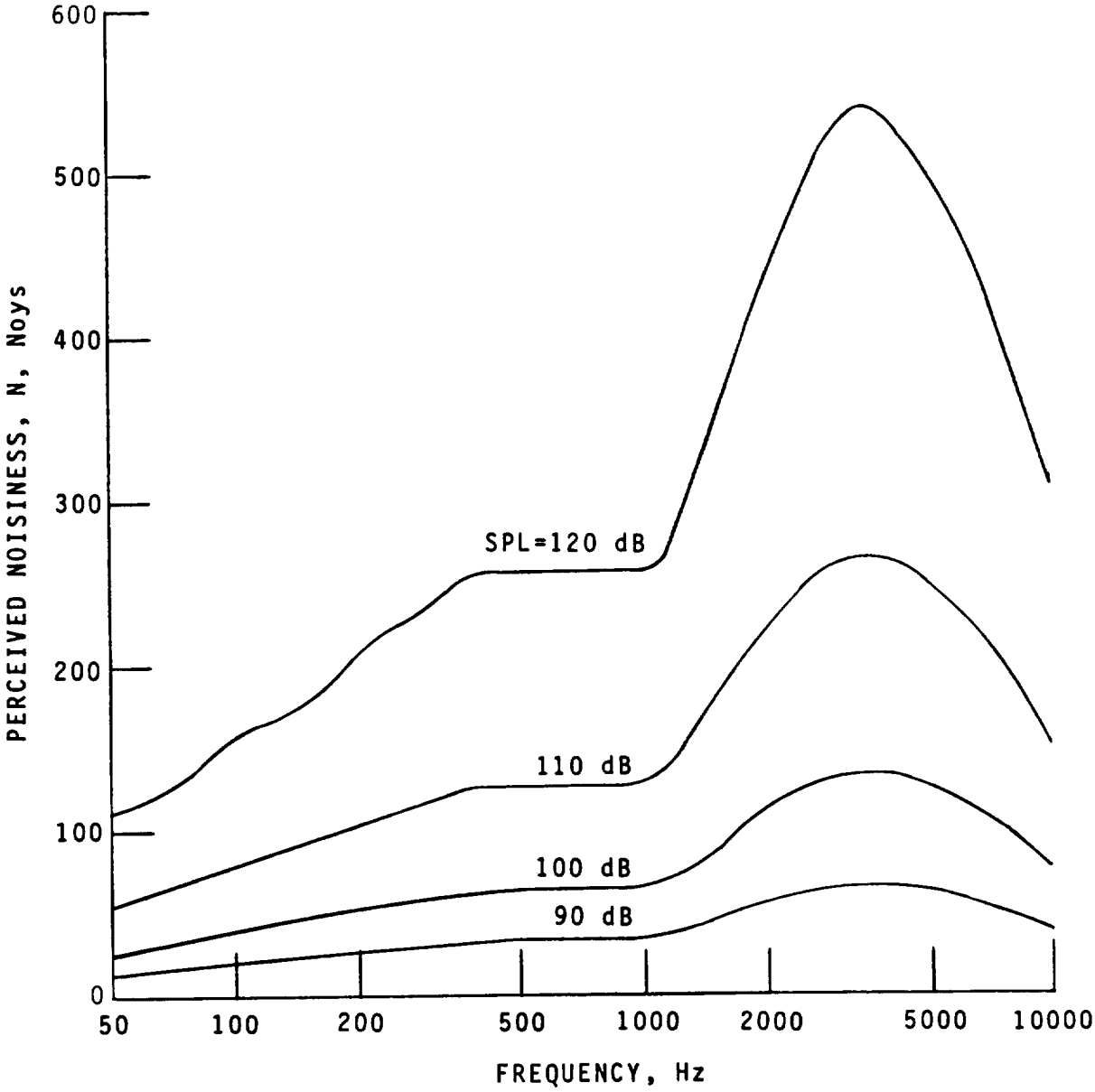

Figure 3.- Perceived noisiness of sound pressure levels.

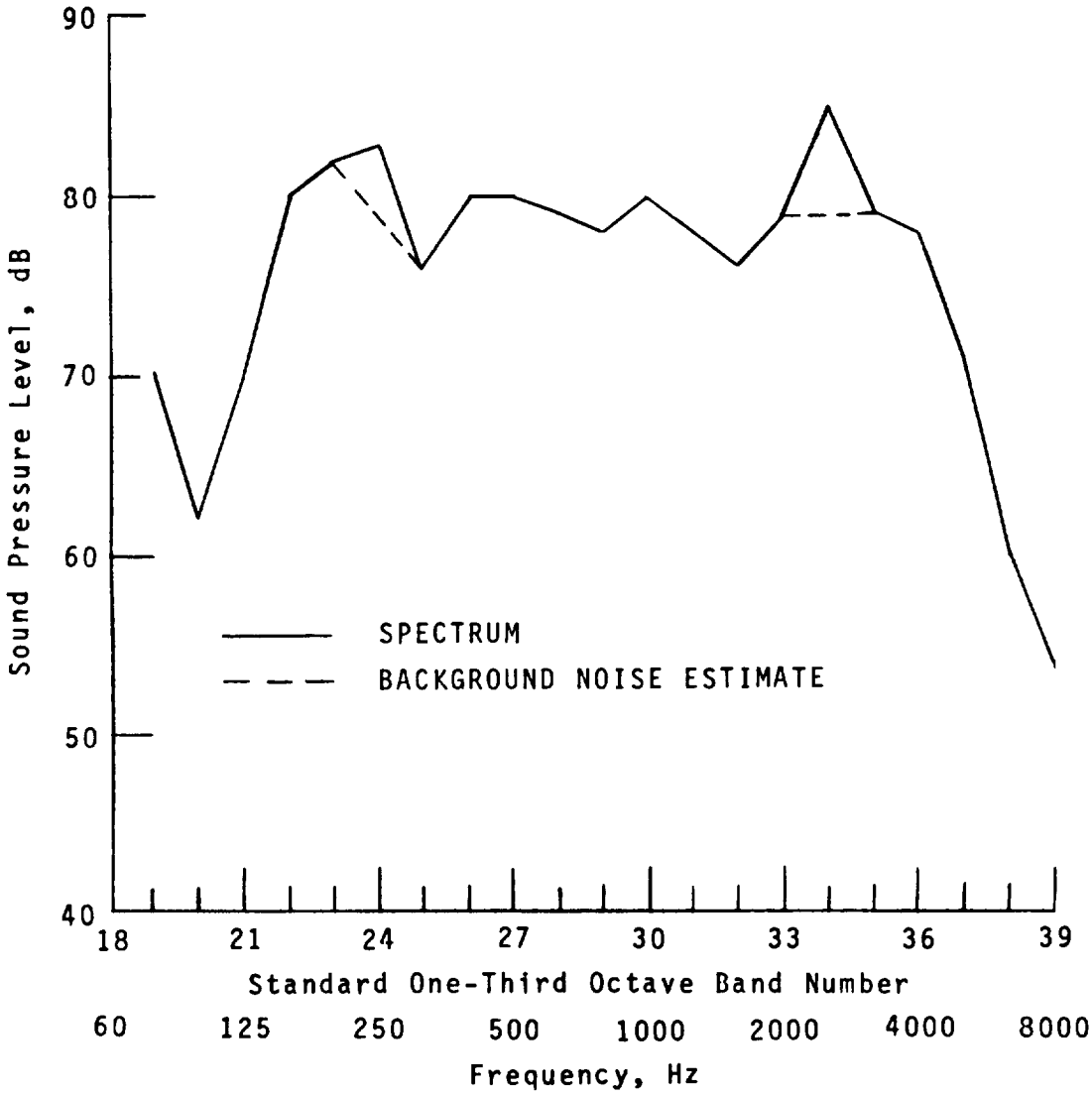

Figure 4.- Example spectrum for computation of tone-corrected perceived noise level.

6.2 EFFECTIVE NOISE MODULE

INTRODUCTION

The Noise Levels Module (LEV) computes various noise level scales which are a function of observer location and time. For consideration of the impact of noise due to airport terminal operations, cumulative exposure to noise is an important consideration. The Effective Noise Module (EFF) computes time-averaged indexes of noise exposure.

The most commonly used noise exposure index is the effective perceived noise level (EPNL), which is incorporated into this module. There are a variety of other cumulative exposure indexes; however, they require data from multiple take-offs and landings. Multiple take-off and landing problems are considered in Levels I and II of ANOPP.

This module computes a table of EPNL as a function of observer position, from a table of tone-corrected perceived noise level produced by the LEV module.

SYMBOLS

EPNL	effective perceived noise level, EPNdB
n	number of time segments
o	observer index
PNLT	tone-corrected perceived noise level, PNdB
$\langle pnlt^2 \rangle$	mean-square equivalent of PNLT
t	time, s
Δt	reception time increment, s

INPUT

The input is a table of the tone-corrected perceived noise level produced by the LEV module.

Input Constant

Δt	reception time increment, s

Tone-Corrected Perceived Noise Level Table

t	time, s
o	observer index
PNLT(t,o)	tone-corrected perceived noise level, PNdB

OUTPUT

The output is a table of the effective perceived noise level and initial, maximum, and final PNLT values at each observer.

Effective Perceived Noise Level Table

o	observer index
n(o)	number of time segments
EPNL(o)	effective perceived noise level, EPNdB
$PNLT_i(o)$	initial PNLT value, PNdB
$PNLT_{max}(o)$	maximum PNLT value, PNdB
$PNLT_f(o)$	final PNLT value, PNdB

METHOD

The computation of EPNL requires the time average of the PNLT. First, the PNLT is converted back to mean-square pressure by the relation

$$\langle pnlt^2 \rangle = 10^{PNLT/10} \tag{1}$$

The EPNL can be computed in integral form as

$$EPNL = 10 \log_{10} \int_{t_i}^{t_f} \langle pnlt^2 \rangle \, dt \tag{2}$$

where t_i and t_f are the initial and final times for each segment of the PNLT data. The segments are determined by comparing the reception time increment Δt used in the Geometry Module to the differences in tabulated time. If the tabulated time entries are more than Δt apart, then a new segment is started. In addition to the value of the EPNL, the initial, maximum, and final PNLT values are printed for each observer to allow assessment of the quality of the EPNL predictions.

7. UTILITIES

7.1 THERMODYNAMIC UTILITIES

INTRODUCTION

The prediction of aircraft-engine noise requires detailed knowledge of the thermodynamics of the engine. The gas properties of the fuel-air mixture are needed to analyze the thermodynamic processes. All data on engine processes are stored as total variables in ANOPP. The capability to convert these to static variables is needed for the noise-prediction modules. The engine utilities perform both of these functions within ANOPP. This allows increased efficiency in the design of the functional modules.

A brief description of each utility in ANOPP is given in the following:

1. Gas-Properties Utility - Computes the ratio of specific heats, specific enthalpy, and specific entropy function as a function of temperature for given values of absolute humidity, fuel-to-air ratio, and ambient temperature.

2. Flow-Variables Utility - Computes the static pressure, static temperature, and Mach number for given values of mass flow rate, total pressure, total temperature, and gas properties.

The inputs, outputs, and method for each utility are presented in detail herein. The ranges of the input variables are given in table I. All methods are extracted from references 1 to 3; however, they are documented in any standard gas dynamics text. All thermodynamic utilities are available for use in any module in ANOPP.

SYMBOLS

A	flow cross-sectional area, m^2 (ft^2)
c_p	specific heat at constant pressure, $m^2/K\text{-}s^2$ ($ft^2/{}^oR\text{-}s^2$)
f	fuel-to-air ratio
H_a	absolute humidity, percent mole fraction
h	specific enthalpy, m^2/s^2 (ft^2/s^2)
M	Mach number
m	mass, kg (slugs)
$\dot{m}$	mass flow rate, kg/s (slugs/s)

p	pressure, Pa (lb/ft^2)
R	dry-air gas constant, $m^2/K\text{-}s^2$ ($ft^2/{}^oR\text{-}s^2$)
$\bar{R}$	universal gas constant, $kg\text{-}m^2/K\text{-}s^2$ ($slugs\text{-}ft^2/{}^oR\text{-}s^2$)
R	gas constant, $m^2/K\text{-}s^2$ ($ft^2/{}^oR\text{-}s^2$)
T	temperature, K (^oR)
U	velocity, m/s (ft/s)
W_i	molecular weights of gas constituents
X_i	mass fractions of gas constituents
γ	ratio of specific heats
ρ	density, kg/m^3 ($slugs/ft^3$)
ϕ	entropy function, $m^2/K\text{-}s^2$ ($ft^2/{}^oR\text{-}s^2$)

Subscripts:

a	air
r	reference value (see table III)
s	static
t	total
∞	ambient

Superscript:

*	dimensionless quantity

GAS-PROPERTIES UTILITY

Input

f	fuel-to-air ratio
H_a	absolute humidity, percent mole fraction
T_∞^*	ambient temperature, re T_r
T^*	local temperature, re T_∞

Output

The gas-properties table can be interpolated to provide the gas-properties data when needed within ANOPP. The gas constant is also provided.

R^* gas constant, re R

Gas-Properties Table

T^* temperature, re T_∞

$h^*(T^*)$ specific enthalpy, re RT_∞

$\phi^*(T^*)$ specific entropy function, re R

$\gamma(T^*)$ ratio of specific heats

Method

The constituents of the gas within the flow are those of dry air (nitrogen, oxygen, and argon) and the products of combustion (carbon dioxide and water). The amounts of the other gas constituents are assumed to be negligible. Table II gives the five gas constituents and their molecular weights. The mass of each gas constituent is given by

$$\begin{bmatrix} m_1 \\ m_2 \\ m_3 \\ m_4 \\ m_5 \end{bmatrix} = m_a \begin{bmatrix} 0.75558 \\ 0.23154 - 3.43185f \\ 3.13753f \\ 0.00622H_a + 1.28432f \\ 0.01289 \end{bmatrix} \tag{1}$$

The amount of fuel that can be burned is limited to the availability of oxygen in the air. Therefore, the value of the fuel-to-air ratio f cannot exceed 0.06767. The constants used in equations (1) are summarized in table III. Then, the mass fraction X_i of each constituent gas is

$$\begin{bmatrix} X_1 \\ X_2 \\ \cdot \\ \cdot \\ \cdot \\ X_5 \end{bmatrix} = \frac{1}{m} \begin{bmatrix} m_1 \\ m_2 \\ \cdot \\ \cdot \\ \cdot \\ m_5 \end{bmatrix} \tag{2}$$

where the total mass m is

$$m = \sum_{i=1}^{5} m_i \tag{3}$$

The dimensionless gas constant R for each constituent gas can be computed from the universal gas constant $\bar{R}$ as

$$\begin{bmatrix} R_1^* \\ R_2^* \\ \cdot \\ \cdot \\ \cdot \\ R_5^* \end{bmatrix} = \frac{1}{R} \begin{bmatrix} \bar{R}/W_1 \\ \bar{R}/W_2 \\ \cdot \\ \cdot \\ \cdot \\ \bar{R}/W_5 \end{bmatrix} \tag{4}$$

where R is the dry-air gas constant and W_i is the molecular weight of the ith gas constituent given in table II. The dimensionless gas constant of the mixture is then given by the following matrix product:

$$R^* = \begin{bmatrix} X_1, & X_2, & \ldots, & X_5 \end{bmatrix} \begin{bmatrix} R_1^* \\ R_2^* \\ \cdot \\ \cdot \\ \cdot \\ R_5^* \end{bmatrix} \tag{5}$$

The dimensionless gas constant R^* is given as a function of fuel-to-air ratio and absolute humidity in table IV.

The dimensionless specific heat at constant pressure c_p^* (which is computed from $c_p^* = c_p/R$) can be expressed as follows:

$$c_p^*(T^*) = \begin{bmatrix} R_1^* X_1, & R_2^* X_2, & \ldots, & R_5^* X_5 \end{bmatrix} \begin{bmatrix} c_{p,1}^*(T/T_r) \\ c_{p,2}^*(T/T_r) \\ \cdot \\ \cdot \\ \cdot \\ c_{p,5}^*(T/T_r) \end{bmatrix} \tag{6}$$

where X_i and R_i^* are the component mass fractions and gas constants from equations (2) and (4) and $T/T_r = T^*T_\infty^*$. The values of the component specific heats at constant pressure $c_{p,i}^*$ are given in table V. Finally, the ratio of specific heats γ is

$$\gamma = \frac{c_p^*}{c_p^* - 1} \tag{7}$$

The ratio of specific heats as a function of temperature and fuel-to-air ratio is plotted in figure 1.

The enthalpy per unit mass of a fluid is defined as

$$h = \int_{T_\infty}^{T} c_p(T/T_r)\, dT \tag{8}$$

Expressed in dimensionless form, this becomes the following:

$$h^*(T^*) = \int_1^{T^*} c_p^*\left(T^*T_\infty^*\right) dT^* \tag{9}$$

Equation (9) can be expressed in terms of an absolute scale T/T_r as

$$h^*(T^*) = \frac{1}{T_\infty^*}\int_1^{T/T_r} c_p^*\, d\left(\frac{T}{T_r}\right) - \frac{1}{T_\infty^*}\int_1^{T_\infty^*} c_p^*\, d\left(\frac{T}{T_r}\right) \tag{10}$$

or

$$h^*(T^*) = \left[h_r^*\left(T^*T_\infty^*\right) - h_r^*\left(T_\infty^*\right)\right]\Big/T_\infty^* \tag{11}$$

In general, the specific enthalpy is a function of the fuel-to-air ratio and the absolute humidity. Then the specific enthalpy h_r^* is expressed in terms of the component specific enthalpies of table V as

$$h_r^* = \left[R_1^*X_1,\ R_2^*X_2,\ \ldots,\ R_5^*X_5\right]\begin{bmatrix} h_{r,1}^* \\ h_{r,2}^* \\ \cdot \\ \cdot \\ \cdot \\ h_{r,5}^* \end{bmatrix} \tag{12}$$

The specific enthalpy is plotted as a function of temperature and fuel-to-air ratio for zero absolute humidity in figure 2.

The entropy function ϕ per unit mass of a fluid is given by

$$\phi = \int_{T_\infty}^{T} \frac{c_p}{T} \, dT \tag{13}$$

which may be expressed in dimensionless form as

$$\phi^* = \int_1^{T^*} \frac{c_p^*}{T^*}\left(T^* T_\infty^*\right) \, dT^* \tag{14}$$

Equation (14) can be expressed in terms of T/T_r as

$$\phi^*(T^*) = \int_1^{T/T_r} \frac{c_p^*}{(T/T_r)} \, d(T/T_r) - \int_1^{T_\infty^*} \frac{c_p^*}{d(T/T_r)} \, d(T/T_r) \tag{15}$$

or

$$\phi^*(T^*) = \phi_r^*\left(T^* T_\infty^*\right) - \phi_r^*\left(T_\infty^*\right) \tag{16}$$

In general, the specific entropy function is a function of the fuel-to-air ratio and absolute humidity. Then the specific entropy function ϕ_r^* is expressed in terms of the component specific entropy functions of table V as

$$\phi_r^* = \left[R_1^* x_1, \; R_2^* x_2, \; \ldots, \; R_5^* x_5\right] \begin{bmatrix} \phi_{r,1}^* \\ \phi_{r,2}^* \\ \cdot \\ \cdot \\ \cdot \\ \phi_{r,5}^* \end{bmatrix} \tag{17}$$

The specific entropy function is plotted as a function of temperature and fuel-to-air ratio for zero absolute humidity in figure 3.

The gas properties table is formed from equations (7), (12), and (17). It can be interpolated to determine γ, h^*, or ϕ^* for a given value of T^*. Alternately, the temperature T^* can be determined for a given value of h^* or ϕ^*.

FLOW-VARIABLES UTILITY

Input

The inputs to this utility are the gas-properties table and the total flow variables.

Total Flow Variables

$\dot{m}_t^*$	total mass flow rate, re $Ap_t/\sqrt{RT_t}$
p_t^*	total pressure, re p_∞
T_t^*	total temperature, re T_∞

Gas-Properties Table

T^*	temperature, re T_∞
$h^*(T^*)$	specific enthalpy, re RT_∞
$\phi^*(T^*)$	specific entropy function, re R
$\gamma(T^*)$	ratio of specific heats

Output

The outputs are the static flow variables.

Static Flow Variables

M	Mach number
p_s^*	static pressure, re p_∞
T_s^*	static temperature, re T_∞

Method

The computation can be performed with either constant ratio of specific heats or variable ratio of specific heats.

Constant Ratio of Specific Heats

As derived in reference 2, the total mass flow rate $\dot{m}_t^*$ is related to the Mach number as follows:

$$\dot{m}_t^* = \sqrt{\gamma} M \left(1 + \frac{\gamma - 1}{2} M^2\right)^{-\frac{1}{2}\left(\frac{\gamma+1}{\gamma-1}\right)} \tag{18}$$

where the ratio of specific heats γ is determined from T_t^* using the gas-properties table. Given the mass flow rate, the Mach number cannot be determined in closed form from equation (18). In addition, the equation has two roots, one for subsonic and one for supersonic flow. The subsonic root is the one of interest here, so the interval-halving technique (ref. 4) is used to find the Mach number value. The Mach number is plotted versus the dimensionless total mass flow rate in figure 4.

From the energy equation for the adiabatic flow of a perfect gas with constant specific heats, the expression for the stagnation-temperature ratio (ref. 2) is

$$\frac{T_t^*}{T_s^*} = 1 + \frac{\gamma - 1}{2} M^2 \tag{19}$$

Rearranging yields

$$T_s^* = T_t^* \Big/ \left(1 + \frac{\gamma - 1}{2} M^2\right) \tag{20}$$

which is plotted in figure 5 for $\gamma = 1.4$.

Similarly, for an isentropic process, the stagnation-pressure ratio is related to the stagnation-temperature ratio by the following relation:

$$\frac{T_s^*}{T_t^*} = \left(\frac{p_s^*}{p_t^*}\right)^{\frac{\gamma-1}{\gamma}} \tag{21}$$

After substituting equation (19) and rearranging, the static pressure p_s^* is

$$p_s^* = p_t^* \Big/ \left(1 + \frac{\gamma - 1}{2} M^2\right)^{\frac{\gamma}{\gamma-1}} \tag{22}$$

which is also plotted in figure 5 for $\gamma = 1.4$.

Variable Ratio of Specific Heats

Computation of the static temperature and static pressure using a variable ratio of specific heats requires two relations. The first is derived from continuity and the first law of thermodynamics, and the second is derived from the second law of thermodynamics. The two equations are solved simultaneously.

The continuity relation is

$$\dot{m} = \rho_s U A \tag{23}$$

and, from the first law of thermodynamics,

$$U = \sqrt{2(h_t - h_s)} \tag{24}$$

Substituting equation (24) into (23) and applying the ideal-gas law yields

$$\dot{m} = \frac{p_s}{RT_s} A \sqrt{2(h_t - h_s)} \tag{25}$$

By rearranging and expressing in dimensionless form, equation (25) becomes

$$\dot{m}_t^* = \frac{\sqrt{T_t^*}}{T_s^*} \frac{p_s^*}{p_t^*} \sqrt{2\left(h_t^* - h_s^*\right)} \tag{26}$$

From the second law of thermodynamics, the change in entropy Δs is given by

$$\Delta s = R \ln\left(\frac{p_s}{p_t}\right) + \phi_t - \phi_s \tag{27}$$

where ϕ is the entropy function. For an isentropic process, $\Delta s = 0$, so by rearranging yields the following:

$$\ln\left(\frac{p_s}{p_t}\right) = \frac{-(\phi_t - \phi_s)}{R} \tag{28}$$

By taking the exponential of both sides and putting in dimensionless form, equation (28) becomes

$$\frac{p_s^*}{p_t^*} = \exp\left[-\left(\phi_t^* - \phi_s^*\right)\right] \tag{29}$$

Equations (26) and (29) can be solved simultaneously for the static temperature and static pressure. Two roots exist, one for subsonic flow and one for supersonic flow. To ensure that the subsonic flow case is determined, the equations are solved using an interval-halving technique. The static-to-total temperature and pressure ratios computed with both constant and variable ratios of specific heats are given in tables VI and VII.

From the continuity equation (eq. (23)), the Mach number can be expressed as

$$M = \frac{\dot{m}}{\rho_s A \sqrt{\gamma R T_s}} \tag{30}$$

Applying the perfect-gas law and expressing in dimensionless form yields

$$M = \frac{\dot{m}_t}{\sqrt{\gamma}} \frac{p_t^*}{p_s^*} \sqrt{\frac{T_s^*}{T_t^*}} \tag{31}$$

Table VIII compares the Mach numbers for constant and variable ratios of specific heats.

REFERENCES

1. McBride, Bonnie J.; Heimel, Sheldon; Ehlers, Janet G.; and Gordon, Sanford: Thermodynamic Properties to 6000° K for 210 Substances Involving the First 18 Elements. NASA SP-3001, 1963.

2. Shapiro, Ascher H.: The Dynamics and Thermodynamics of Compressible Fluid Flow. Volume I. Ronald Press Co., c.1953.

3. Liepmann, H. W.; and Roshko, A.: Elements of Gasdynamics. John Wiley & Sons, Inc., c.1957.

4. Beckett, Royce; and Hurt, James: Numerical Calculations and Algorithms. McGraw-Hill Book Co., c.1967.

TABLE I.- RANGES OF INPUT PARAMETERS

Input parameter	Minimum	Maximum
f	0	0.06767
H_a, percent . . .	0	4
$\dot{m}_t^*$	0	0.6847
p_t^*	0.1	10.0
T_a^*	0.8	1.2
T_t^*	0.5	7.0

TABLE II.- GAS CONSTITUENTS

Index	Constituent	Molecular weight
1	Nitrogen (N_2)	28.01340
2	Oxygen (O_2)	31.99880
3	Carbon dioxide (CO_2)	44.00995
4	Water (H_2O)	18.01534
5	Argon (Ar)	39.94800

TABLE III.- STORED PRIMARY CONSTANTS

Mass fraction of nitrogen in dry air	0.75558
Mass fraction of oxygen in dry air	0.23154
Mass fraction of argon in dry air	0.01289
Mass of oxygen required per unit mass of fuel burned	3.42185
Mass of water produced per unit mass of fuel burned	1.28432
Mass of carbon dioxide produced per unit of fuel burned	3.13753
Mass fraction of water per percent mole fraction	0.00622
Standard sea level temperature, K	288.15
Universal gas constant, kg-m^2/K-s^2	8314.32

TABLE IV.- VARIATION IN DIMENSIONLESS GAS CONSTANT R^*

f	R^* for H_a, percent mole fraction, of -	
	0	1.2
0.000	1.00016	1.00763
.005	1.00032	1.00775
.010	1.00048	1.00787
.015	1.00064	1.00799
.020	1.00079	1.00811
.025	1.00095	1.00822
.030	1.00110	1.00834
.035	1.00125	1.00845
.040	1.00140	1.00857
.045	1.00155	1.00868
.050	1.00170	1.00879
.055	1.00184	1.00890
.060	1.00199	1.00901
.065	1.00213	1.00912

TABLE V.- SPECIFIC HEAT AT CONSTANT PRESSURE, SPECIFIC ENTHALPY, AND SPECIFIC ENTROPY FUNCTION FOR THE GAS CONSTITUENTS

(a) Specific heat at constant pressure

T/T_r	$c^*_{p,i}$ for -				
	N_2	O_2	CO_2	H_2O	Ar
0.347041	3.50040	3.50065	3.51268	4.00582	2.50000
.694083	3.50085	3.50306	3.89134	4.01025	2.50000
1.041124	3.50296	3.53436	4.47561	4.03953	2.50000
1.388166	3.51791	3.62112	4.96976	4.11944	2.50000
1.735207	3.55781	3.73957	5.36648	4.23503	2.50000
2.082249	3.62147	3.85979	5.69115	4.36677	2.50000
2.429290	3.69901	3.96712	5.96077	4.50726	2.50000
2.776332	3.78063	4.05755	6.18585	4.65445	2.50000
3.123373	3.85959	4.13278	6.37410	4.80652	2.50000
3.470415	3.93245	4.19482	6.53181	4.96045	2.50000
3.817456	3.99792	4.24675	6.66435	5.11307	2.50000
4.164498	4.05584	4.29113	6.77616	5.26152	2.50000
4.511593	4.10666	4.32998	6.87102	5.40362	2.50000
4.858581	4.15114	4.36495	6.95198	5.53808	2.50000
5.205622	4.19004	4.39731	7.02153	5.66408	2.50000
5.552664	4.22416	4.42796	7.08171	5.78153	2.50000
5.899705	4.25415	4.45749	7.13409	5.89052	2.50000
6.246746	4.28062	4.48633	7.18004	5.99142	2.50000
6.593788	4.30407	4.51476	7.22054	6.08471	2.50000
6.940829	4.32495	4.54294	7.25652	6.17096	2.50000

TABLE V.- Continued

(b) Specific enthalpy

T/T_r	h_r^* for -				
	N_2	O_2	CO_2	H_2O	Ar
0.347041	-2.28601	-2.29021	-2.55053	-2.62091	-1.63240
.694083	-1.07126	-1.07511	-1.28077	-1.23013	-.76479
1.041124	.12148	.14453	.17217	.16537	.10281
1.388166	1.36173	1.38477	1.81442	1.57972	.97042
1.735207	2.58870	2.66151	3.61035	3.02883	1.83802
2.082249	3.83383	3.98052	5.53079	4.52107	2.70562
2.429290	5.10377	5.33916	7.55409	6.06063	3.57323
2.776332	6.40164	6.73204	9.66296	7.65032	4.44083
3.123373	7.72763	8.15373	11.84343	9.29187	5.30843
3.470415	9.07981	9.59899	14.08363	10.98651	6.17604
3.817456	10.45610	11.06399	16.37411	12.73459	7.04364
4.164498	11.85386	12.54575	18.70686	14.53505	7.91125
4.511593	13.27049	14.04183	21.07541	16.38582	8.77898
4.858581	14.70352	15.55066	23.47435	18.28460	9.64645
5.205622	16.15106	17.07119	25.89930	20.22879	10.51406
5.552664	17.61117	18.60255	28.34679	22.21507	11.38166
5.899705	19.08245	20.14439	30.81366	24.24064	12.24926
6.246746	20.56351	21.69635	33.29764	26.30253	13.11687
6.593788	22.05331	23.25827	35.79664	28.39831	13.98447
6.940829	23.55061	24.82997	38.30874	30.52499	14.85207

TABLE V.- Concluded

(c) Specific entropy function

T/T_r	ϕ_r^* for -				
	N_2	O_2	CO_2	H_2O	Ar
0.347041	-3.67792	-3.58194	-4.01072	-4.21447	-2.64578
.694083	-1.25146	-1.25572	-1.48926	-1.43687	-.91291
1.041124	.16823	.16881	.20020	.19316	.10075
1.388166	1.17751	1.19630	1.55805	1.36507	.81996
1.735207	1.96629	2.01678	2.71120	2.29626	1.37782
2.082249	2.62030	2.70934	3.71927	3.07990	1.83362
2.429290	3.18430	3.31258	4.61744	3.76350	2.21900
2.776332	3.68353	3.84845	5.42656	4.37490	2.55283
3.123373	4.13344	4.33062	6.16832	4.93184	2.84728
3.470415	4.54391	4.76956	6.84830	5.44622	3.11069
3.817456	4.92186	5.17188	7.47726	5.92618	3.34896
4.164498	5.27225	5.54334	8.06208	6.37750	3.56649
4.511593	5.59893	5.88839	8.60831	6.80432	3.76663
4.858581	5.90493	6.21059	9.12052	7.20970	3.95187
5.205622	6.19271	6.51287	9.60259	7.59617	4.12435
5.552664	6.46424	6.79763	10.05774	7.96552	4.28569
5.899705	6.72123	7.06695	10.48864	8.31932	4.43726
6.246746	6.96518	7.32258	10.89774	8.65884	4.58015
6.593788	7.19726	7.56588	11.28707	8.98537	4.71532
6.940829	7.41851	7.79821	11.65839	9.29972	4.84355

TABLE VI.- COMPARISON OF STATIC-TO-TOTAL TEMPERATURE RATIO, T_s^*/T_t^*, FOR CONSTANT AND VARIABLE RATIOS OF SPECIFIC HEATS

$$\left[\dot{m}_t^* = 0.3\sqrt{T_t^*}\right]$$

T^*	T_s^*/T_t^* at constant γ for f of -		T_s^*/T_t^* at variable γ for f of -	
	0	0.05	0	0.05
1.500	0.979	0.980	0.979	0.980
2.000	.971	.973	.971	.972
2.500	.963	.965	.964	.966
3.000	.954	.957	.954	.957
3.200	.951	.954	.950	.953
3.400	.946	.950	.946	.949
3.600	.942	.945	.942	.946
3.800	.937	.941	.936	.940
4.000	.932	.936	.931	.936
4.200	.925	.930	.925	.929
4.400	.918	.922	.918	.922
4.600	.909	.913	.909	.913
4.800	.896	.898	.895	.896

TABLE VII.- COMPARISON OF STATIC-TO-TOTAL PRESSURE RATIO, p_s^*/p_t^*, FOR CONSTANT AND VARIABLE RATIOS OF SPECIFIC HEATS

$$\left[\dot{m}_t^* = 0.3\sqrt{T_t^*}\right]$$

T^*	p_s^*/p_t^* at constant γ for f of -		p_s^*/p_t^* at variable γ for f of -	
	0	0.05	0	0.05
1.500	0.927	0.926	0.930	0.930
2.000	.899	.898	.895	.894
2.500	.868	.868	.872	.873
3.000	.835	.833	.836	.834
3.200	.820	.818	.819	.818
3.400	.804	.802	.803	.801
3.600	.788	.785	.788	.787
3.800	.770	.766	.766	.762
4.000	.750	.746	.751	.748
4.200	.728	.723	.726	.720
4.400	.703	.696	.702	.696
4.600	.673	.662	.677	.666
4.800	.633	.612	.630	.608

TABLE VIII.- COMPARISON OF MACH NUMBER, M, FOR CONSTANT AND VARIABLE RATIOS OF SPECIFIC HEATS

$$\left[\dot{m}_t^* = 0.3\sqrt{T_t^*}\right]$$

T^*	M at constant γ for f of -		M at variable γ for f of -	
	0	0.05	0	0.05
1.500	0.332	0.336	0.331	0.335
2.000	.396	.402	.398	.403
2.500	.459	.466	.457	.463
3.000	.524	.532	.522	.531
3.200	.551	.560	.551	.559
3.400	.579	.589	.578	.589
3.600	.607	.619	.606	.616
3.800	.638	.650	.640	.653
4.000	.671	.685	.669	.682
4.200	.706	.723	.706	.723
4.400	.747	.766	.745	.765
4.600	.794	.820	.788	.814
4.800	.857	.900	.858	.902

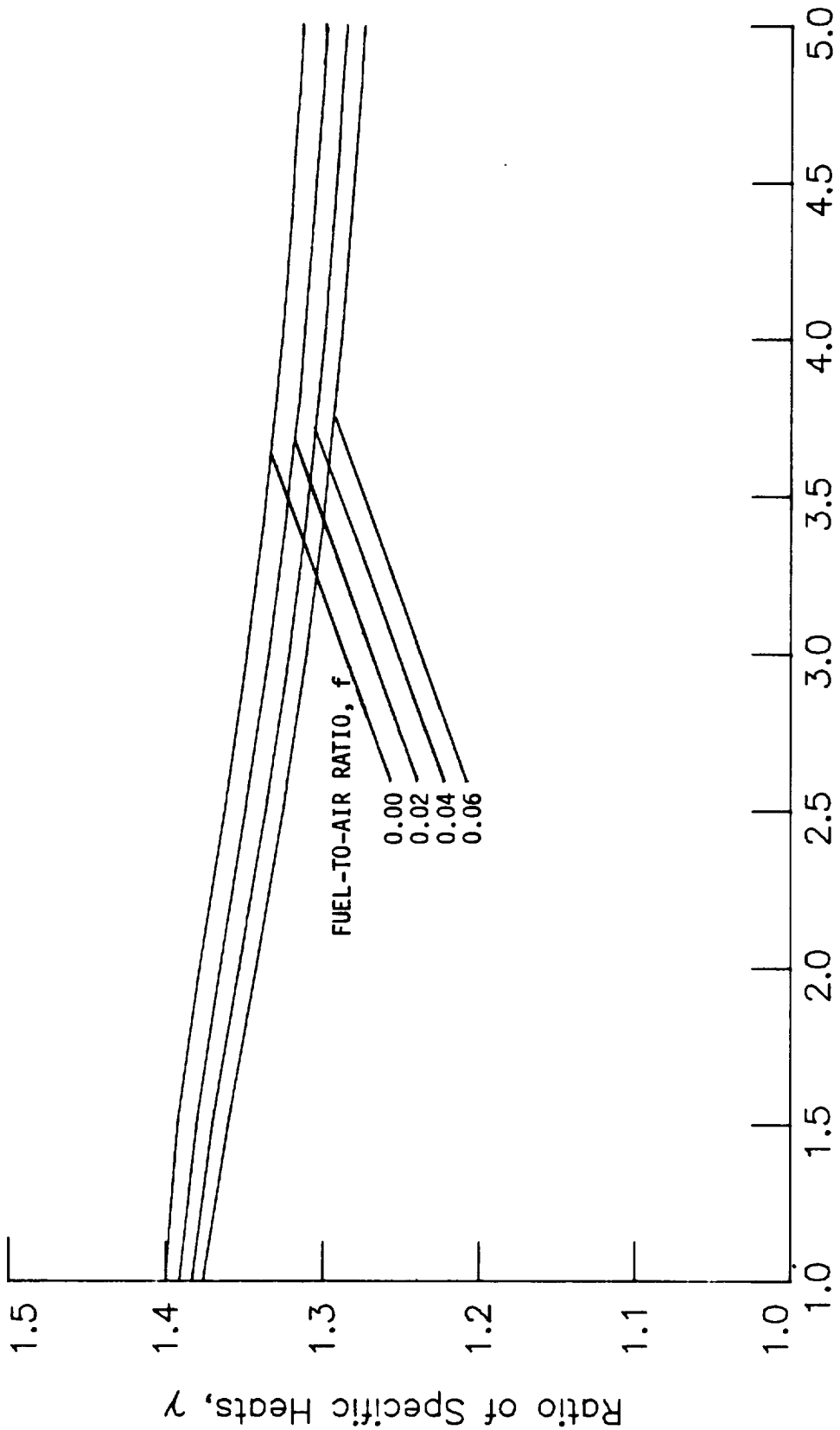

Figure 1.- Ratio of specific heats.

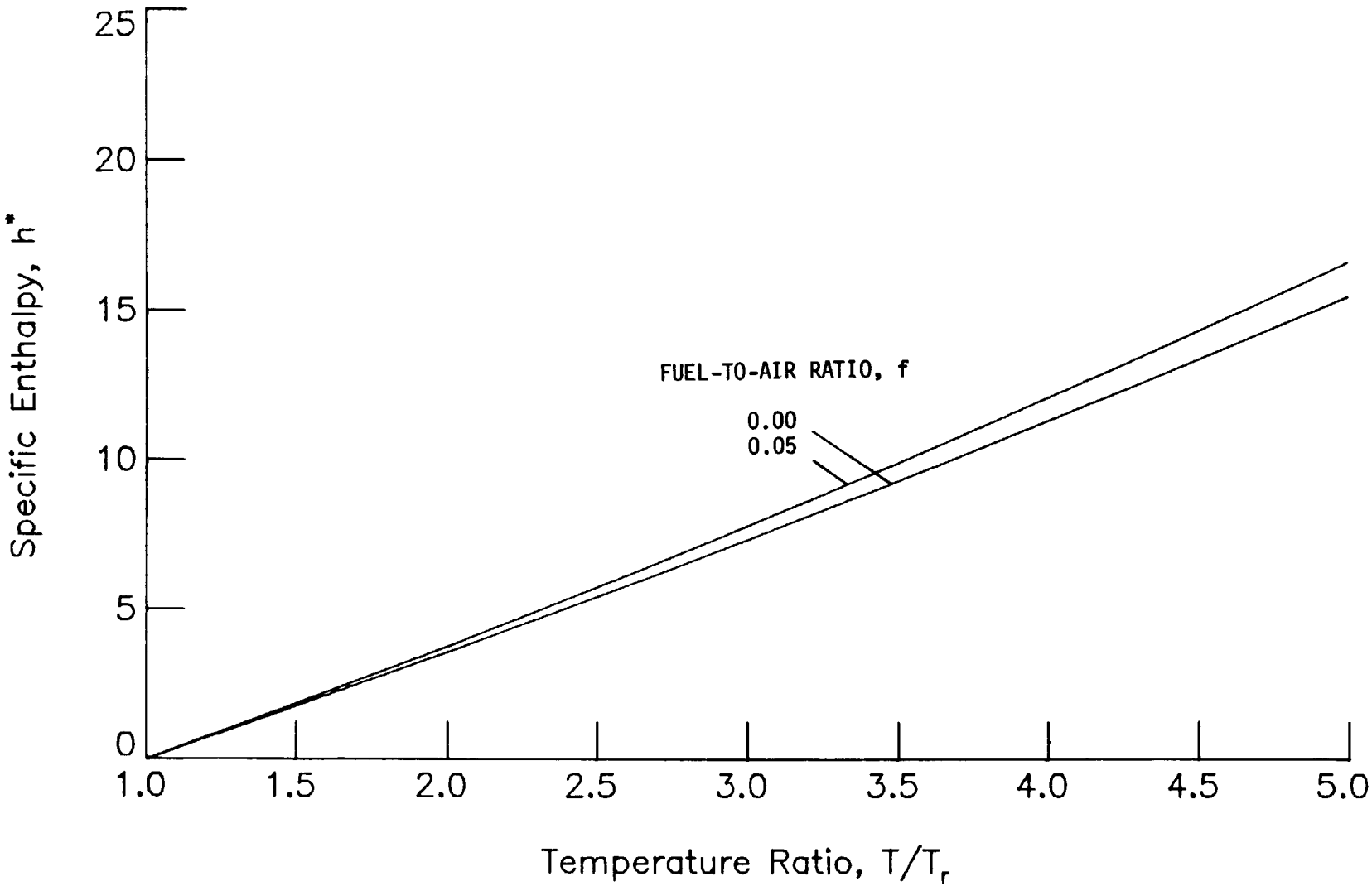

Figure 2.- Specific enthalpy.

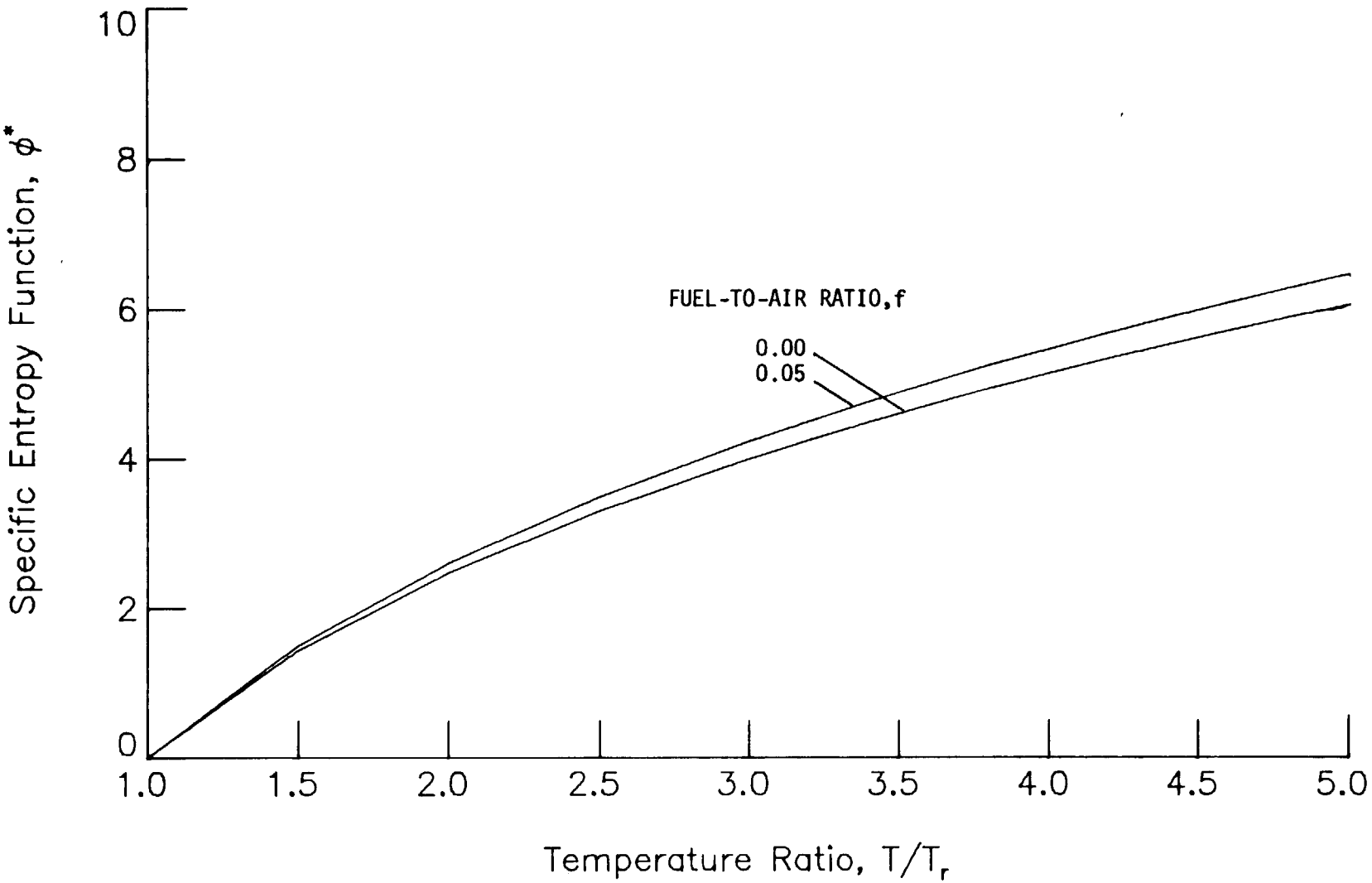

Figure 3.- Specific entropy function.

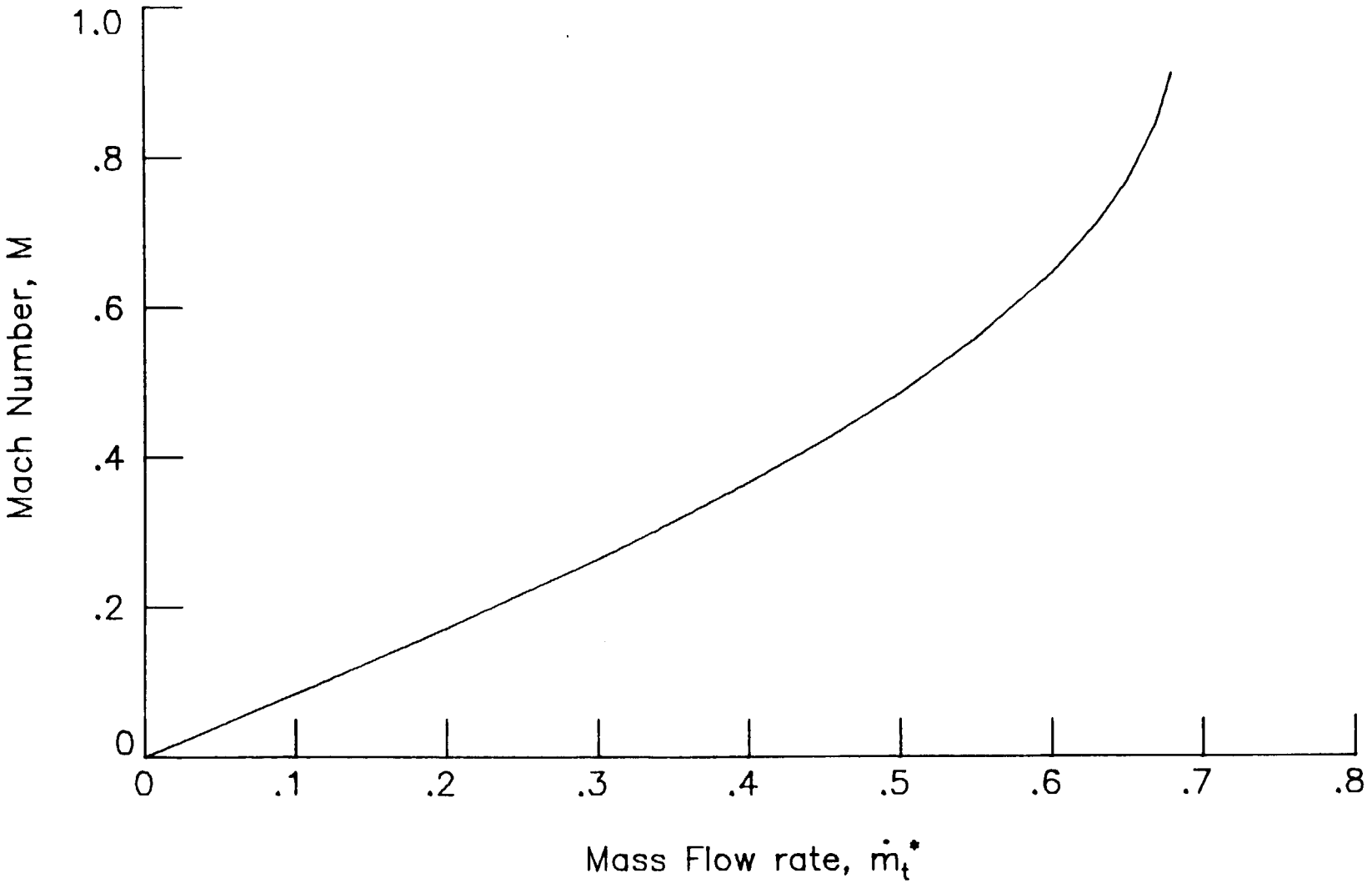

Figure 4.- Mach number referred to total variables for a constant ratio of specific heats. $\gamma = 1.4$.

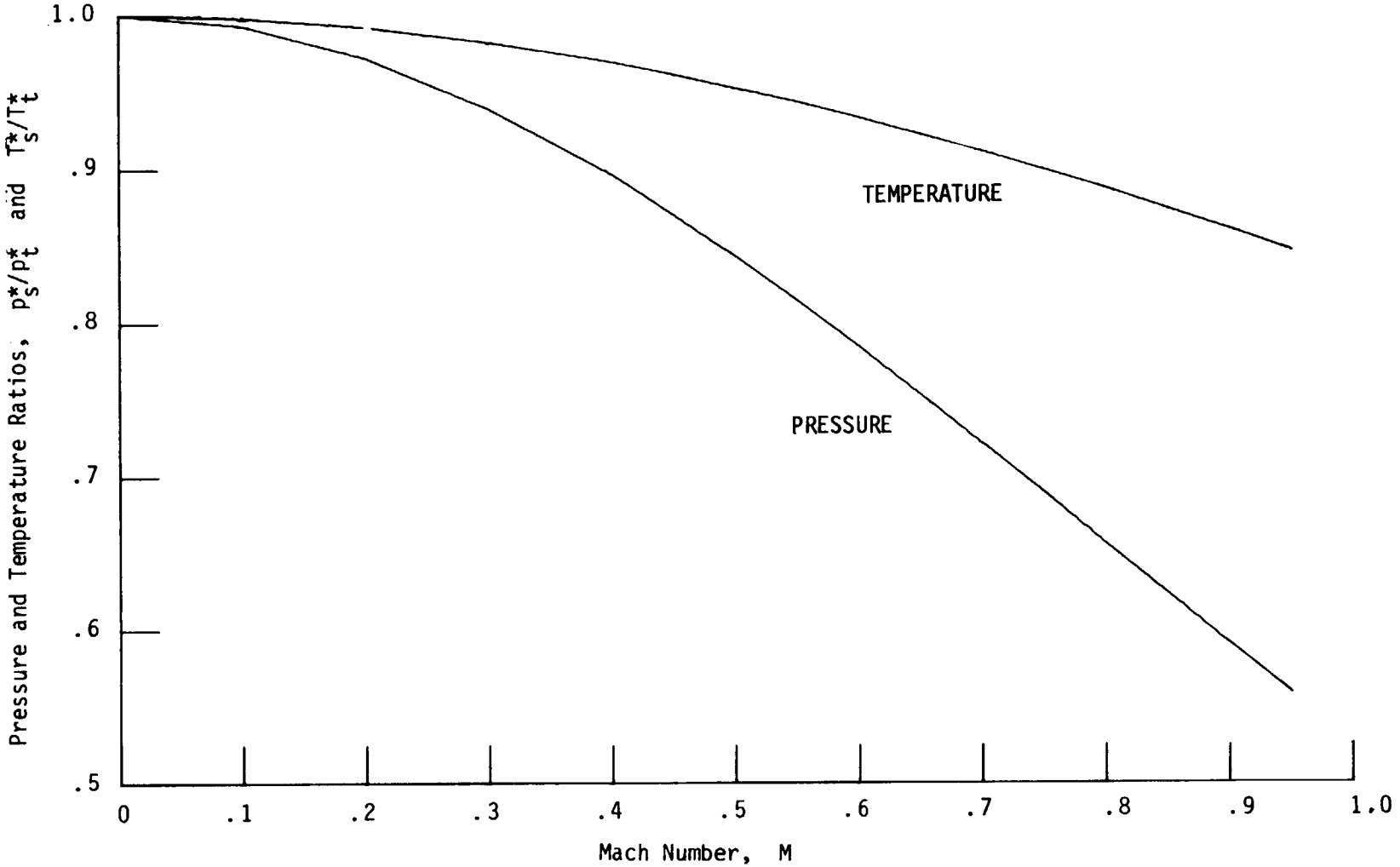

Figure 5.- Static-to-total temperature and pressure ratios for a constant ratio of specific heats. $\gamma = 1.4$.